Energy bands: Chern numbers and symmetry

AUTHOR(S):

Iwai, T.; Zhilinskii, B.

CITATION:

Iwai, T. ...[et al]. Energy bands: Chern numbers and symmetry. Annals of Physics 2011, 326(12): 3013-3066

ISSUE DATE:

2011-12

URL:

http://hdl.handle.net/2433/150445

Energy bands: Chern numbers and symmetry.

T. Iwai[a], B. Zhilinskii[a,b]

[a] *Kyoto University, Kyoto, Japan*
[b] *Université du Littoral Côte d'Opale, 59140 Dunkerque, France*

Abstract

Energy bands formed by rotation-vibrational states of molecules in the presence of symmetry and their qualitative modifications under variation of some control parameters are studied within the semi-quantum model. Rotational variables are treated as classical whereas a finite set of vibrational states is considered as quantum. In the two-state approximation the system is described in terms of a fiber bundle with the base space being a two-dimensional sphere, the classical phase space for rotational variables. Generically this rank two complex vector bundle can be decomposed into two complex line bundles characterized by topological invariant, first Chern class. General method of explicit calculation of Chern classes and of their possible modifications under variation of control parameters in the presence of symmetry is suggested. The construction of iso-Chern diagrams which split the space of control parameters into connected domains with fixed Chern numbers is suggested. Detailed analysis of rovibrational model Hamiltonian for D_3 invariant molecule possessing two vibrational states transforming according to two-dimensional irreducible representation is done to illustrate non-trivial restrictions imposed by symmetry on possible values of Chern classes.

Keywords: energy bands, fiber bundle, Chern class, molecules

1. INTRODUCTION

Qualitative understanding of many physical phenomena is based on the construction of a model associated with topological and symmetry notions [45, 44, 27]. The interrelation between physical and mathematical ideas here

Email addresses: iwai@amp.i.kyoto-u.ac.jp (T. Iwai), zhilin@univ-littoral.fr (B. Zhilinskii)

is so important that many new mathematical ideas are tightly related to preliminary physical constructions [9]. The most intensive such collaboration between mathematicians and physicists is in the field of high-energy and solid state physics. Description of finite particle quantum systems (atoms and molecules) is often considered as being more related to the domain of direct extensive numerical calculation based on the study of multi-particle Schrödinger equation. Nevertheless, it turns out that many sophisticated mathematical constructions are extremely adequate for the description of qualitative features of simple isolated quantum systems. [22, 33, 16, 11]. In some way the finite particle systems have even certain advantage from the point of view of the verification of adequacy of mathematical models due to a large amount of very detailed information about energy spectra of finite quantum systems and their variation as a function of some control parameters, whereas many mathematical applications to high-energy physics, gravitation, cosmology and so on either could not be verified experimentally at present, or can be compared with a very restrictive set of experimental data.

In this paper we discuss qualitative aspects related to such well known molecular notion as energy bands and their rearrangement from the point of view of vector bundles, their characteristic classes (Chern classes), associated topological quantum numbers and especially from the point of view of symmetry and its consequences on the possible values of topological quantum numbers and their modifications.

The relevance of Chern numbers to the notion of reorganization of energy bands in molecules was initially suggested in [35], where the reorganization of energy bands was related to the modifications of the Chern number associated with corresponding singularity. This initial paper was inspired by the manifestation of the "diabolic type" singularities in the adiabatic study of the evolution of quantum systems and appearance of geometrical Berry phase [17]. Further studies of essentially the same model [13, 14, 15] allowed to formulate more concrete relation between Chern numbers and the numbers of states in the bands. Moreover, the extension of the model to purely classical treatment reveals an interesting relation [40, 18] between redistribution of bands (accompanied by Chern number variation) and Hamiltonian monodromy phenomenon [30, 10, 8]. This correspondence in its turn stimulated further generalizations of the Hamiltonian monodromy to fractional monodromy phenomenon [32, 31, 20] which is ultimately related to specific symmetry of the problem.

From the physical point of view the most spectacular appearance of the Chern numbers is related to the description of the quantum Hall effect [3]. Here the topological origin of Chern numbers is responsible for an appearance of plateau of conductivity and for its persistence even in presence of perturbations naturally existing for real materials. It was noted that appearance of nontrivial Chern numbers for quantum Hall effect is related to breaking of time reversal invariance. For time reversal invariant systems new interesting topological phenomena are the Quantum Spin Hall Effect and Topological insulators [25, 29]. Further attempt to classify topological phases is based on the construction of "periodic table" taking into account the topology and symmetry of the emergent phases [26]. One of the simplest cases is the Z_2 topological invariant appearing for specific phases of topological insulators.

From the mathematical point of view the problem of description of quantum Hall effect by Chern numbers is the description of stratification of the set of eigenvalues and eigenfunctions of a family of Hermitian matrices [2, 1, 33]. Alternatively it is possible to study the singularities appearing in families of dynamical systems depending on some control parameters. In any approach the presence or absence of symmetry strongly modify the results because the notion of generic system itself depends on symmetry restrictions imposed on the problem. Instead of trying to develop general equivariant formalism we study in this article several concrete examples possessing different symmetry.

We work below within the model inspired largely by the molecular physics which assumes generically the existence of certain limiting cases consisting in splitting of dynamical variables (or equivalently classical motions) in several types (electronic, vibrational and rotational) which can be relatively well characterized by different scale of corresponding energy excitations, or characteristic times. In majority of systems due to rovibronic (rotational-vibrational-electronic) coupling the reorganization of energy levels and corresponding eigenfunctions takes place which does not allow a simple splitting of quantum energy levels and even the associated classical motions into rotational, vibrational and electronic ones [19, 23, 21].

At the same time very often the coupling of different degrees of freedom results after a short transition region in appearance of a new set of approximate integrals of motion, which allows to see again an almost regular type of motion in classical mechanics with another set of approximate integrals of motion. In quantum mechanics this corresponds to formation of another system of energy levels classified by a new set of approximate but good quantum numbers. Restructuring the set of energy levels under the variation of

some control parameters is precisely the qualitative phenomenon which we addressed in this paper from both topological and symmetry point of view.

We start in section 2 by introducing the notion of bands and their rearrangements. The adiabatic separation of variables into slow and fast ones and the assignment of respective variables for classical and quantum descriptions of motions suggests us to introduce a semi-quantum model whose Hamiltonian is a matrix-valued function defined on the manifold associated with the classical variables. The rearrangement of bands may be linked with topological change in bundle structure associated with the Hamiltonian depending on control parameters.

By using very simple model of two angular momentum coupling in the presence of continuous $SO(2)$ symmetry, several concrete examples of exactly solvable quantum problems showing redistribution phenomenon are treated in section 3. For generality, the $SO(2)$ action on two angular momenta is weighted.

Systematic construction of semi-quantum model within coherent state approach is discussed in section 4.

The formalism of fibre bundles and the basic approach of Chern number calculation used further in this article is described in section 5. A key to constructing a complex line bundle associated with a non-degenerate eigenvalue, called an eigen-line bundle in this article, is the exceptional point which is a singularity for normalization of the eigenvector concerned. Evaluation of the Chern numbers results in the calculation of a quantity assigned to the exceptional points. Two methods are presented for the evaluation of Chern numbers, one of which is a winding number method, and the other a linearization approach to winding numbers.

The notion of iso-Cherm diagram is introduced and discussed in section 6. It will be shown that elementary transformation of the Hamiltonian results either in the invariance of the Chern number or in a change in the sign of it. This observation works well in making out the iso-Chern diagram.

Some generalities about construction of effective rotation-vibration Hamiltonians in terms of irreducible tensors in the presence of symmetry are summarized in section 7, and applied to the construction of $SO(2)$ and D_3 invariant Hamiltonian models.

In section 8, the evaluation of Chern numbers for the $SO(2)$ model is made through the direct calculation of winding numbers for exceptional points.

Finally in section 9 we discuss in details the application of the developped approach to the analysis of D_3 invariant rotation-vibration Hamiltonian for

two vibrational states belonging to irreducible two dimensional representation of D_3 group. The Hamiltonian which is also invariant with respect to time reversal is written in the form of polynomial expansion in rotational tensors and depends on four control parameters. Complete iso-Chern diagram is constructed for this example. Detailed calculation of Chern numbers are given in the appendix. The linearization approach is used to calculate the winding numbers.

Section 10 discusses shortly possible generalizations of our approach.

2. Notion of bands and their rearrangement

Let us start by introducing the energy bands on very simple example of coupling of two angular momenta. Let $\boldsymbol{N}$ and $\boldsymbol{S}$ denote two operators acting each on irreducible finite dimensional vector space V_N and V_S whose dimensions are $\dim V_N = 2N + 1$ and $\dim V_S = 2S + 1$, where N, S are nonnegative integers or half integers. The total space of the problem is the tensor product $V_N \otimes V_S$, which generally could be reducible. The operators acting on that space can be constructed in terms of $S_\alpha \otimes \mathbf{1}$ and $\mathbf{1} \otimes N_\alpha$ operators.

Instead of looking at the total space we can try to introduce an additional classifying operator which split the total space into irreducible subspaces. If the classifying operator commutes with the Hamiltonian of the dynamical system under study, it plays the role of an integral of motion and enables us to split rigorously the total space into subspaces, corresponding to different eigenvalues of the classifying operator.

What kind of classifying operator is interesting depends on the form of the Hamiltonian defined on this total space by the concrete dynamical system. The operator S_z or $S_z \otimes \mathbf{1}$ can be chosen as a classifying operator, for example. It naturally splits the total space into subspaces with fixed value of S_z operator. Each such subspace has the dimension $2N + 1$ coinciding with the dimension of the space V_N. In a similar way it is possible to use the operator $J_z = S_z \otimes \mathbf{1} + \mathbf{1} \otimes N_z$ as a classifying operator. Subspaces associated with different values of J_z have different numbers of states. Another natural classification operator is $\boldsymbol{N} \otimes \boldsymbol{S}$. This operator splits the total space into irreducible subspaces, given by standard Clebsch-Gordan decomposition of the product of two irreps of SU(2) group. Note that in the case of $N \geq S$ the number of irreducible subspaces for S_z and $\boldsymbol{N} \otimes \boldsymbol{S}$ operators are exactly the same, but the dimensions of subspaces are quite different for two

decompositions.

If the Hamiltonian defining dynamical system on the total space commutes with a classifying operator, the whole number of eigenstates of the Hamiltonian can be split into irreducible subspaces which are the invariant subspaces of the classifying operator. From the physical point of view such splitting is often named a band structure. The origin of such terminology becomes especially clear in a limiting situation when all the eigenvalues of the Hamiltonian corresponding to the same eigenvalue of the classifying operator are very close in value (their energy) being at the same time quite distant from energy eigenvalues corresponding to another eigenvalue of the classifying operator. Energy eigenstates corresponding to each irreducible subspace of classifying operator form an "energy band".

From the physical point of view there is a quite important and interesting question: Is it possible to generalize the notion of bands to slightly perturbed (deformed) systems, when the classifying operator does not commute exactly with the Hamiltonian. And even more interesting: Is it possible to describe and to characterize the reorganization of bands which can be easily imagined by constructing a parameter dependent family of Hamiltonians having at different limits the Hamiltonians commuting with different classifying operators, giving the decomposition into different systems of bands.

One of the possibility to realize such a construction is based on the adiabatic separation of variables responsible for an intra-band structure (so called slow motion) and inter-band structure (fast motion). After using classical variables for slow motion and quantum description for fast motion, we obtain so called a semi-quantum model [38, 40, 14, 47], where the classical phase space for slow variables can be considered as a base space for a vector bundle, whose fibers are quantum eigenfunctions associated to each point of the classical phase space. The Hamiltonian in this model is a matrix valued function defined over the classical limit manifold, the classical phase space for "slow" classical variables. The rank of the vector bundle is the number of quantum states taken into account in the model.

The situation becomes simple in the case of a fiber bundles over a base space being classical phase space for a one-degree-of-freedom system. If the energy surface associated with each quantum eigenfunction and considered as a function over the classical phase space is isolated as a whole, *i.e.*, possesses no degeneracy points with another energy surface, the fiber bundle can be decomposed into line bundles. The topology of each bundle with complex

line fibers can be topologically characterized by the corresponding first Chern class. Now, if we deform the problem in such a way that the classifying operator does not commute with the Hamiltonian, the topology of each line bundle cannot change as long as energy surfaces remain isolated. The only possibility for qualitative modifications of bands can appear along with formation of degeneracy points between different energy surfaces. Such degeneracy points do not appear for a generic bundle over base space of real dimension 2, because the real codimension of degeneracy is three [2]. At the same time the one-parameter family of Hamiltonians have generically isolated degeneracies which can result in qualitative modifications of bands. Type of degeneracy and corresponding modifications of bands depends strongly on symmetry of the problem or more exactly on the action of the symmetry group of the problem on classical phase space variables and on quantum states taken into account. In spite of a large variety of different symmetry groups and their different possible actions on classical and quantum variables we try in this paper to describe some generic type of behavior for a semi-quantum model and to compare it with completely quantum description of possible splitting of the whole system of energy levels into bands and possible rearrangements of bands.

3. Preliminary analysis of model examples

The simplest family of Hamiltonians describing coupling of two angular momenta is given by the operator

$$H_{1:1}(t) \quad = (1-t)\mathbf{1}\otimes S_z + t\ \boldsymbol{N}\otimes\boldsymbol{S}, \quad 0\le t\le 1, \tag{1}$$

which admits the existence of additional integral of motion due to presence of axial symmetry whose action on N_α and S_α variables is diagonal. This family of operators is studied from different points of view in [35, 40, 18, 13, 14]. In spite of the fact that $J_z = \mathbf{1}\otimes S_z + N_z\otimes\mathbf{1}$ operator is the integral of motion for any values of parameter t two other classifying operators are more appropriate to describe the system of bands. At t close to zero the operator $\mathbf{1}\otimes S_z$ is used whereas for t close to 1 the operator $\boldsymbol{N}\otimes\boldsymbol{S}$ is a natural candidate. The rearrangement between these two band systems takes place at $t\sim 1/2$ [40, 13].

3.1. A 1 : 2 resonance model

Another family of operators constructed with angular momenta is designed to model on the compact phase space the $1:2$ and $1:(-2)$ resonance

situations widely studied for linear oscillators [7, 31]. We take the Hamiltonian of the form

$$H_{1:2}(t) = (1-t)\ \mathbf{1}\otimes S_z + t\ \left(N_z\otimes S_z + N_-^2\otimes S_+ + N_+^2\otimes S_-\right), \quad 0\le t\le 1, \tag{2}$$

essentially corresponding to that studied in [20]. This family again has an integral of motion related to the $U(1)$ or $SO(2)$ action on S_α and N_α variables but now this action is weighted (has different weights). We study the implications of symmetry group actions on the redistribution phenomenon with the simple example of model (2).

In analogy to the analysis of model (1) [35, 40, 13] showing the redistribution of only one energy level between two bands under variation of the control parameter t, we study the model Hamiltonian (2) within purely quantum approach by imposing $S = 1/2$ and $N = 1$. The total space is spanned by six states which we choose to be eigenstates of $\mathbf{1}\otimes S_z$ and $N_z\otimes\mathbf{1}$ operators. One can check that the operator

$$J_z = 2(\mathbf{1}\otimes S_z) + N_z\otimes\mathbf{1} \tag{3}$$

commute with the Hamiltonian (2) and we can immediately block diagonalize the Hamiltonian by going to eigenspaces of J_z. Fortunately, for $S = 1/2$ and $N = 1$ there are five different subspaces corresponding to different eigenvalues of $J_z = 2, 1, 0, -1, -2$. Only $J_z = 0$ subspace has dimension two. All others are one-dimensional. We denote the basis states by

$$|J_z = 2; N_z = 1, S_z = +\rangle, \tag{4a}$$
$$|J_z = 1; N_z = 0, S_z = +\rangle, \tag{4b}$$
$$|J_z = 0; N_z = -1, S_z = +\rangle, |J_z = 0; N_z = 1, S_z = -\rangle, \tag{4c}$$
$$|J_z = -1; N_z = 0, S_z = -\rangle, \tag{4d}$$
$$|J_z = -2; N_z = -1, S_z = -\rangle. \tag{4e}$$

The eigenvalues exhibit the following behavior as a function of t: Four of six eigenvalues are obtained directly as

$$E(J_z = 2) = \frac{1-t}{2} + \frac{t}{2}; \tag{5a}$$
$$E(J_z = 1) = \frac{1-t}{2}; \tag{5b}$$
$$E(J_z = -1) = \frac{t-1}{2}; \tag{5c}$$
$$E(J_z = -2) = \frac{t-1}{2} + \frac{t}{2}. \tag{5d}$$

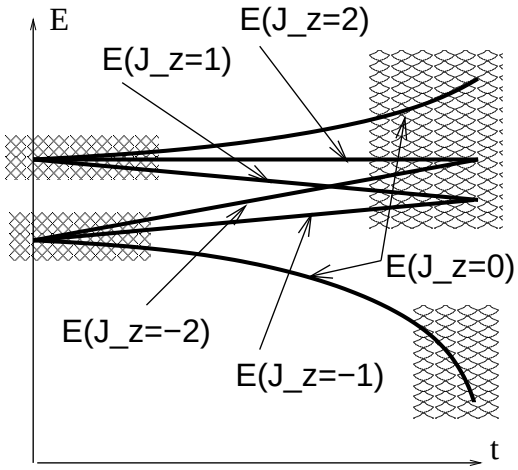

Figure 1: Redistribution of energy levels for model 2 in the case of $N = 1$.

The other two eigenvalues corresponding to the subspace with $J_z = 0$ should be obtained by diagonalizing the 2×2 matrix with matrix elements $\langle 1/2|S_+|-1/2\rangle = 1$ and $\langle 1|N_+^2|-1\rangle = 2$. The matrix has the form

$$\begin{pmatrix} \frac{1-t}{2} - \frac{t}{2} & 2t \\ 2t & \frac{t-1}{2} - \frac{t}{2} \end{pmatrix}, \tag{6}$$

and its eigenvalues are

$$E_{1,2} = \frac{-t \pm \sqrt{17t^2 - 2t + 1}}{2}. \tag{7}$$

At $t = 1$ we have $E_{1,2}(t = 1) = \{3/2, -5/2\}$.

Figure 1 shows schematically the variation of eigenvalues with t. Near the $t = 0$ and $t = 1$ limits the energy levels forming bands are marked by hatching. Eventually it is not obvious that near $t = 1$ limit the energy levels should be grouped in the manner shown in that picture. One needs to apply more serious arguments than simply existence of the energy gap in order to justify the existence of two isolated bands near $t = 1$ limit.

3.2. A $1 : K$ resonance model

For a generalization of the $1 : 2$ resonance model, we consider the Hamiltonian $H_{1:K}(t)$ in the form of $1 : K$ resonance and the symmetry operator

J_z, which are given, respectively, by

$$H_{1:K}(t) = (1-t)\,(\mathbf{1}\otimes S_z) + t(N_z\otimes S_z + N_-^K\otimes S_+ + N_+^K\otimes S_-), \tag{8}$$

and

$$J_z = K\,(\mathbf{1}\otimes S_z) + N_z\otimes\mathbf{1}, \tag{9}$$

where S and N are not restricted to $1/2$ and 1, respectively. Since $N_\pm$ are nilpotent, that is,

$$N_\pm^K = 0 \quad \text{for} \quad K \geq \dim V_N = 2N+1, \tag{10}$$

the range of K is restricted to $1 \leq K \leq 2N$. In a similar manner to that in Sec. 3.1, we can find invariant subspaces for the Hamiltonian $H_{1:K}$,

$$W_{N,S}^{(\ell)} = \mathrm{span}\{|m\rangle\otimes|r\rangle;\ m+Kr=\ell,\ |m|\leq N,\ |r|\leq S\}, \tag{11}$$

where $|m\rangle := |N\,m\rangle$ and $|r\rangle := |S\,r\rangle$ are the basis vectors of V_N and V_S, respectively. Note that J_z has a single eigenvalue $m+Kr=\ell$ on $W_{N,S}^{(\ell)}$. In each subspace $W_{N,S}^{(\ell)}$, the Hamiltonian $H_{1:K}$ is expressed as a matrix of smaller size. In particular, for $\ell = -N-KS$, one obtains $\dim W_{N,S}^{(-N-KS)} = 1$ and

$$H_{1:K}(t)|-N\rangle\otimes|-S\rangle = (-S+S(1+N)t)|-N\rangle\otimes|-S\rangle. \tag{12}$$

We note here that for $(N,S)=(1,\frac{1}{2})$ and $K=2$ the eigenvalue shown in the equation (12) reduces to (5d). The above equation implies that for $t=0$, $|-N\rangle\otimes|-S\rangle$ is an eigenvector associated with the lowest eigenvalue $-S$ of $H_{1:K}(0) = \mathbf{1}\otimes S_z$, but for $t=1$, the same vector $|-N\rangle\otimes|-S\rangle$ is an eigenvector with the eigenvalue SN which is not the lowest one. This implies that the reordering[1] of energy eigenvalues must occur as t ranges from zero to one. In addition, the same argument as in (12) can be carried on to see that $|S\rangle\otimes|N\rangle$ is an eigenvector associated with the eigenvalue S of $H_{1:K}(0) = \mathbf{1}\otimes S_z$, and also an eigenvector associated with the eigenvalue NS of $H_{1:K}(1)$. It then turns out that the level NS is degenerate, *i.e.*, the eigenspace associated with NS is of dimension two at least.

[1]We use here the word "reodering" because we speak about process which can equally occur within one band as well as between several bands. We reserve the notion "redistribution" for process consisting in passing of energy levels from one band to another.

If $S = \frac{1}{2}$, we can say more about reordering of eigenvalues in a simple manner. We note that $\dim W^{(\ell)}_{N,\frac{1}{2}} = 1$ for $\ell = -N + \kappa - \frac{1}{2}K$ and for $\ell = N-\kappa+\frac{1}{2}K$ with $0 \le \kappa \le K-1$. As is easily verified, the states $|-N+\kappa\rangle\otimes|-\frac{1}{2}\rangle$ and $|N-\kappa\rangle \otimes |\frac{1}{2}\rangle$ belonging to $W^{(-N+\kappa-\frac{1}{2}K)}_{N,\frac{1}{2}}$ and to $W^{(N-\kappa+\frac{1}{2}K)}_{N,\frac{1}{2}}$, respectively, with $0 \le \kappa \le K-1$ are eigenvectors associated with the same eigenvalue $\frac{1}{2}(N-\kappa)$ of the Hamiltonian $H_{1:K}(1)$, but they are associated with different eigenvalues $-\frac{1}{2}$ and $\frac{1}{2}$ of $H_{1:K}(0) = \mathbf{1} \otimes S_z$, respectively. Further, for ℓ with $-N + \frac{1}{2}K \le \ell \le N - \frac{1}{2}K$, one has $\dim W^{(\ell)}_{N,\frac{1}{2}} = 2$, and the eigenvalues obtained from the eigenvalue equation for $H_{1:K}(1)$ restricted to $W^{(\ell)}_{N,\frac{1}{2}}$ with $-N + \frac{1}{2}K \le \ell \le N - \frac{1}{2}K$ will be non-degenerate in general. Thus, the K vectors $|-N+\kappa\rangle \otimes |-\frac{1}{2}\rangle$ out of $|m\rangle \otimes |-\frac{1}{2}\rangle$ and those $|N-\kappa\rangle \otimes |\frac{1}{2}\rangle$ out of $|m\rangle \otimes |\frac{1}{2}\rangle$ with $0 \le \kappa \le K-1$ and $|m| \le N$ are distinguishable from others in the sense that they are responsible for the reordering of eigenvalues. Thus the number K is viewed as characteristic of the reordering of eigenvalues. The number K will be further interpreted as a characteristic of the possible modifications of the Chern number when the model is modified into a semi-quantum system (see Sec. 8).

If $N = 1$ and $K = 2$ in addition, the pair of states $|-1\rangle \otimes |-\frac{1}{2}\rangle$ and $|1\rangle \otimes |\frac{1}{2}\rangle$ and the pair of states $|0\rangle \otimes |-\frac{1}{2}\rangle$ and $|0\rangle \otimes |\frac{1}{2}\rangle$ are eigenvectors associated with the eigenvalues $\frac{1}{2}$ and 0, respectively. In fact, Fig. 1 shows that both the eigenvalues $\frac{1}{2}$ and 0 are doubly degenerate at $t = 1$.

In conclusion of this subsection, we note that the operator J_z given in (9) generates the weighted diagonal $U(1)$ action on $V_N \otimes V_S$,

$$e^{-itN_z} \otimes e^{-itKS_z}. \tag{13}$$

The operators $N_\pm, N_z$ and $S_\pm, S_z$ transform according to

$$e^{-itN_z} N_\pm e^{itN_z} = e^{\mp it} N_\pm, \quad e^{-itN_z} N_z e^{itN_z} = N_z, \tag{14a}$$

$$e^{-itKS_z} S_\pm e^{itKS_z} = e^{\mp itK} S_\pm, \quad e^{-itKS_z} S_z e^{itKS_z} = S_z, \tag{14b}$$

respectively, which are easily verified by showing that both sides of each equation satisfy the same differential equation with the same initial value as matrix-valued functions in t. From these formula, the Hamiltonian (8) is shown to be invariant under the weighted $U(1)$ action (13).

4. Classical limit and semi-quantum Hamiltonians

4.1. Averaging with the coherent states

We now treat $\boldsymbol{N}$ as classical variables and $\boldsymbol{S}$ as quantum variables. To make $\boldsymbol{N}$ into classical variables, we take the averages of them with the coherent states which are defined to be the orbit, $|\mathbf{J}\rangle := D^N(g)|N\rangle$, of the maximum weight vector $|N\rangle$ in V_N, where $D^N(g)$ is the representation matrix for $g \in SU(2)$, and g is expressed as the representation matrix with $N = \frac{1}{2}$,

$$g = e^{-i\phi N_z} e^{-i\theta N_y} e^{-i\psi N_z} \in SU(2). \tag{15}$$

Since the adjoint action of $SU(2)$ on the Lie algebra $su(2)$ induces the $SO(3)$ action

$$D^N(g) N_k D^N(g)^\dagger = \sum_{p=1}^{3} a_{pk} N_p, \quad \sum_{p=1}^{3} a_{pk} a_{p\ell} = \delta_{k\ell}, \tag{16}$$

we verify that

$$\langle \mathbf{J}|N_k|\mathbf{J}\rangle = \langle N|D^N(g)^\dagger N_k D^N(g)|N\rangle = \sum_p a_{kp}\langle N|N_p|N\rangle = N a_{k3} =: x_k, \tag{17}$$

where we have used the fact that all the diagonal matrix elements $\langle m|N_p|m\rangle$ vanish for $p = 1, 2$. From (16) as the definition of (a_{pk}) and (17), we see that $\boldsymbol{x} = (x_k)$ is restricted to the two-sphere of radius N,

$$\boldsymbol{x} = \begin{pmatrix} N\sin\theta\cos\phi \\ N\sin\theta\sin\phi \\ N\cos\theta \end{pmatrix} \in S^2(N) = \{\boldsymbol{x} \in \mathbf{R}^3; \sum_{k=1}^{3} x_k^2 = N^2\}. \tag{18}$$

As is expected, we have thus verified that the classical variables associated with $\boldsymbol{N}$ are the $\boldsymbol{x}$ given in (17). In particular, we have

$$\langle \mathbf{J}|N_\pm|\mathbf{J}\rangle = x \pm iy, \quad \langle \mathbf{J}|N_z|\mathbf{J}\rangle = z, \tag{19}$$

where $(x, y, z) = (x_1, x_2, x_3)$.

The transformation (16) of N_k is averaged to yield

$$\langle \mathbf{J}|D^N(g) N_k D^N(g)^\dagger|\mathbf{J}\rangle = \sum_{p,k} a_{pk}\langle \mathbf{J}|N_p|\mathbf{J}\rangle = \sum a_{pk} x_p, \tag{20}$$

which implies that the classical variables are subject to the transformation

$$\boldsymbol{x} \mapsto A^{-1}\boldsymbol{x}, \quad A = (a_{kj}) \in SO(3). \tag{21}$$

In particular, Eqs. (14a) and (19) are put together to give rise to the $SO(2)$ action on the sphere $S^2(N)$,

$$\boldsymbol{x} \ \mapsto \ A_t^{-1}\boldsymbol{x}, \quad A_t = e^{t\widehat{\boldsymbol{e}}_3}, \tag{22}$$

where $\widehat{\boldsymbol{e}}_3$ denotes the antisymmetric 3×3 matrix associated with the vector $\boldsymbol{e}_3$, the unit vector along the z axis in the positive direction.

To make the Hamiltonian (8) into a semi-quantum operator, we have to average $N_\pm^K$ with the coherent states $|\mathbf{J}\rangle$. A question here arises as to whether $\langle\mathbf{J}|N_\pm^K|\mathbf{J}\rangle$ are equal to $(x \pm iy)^K$, respectively, or not. As was mentioned in (10), the operators $N_\pm$ are nilpotent, so that the averages of $N_\pm^K$ must vanish identically for $K \geq 2N+1$, but $(x \pm iy)^N$ never vanish identically. This suggests that $\langle\mathbf{J}|N_\pm^K|\mathbf{J}\rangle \neq (x-iy)^N$ even for $0 < K < 2N+1$. Another question is as follows: To what extent, are $\langle\mathbf{J}|N_\pm^K|\mathbf{J}\rangle$ and $(x \pm iy)^K$ different to each other ? Calculating $\langle N|D^N(g)N_-D^N(g)^\dagger D^N(g)N_-D^N(g)^\dagger|N\rangle$ by the use of the formula (16), we can show that

$$\langle N|D^N(g)N_-^2D^N(g)^\dagger|N\rangle = N\big(N-\frac{1}{2}\big)\frac{(x-iy)^2}{|\boldsymbol{x}|^2}, \quad |\boldsymbol{x}| = N. \tag{23}$$

To get the average of N_-^K, we note that $\langle N|D^N(g)N_-^KD^N(g)^\dagger|N\rangle$ should vanish for N subject to $2N+1 \leq K$. On account of this, the average we want should take the form

$$\langle N|D^N(g)N_-^KD^N(g)^\dagger|N\rangle = \frac{1}{N^K}N\big(N-\frac{1}{2}\big)\cdots\big(N-\frac{K-1}{2}\big)(x-iy)^K. \tag{24}$$

As is expected, this equation shows that $\langle N|D^N(g)N_-^KD^N(g)^\dagger|N\rangle$ becomes equal to $(x-iy)^K$ in the fully classical limit as $N \to \infty$.

Now the Hamiltonian (2) is averaged into

$$\overline{H}_{1:2}(t) = (1-t)S_z + t\left(zS_z + (1-\frac{1}{2N})\big((x-iy)^2S_+ + (x+iy)^2S_-\big)\right). \tag{25}$$

This Hamiltonian is expected to be $SO(2)$ invariant.

4.2. Semi-quantum Hamiltonians with weighted $SO(2)$ symmetry

In what follows, we assume that N is sufficiently large, so that we may think of functions $f(\boldsymbol{x})$ on $S^2(N)$ in semi-quantum systems. With this in mind, we now study from the viewpoint of $SO(2)$ symmetry the Hamiltonian of the form

$$H(\boldsymbol{x}) = \sum_{k=1}^{3} f_k(\boldsymbol{x}) S_k, \tag{26}$$

where f_k are real-valued functions on the sphere $S^2(N)$. Our question is as to when this Hamiltonian is invariant with respect to the $SO(2)$ action associated with the $1 : K$ diagonal action (13). From (14b) and (22), it follows that the above Hamiltonian transforms according to

$$\sum_{k=1}^{3} f_k(\boldsymbol{x}) S_k \;\mapsto\; \sum_{k,\ell=1}^{3} f_k(A_t^{-1}\boldsymbol{x}) b_{k\ell} S_\ell, \tag{27}$$

where

$$(b_{k\ell}) = e^{-tK\widehat{\boldsymbol{e}}_3} = A_t^{-K}, \tag{28}$$

Then, the Hamiltonian (26) is invariant under the K-weighted $SO(2)$ action, if and only if

$$f_k(A_t^{-1}\boldsymbol{x}) = \sum_{\ell=1}^{3} b_{k\ell} f_\ell(\boldsymbol{x}). \tag{29}$$

We here introduce the vector notation for the functions f_k by $\boldsymbol{F}(\boldsymbol{x}) = \sum_k f_k(\boldsymbol{x})\boldsymbol{e}_k$, where $\boldsymbol{e}_k$ are the standard basis vectors in $\mathbf{R}^3$. Then, the above equation is put in the form

$$\boldsymbol{F}(A_t^{-1}\boldsymbol{x}) = A_t^{-K}\boldsymbol{F}(\boldsymbol{x}). \tag{30}$$

We call $\boldsymbol{F}$ satisfying the above equation to be K-weighted $SO(2)$ equivariant.

To find such a function, let us introduce

$$w = x + iy, \quad \overline{w} = x - iy, \quad h(\boldsymbol{x}) = f_1(\boldsymbol{x}) + if_2(\boldsymbol{x}). \tag{31}$$

Then, the above K-weighted $SO(2)$ equivariance is put in the form

$$h(e^{-it}w, e^{it}\overline{w}, z) = e^{-iKt}h(w, \overline{w}, z), \quad f_3(e^{-it}w, e^{it}\overline{w}, z) = f_3(w, \overline{w}, z). \tag{32}$$

Note that we have a similar condition for $\overline{h(\boldsymbol{x})} = f_1(\boldsymbol{x}) - if_2(\boldsymbol{x})$. Differentiating h, $\overline{h}$, and f_3 with respect to t, we find that

$$w\frac{\partial h}{\partial w} = Kh, \quad \overline{w}\frac{\partial \overline{h}}{\partial \overline{w}} = K\overline{h}, \quad \frac{\partial h}{\partial \overline{w}} = 0, \quad \frac{\partial f_3}{\partial w} = \frac{\partial f_3}{\partial \overline{w}} = 0. \tag{33}$$

This implies that h is a homogeneous function of degree K in w and independent of $\overline{w}$, and that f_3 is independent of both w and $\overline{w}$. Examples of h and f_3 are given by

$$h(\boldsymbol{x}) = h(z)(x+iy)^K, \quad \overline{h(\boldsymbol{x})} = h(z)(x-iy)^K, \quad f_3(\boldsymbol{x}) = f(z), \tag{34}$$

where $h(z)$ and $f(z)$ are both real functions depending on z only. Then, the Hamiltonian which is invariant under the K-weighted $SO(2)$ action takes the form

$$H_K(\boldsymbol{x}) = \frac{1}{2}h(z)(x-iy)^K S_+ + \frac{1}{2}h(z)(x+iy)^K S_- + f(z)S_z. \tag{35}$$

It is to be noted again that N should be sufficiently large, namely $N > (K-1)/2$. For $s = \frac{1}{2}, 1$, we have the Hamiltonians of the form

$$H_K(\boldsymbol{x}) = \begin{pmatrix} f(z) & \frac{1}{2}h(z)(x-iy)^K \\ \frac{1}{2}h(z)(x+iy)^K & -f(z) \end{pmatrix}, \tag{36a}$$

$$H_K(\boldsymbol{x}) = \begin{pmatrix} f(z) & \frac{1}{\sqrt{2}}\Big(h(z)(x-iy)^K\Big) & 0 \\ \frac{1}{\sqrt{2}}\Big(h(z)(x+iy)^K\Big) & 0 & \frac{1}{\sqrt{2}}\Big(h(z)(x-iy)^K\Big) \\ 0 & \frac{1}{\sqrt{2}}\Big(h(z)(x+iy)^K\Big) & -f(z) \end{pmatrix}, \tag{36b}$$

respectively.

The Hamiltonian (25) is now extended in an $SO(2)$ invariant manner to

$$\overline{H}_{1:K}(t) = (1-t)S_z + tH_K(\boldsymbol{x}), \quad 0 \le t \le 1. \tag{37}$$

If $f(z) = z$, $\frac{1}{2}h(z) = 1 - \frac{1}{2N}$, and $K = 2$, Eq. (37) becomes (25). The redistribution of energy levels for the Hamiltonian (8) will give rise to a corresponding phenomenon on the semi-quantum Hamiltonian (37). Since (37) is defined on the sphere $S^2(N)$, at each point of $S^2(N)$ there is attached the eigenspace associated with an eigenvalue of (37), which would form a

complex line bundles if all eigenvalues are different from one another on the whole sphere $S^2(N)$. Then, we would obtain the direct sum of line bundles associated with respective eigenvalues. However, this is not the case for all $0 \leq t \leq 1$. In fact, if we take up a point $-N\boldsymbol{e}_3$, the south pole of $S^2(N)$, the Hamiltonian at $-N\boldsymbol{e}_3$ is expressed as

$$\overline{H}_{1:K}(t)|_{\boldsymbol{x}=-N\boldsymbol{e}_3} = ((1-t) + tf(N))S_z. \tag{38}$$

If $t = 1/(1 - f(-N))$ is in the interval $0 \leq t \leq 1$, which is the case for $f(z) = z$, then all the eigenvalues of the Hamiltonian vanish at the north pole for $t = 1/(1 - f(-N))$. This means that we have no way to single out a one-dimensional subspace at $z = -N\boldsymbol{e}_3$ for $t = 1/(1 - f(-N))$. Thus we fail to construct a line bundle over $S^2(N)$ for $t = 1/(1 - f(-N))$. However, for $t \neq 1/(1 - f(-N))$, all the eigenvalues are different to one another for $\overline{H}_{1:K}(t)|_{\boldsymbol{x}=-N\boldsymbol{e}_3}$, and we expect that line bundles can be formed over $S^2(N)$ for $t \neq 1/(1 - f(-N))$. However, the degeneracy at $t = 1/(1 - f(-N))$ implies that the bundle structure over $S^2(N)$ may changes when the control parameter t passes the value $t = 1/(1 - f(-N))$. In fact, while the bundle structure associated with $\overline{H}_{1:K}(0) = S_z$ is trivial, that associated with $\overline{H}_{1:K}(1) = H_K(\boldsymbol{x})$ is not so. The change in the bundle structure is viewed as the correspondent to the redistribution of energy levels. The Chern numbers of the bundles associated with $H_K(\boldsymbol{x})$ will be evaluated in section 8.

5. Chern class analysis of a two-state model

We leave for a moment the symmetry aspects of Hamiltonians and analyse Chern classes for bundles formed by eigenvectors of an arbitrary 2×2 Hermitian matrix defined as a Hamiltonian on the two-sphere. Let the 2×2 Hermitian matrix

$$\begin{pmatrix} a_{11} & a_{12} + ib_{12} \\ a_{12} - ib_{12} & a_{22} \end{pmatrix} \tag{39}$$

has its elements $a_{ij}(x, y, z)$ and $b_{12}(x, y, z)$ defined on the two-dimensional sphere, parameterized by x, y, z, subject to the condition $x^2 + y^2 + z^2 = \rho^2$ with $\rho > 0$. Such a matrix has no degeneracy points of its two eigenvalues in general. Hermitian matrices with degeneracy of eigenvalues have codimension 3 in the space of Hermitian matrices and consequently are not generically present in the chosen family depending on two parameters. The eigenspaces

of the matrix (39) form a bundle of rank two over the base space which is two-dimensional sphere. In the absence of degeneracy points of eigenvalues this vector bundle decomposes into the direct sum of two complex line bundles whose fibers are eigenspaces associated with respective eigenvalues. Each such complex line bundle, which we call an eigen-line bundle, is characterized by a Chern number. For topological reason, small continuous deformation of a Hamiltonian can not alter the Chern number which is a topological invariant for a complex line bundle. This is a key idea to iso-Chern diagrams to be treated in Sec. 6. We can calculate explicitly the Chern number by analyzing eigenvectors of (39).

5.1. Setting up a complex line bundle

As soon as we suppose that two eigenvalues λ_1, λ_2 are nowhere degenerate we can admit that $\lambda_1 > \lambda_2$ everywhere. Let us consider the eigenvector associated to the eigenvalue λ_1. We denote this eigenvector by

$$\begin{pmatrix} C_1 \\ C_2 \end{pmatrix}, \tag{40}$$

where C_1 and C_2 are complex numbers satisfying normalization condition $|C_1|^2 + |C_2|^2 = 1$. Two possible alternative equations for C_1, C_2 follow from the eigenvalue equation for the matrix (39). We have from the first and the second row of the eigenvalue equation the relations

$$(a_{11} - \lambda_1)C_1^{\rm up} + (a_{12} + ib_{12})C_2^{\rm up} = 0, \tag{41}$$

and

$$(a_{12} - ib_{12})C_1^{\rm down} + (a_{22} - \lambda_1)C_2^{\rm down} = 0, \tag{42}$$

respectively. Naturally, both relations give the same eigenvector up to phase factor but the definition domain for these two representations of the same eigenvector could be different. Each of them can be defined only in its proper domain in the base space S^2. This is why we have denoted them differently by $C_\alpha^{\rm up}$ and $C_\alpha^{\rm down}$.

The solution to (41) yields the normalized eigenvector of the form

$$\begin{pmatrix} C_1^{\rm up} \\ C_2^{\rm up} \end{pmatrix} = \frac{1}{\sqrt{(\lambda_1 - a_{11})^2 + a_{12}^2 + b_{12}^2}} \begin{pmatrix} a_{12} + ib_{12} \\ \lambda_1 - a_{11} \end{pmatrix}. \tag{43}$$

This vector is well defined everywhere on the sphere except at points where the norm of the vector goes through zero. The exceptional points occur if three conditions are satisfied:

$$a_{12} = 0, \quad b_{12} = 0, \quad a_{11} = \lambda_1. \tag{44}$$

The first two conditions $a_{12} = b_{12} = 0$ generically lead to a number of isolated solutions described as isolated points on the sphere. By substituting $a_{12} = 0$ and $b_{12} = 0$ into $a_{11} = \lambda_1$ we get

$$a_{11} = \frac{1}{2}\left(a_{11} + a_{22} + |a_{11} - a_{22}|\right). \tag{45}$$

One should be reminded that λ_1 is chosen as the highest eigenvalue,

$$\lambda_{1,2} = \frac{1}{2}\Big(a_{11} + a_{22} \pm \sqrt{(a_{11} - a_{22})^2 + 4a_{12}^2 + 4b_{12}^2}\Big), \tag{46}$$

so that the sign plus before the square root should be chosen for the λ_1 eigenvalue.

We rewrite Eq. (45) as

$$a_{11}(\theta, \phi) - a_{22}(\theta, \phi) = |a_{11}(\theta, \phi) - a_{22}(\theta, \phi)| \tag{47}$$

to specify two parameters θ, ϕ assigning the points on the base space.

It is clear that the equation (47) is automatically satisfied in the region where $a_{11} - a_{22} \geq 0$ and it is not satisfied in the region where $a_{11} - a_{22} < 0$. However, if $a_{11} - a_{22} = 0$ in addition to $a_{12} = b_{12} = 0$, the eigenvalues are degenerate. Put another way, exceptional points determined by $a_{12} = b_{12} = 0$ become degeneracy points. We exclude such a case in order to define the eigen-line bundle associated with the eigenvalue λ_1 larger than λ_2.

Now we define the domain $U_{\rm up}$ to be the subset of the sphere where the eigenvector (43) is well defined. This domain includes the whole sphere with exception of a number of isolated points which can be found as a solution of the following system of equations and an inequality:

$$a_{12} = 0; \tag{48a}$$
$$b_{12} = 0; \tag{48b}$$
$$a_{11} - a_{22} > 0. \tag{48c}$$

Now we can analyse the second equation (42) for the same eigenvector associated with the highest eigenvalue. The solution to (42) provides the normalized eigenvector of the form

$$\begin{pmatrix} C_1^{\text{down}} \\ C_2^{\text{down}} \end{pmatrix} = \frac{1}{\sqrt{(\lambda_1 - a_{22})^2 + a_{12}^2 + b_{12}^2}} \begin{pmatrix} \lambda_1 - a_{22} \\ a_{12} - ib_{12} \end{pmatrix}. \tag{49}$$

Like (44), the exceptional points occur if three conditions are satisfied:

$$a_{12} = 0, \quad b_{12} = 0, \quad a_{22} = \lambda_1. \tag{50}$$

The first two conditions $a_{12} = b_{12} = 0$ are exactly the same as in (44). They give on the sphere the same system of isolated points as those for "up" expression. But the third condition now rewrites as

$$a_{22} = \frac{1}{2}\left(a_{11} + a_{22} + |a_{11} - a_{22}|\right) \tag{51}$$

or equivalently as

$$a_{22} - a_{11} = |a_{11} - a_{22}|. \tag{52}$$

It is clear that condition (52) is satisfied if $a_{11} - a_{22} \leq 0$. For the same reason as that for "up" expression, we exclude the case of $a_{11} - a_{22} = 0$.

In a similar manner to the previous case we can define the domain U_{down} of the sphere where the eigenvector (49) is well defined. This region includes the whole sphere with exception of a number of isolated points which can be found as a solution of the following system of equations and an inequality:

$$a_{12} = 0; \tag{53a}$$
$$b_{12} = 0; \tag{53b}$$
$$a_{11} - a_{22} < 0. \tag{53c}$$

Schematic summary of generic situation can be given in Figure 2. Generically, $a_{11} - a_{22} = 0$ curve does not pass through the solutions of $a_{12} = b_{12} = 0$. This means that on Figure 2 the black points are not located on the boundary of the hatched region. Otherwise three equations $a_{11} - a_{22} = 0$ and $a_{12} = b_{12} = 0$ are simultaneously satisfied and two eigenvalues are degenerate in the corresponding point.

So far we have obtained two expressions, (43) and (49), of the eigenvector, which are defined on U_{up} and U_{down}, respectively. To get the coefficient of

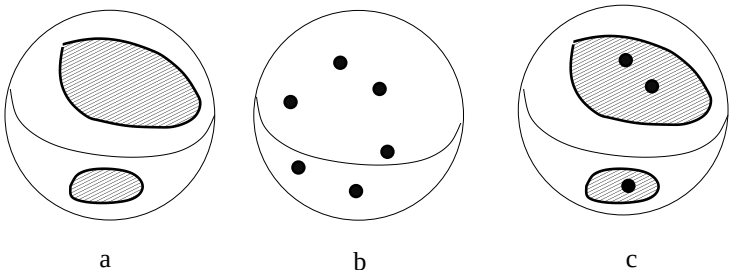

Figure 2: Schematic description of generic situations for regular domains. *a*) - Description on the sphere of regions with $a_{11} - a_{22} \geq 0$. Hatched region - positive values. Boundary black curve - zero value. *b*) - Solutions of $a_{12} = b_{12} = 0$. - isolated black points. *c*) - Description of the regular $U_{\rm up}$ domain. Only black points (which belong to hatched regions) should be excluded from the sphere to get the open set $U_{\rm up}$.

proportionality between (43) and (49) on the intersection $U_{\rm up} \cap U_{\rm down}$, we need to calculate the ratio of the first (or of the second) components of the same eigenvectors defined in different domains. This ratio can be rewritten by using the relation $(\lambda_1 - a_{11})(\lambda_1 - a_{22}) = a_{12}^2 + b_{12}^2$ and calculated as

$$\frac{a_{12} + ib_{12}}{\sqrt{(\lambda_1 - a_{11})^2 + a_{12}^2 + b_{12}^2}} \frac{\sqrt{(\lambda_1 - a_{22})^2 + a_{12}^2 + b_{12}^2}}{\lambda_1 - a_{22}} = \varepsilon \frac{a_{12} + ib_{12}}{\sqrt{a_{12}^2 + b_{12}^2}}, \qquad (54)$$

where $\varepsilon = \mathrm{sgn}(\lambda_1 - a_{22})$. Now we have obtained the transition rule

$$\begin{pmatrix} C_1^{\rm up} \\ C_2^{\rm up} \end{pmatrix} = \varepsilon \frac{a_{12} + ib_{12}}{\sqrt{a_{12}^2 + b_{12}^2}} \begin{pmatrix} C_1^{\rm down} \\ C_2^{\rm down} \end{pmatrix} \quad \text{on} \quad U_{\rm up} \cap U_{\rm down}, \qquad (55)$$

which determines the eigen-line bundle associated with the eigenvalue λ_1. The eigen-line bundle associated with the eigenvalue λ_2 can be constructed in the same manner.

5.2. The Chern class of the eigen-line bundle

For notational simplicity, we denote the transition rule (55) by

$$\boldsymbol{u}_+ = \Phi \boldsymbol{u}_-, \quad \Phi = \varepsilon \frac{a_{12} + ib_{12}}{\sqrt{a_{12}^2 + b_{12}^2}} \in U(1), \qquad (56)$$

where

$$\boldsymbol{u}_+ = \begin{pmatrix} C_1^{\rm up} \\ C_2^{\rm up} \end{pmatrix}, \quad \boldsymbol{u}_- = \begin{pmatrix} C_1^{\rm down} \\ C_2^{\rm down} \end{pmatrix}, \quad \varepsilon = \mathrm{sgn}(\lambda_1 - a_{22}). \qquad (57)$$

The local connection forms are defined on $U_{\rm up}$ and $U_{\rm down}$ to be

$$\omega_+ := \boldsymbol{u}_+^\dagger d\boldsymbol{u}_+, \quad \omega_- := \boldsymbol{u}_-^\dagger d\boldsymbol{u}_-, \tag{58}$$

respectively. Then, when differentiated, the transition equation provides the relation between ω_+ and ω_-,

$$\omega_+ = \Phi^{-1}d\Phi + \omega_- \quad \text{on} \quad U_{\rm up} \cap U_{\rm down}. \tag{59}$$

Let $\Phi = e^{i\varphi}$, where φ is determined within additive constants. Then, one obtains by differentiation $\Phi^{-1}d\Phi = id\varphi$, where $d\varphi$ is defined uniquely on $U_{\rm up} \cap U_{\rm down}$. Since $d(\Phi^{-1}d\Phi) = id(d\varphi) = 0$, the curvature form turns out to be defined globally to be

$$\Omega = \begin{cases} d\omega_- & \text{on} \quad U_{\rm down} \\ d\omega_+ & \text{on} \quad U_{\rm up} \end{cases}. \tag{60}$$

The first Chern number is defined as the integral over the whole sphere

$$c_1 = \frac{i}{2\pi}\int_{S^2} \Omega. \tag{61}$$

If we are given the Hermitian matrix (39) explicitly, we can calculate the above integral to get the Chern number.

5.3. Applying the Stokes theorem

In order to calculate the Chern number according to (61), we first find all "positive" and "negative" exceptional points, where the positive and negative exceptional points means the points determined as solutions to (48) and (53), respectively. Then, we split the whole sphere S^2 into regions S^2_+ and S^2_- in such a way that the local connection form ω_+ has no singularities in S^2_+ and the local connection form ω_- has no singularities in S^2_-. Put another way, the region S^2_+ includes only "negative" exceptional points and the S^2_- only "positive" exceptional points. We can always do that but each region (S^2_+ or S^2_-) may consist of several connected components. The division of the whole sphere S^2 into S^2_+ and S^2_- can be done by a set of closed curves $C_1, C_2, \ldots C_k$. All curves C_i, $i = 1, \ldots, k$ belong to $U_{\rm up} \cap U_{\rm down}$. Each closed curve C_i is always a boundary between the S^2_+ and S^2_- regions. Each curve C_i should be properly oriented. We choose the orientation of C_i in such a way that the boundary of S^2_+ is oriented counterclockwise with respect to the outgoing

normal to the sphere. This automatically leads to reversed orientation of the boundary for the S_2^- region. By the application of the Stokes theorem with this convention, the surface integral over the sphere in (61) can be written in terms of contour integrals as

$$\int_{S^2} \Omega = \int_{S^2_+} d\omega_+ + \int_{S^2_-} d\omega_- = \oint_{C_1+\cdots+C_k} \omega_+ + \oint_{-(C_1+\cdots+C_k)} \omega_- \ . \quad (62)$$

Using the relation (59) between local connection forms ω_+ and ω_-, we rewrite the expression (62) for the integral over the sphere in terms of winding numbers for corresponding contours

$$\begin{aligned} \int_{S^2} \Omega &= \oint_{C_1+\cdots+C_k} \omega_+ - \oint_{(C_1+\cdots+C_k)} \left(\omega_+ - \Phi^{-1} d\Phi\right) \\ &= \sum_{s=1}^{k} \oint_{C_s} \Phi^{-1} d\Phi \\ &= 2\pi i \sum_{s=1}^{k} W[C_s], \end{aligned} \quad (63)$$

where $W[C_s]$ denotes the winding number of the mapping $\Phi : C_s \to U(1)$. Finally, Eqs. (61) and (63) are put together to provide the first Chern number in terms of a sum of winding numbers for appropriately chosen contours

$$c_1 = -\sum_{s=1}^{k} W[C_s]. \quad (64)$$

In the formula (64), the sum of winding numbers are taken for all contours separating the S^2_+ and S^2_- regions with appropriate signs. It can be easily seen that this sum of winding numbers can be transformed into a sum over circles surrounding each one exceptional point with a small neighborhood forming S^2_- region.

Figure 3 gives an example of a transformation of contours. Figure 3, left shows three positive exceptional points surrounded by two circular paths. A continuous deformation of contours leads to a new configuration (represented in Figure 3, right) which shows clearly that the winding numbers can be calculated equally either along two circular paths (Figure 3, left) or along

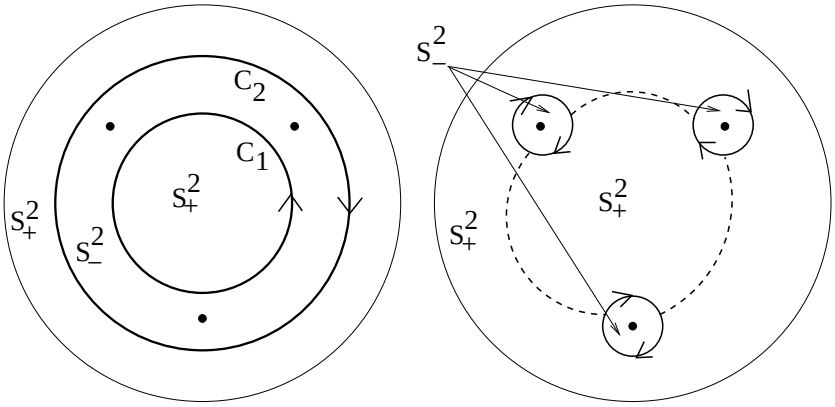

Figure 3: Example of the splitting of the sphere into S^2_+ and S^2_- regions. A part of the sphere is represented which has three "positive" zeros assigned to $U_{\rm up}$ as exceptional points. These zeros are shown by three black dots. They belong to S^2_- region. Left figure gives an example of the choice of two contours, C_1 and C_2, separating S^2_+ and S^2_- regions. The sum of integrals along C_1 and C_2 contours is equivalent to the sum of integrals along three contours surrounding "positive" zeros, as shown in the right figure. Paths shown by dashed lines in the right figure give zero contribution to the sum of contour integrals.

three new paths (Figure 3, right). Each new path surrounds only one exceptional point and its contribution to the Chern number can be evaluated locally using information about transition factor between charts in a small neighborhood of each exceptional point.

From the practical point of view two slightly different approaches are possible to apply in order to calculate Chern numbers for eigen-line bundles of any generic 2×2 Hermitian matrix.

i) One is the application of (64). For each contour separating S^2_+ and S^2_- we find the winding number for the map from this contour with a parameter t to a closed curve $(a_{12}(t), b_{12}(t))$ in $\mathbb{R}^2$ or $a_{12}(t) + ib_{12}(t)$ in $\mathbb{C}$. The Chern number is expressed as an appropriate algebraic sum of winding numbers for all contours. It is useful to choose contours lying on the sphere at a constant value of one of coordinates, say z. In this procedure, the stereographic projection is effectively used. This allows us to check easily the winding numbers by looking at the z dependence of the winding number. The winding number is not defined if the contour goes through an exceptional point. Otherwise the winding number is an integer and remains invariant under continuous deformation of the contour if all exceptional points remain avoided under such

deformation. Computer algebra tools assist us to plot easily corresponding curve on the complex plane and to count the number of times the curve goes around the zero even for rather complicated effective Hamiltonians.

ii) Alternatively it is possible to calculate the Chern number by summing up the local contribution from positive (or negative) exceptional points. For each (say, positive) exceptional point the winding number should be evaluated along an infinitesimal circular contour surrounding this exceptional point. Using Taylor expansion of off-diagonal matrix element near exceptional point allows us to calculate analytically the contribution of this point to the Chern number. In the simplest case of a generic exceptional point the linear approximation is sufficient and this approach in this case can be named the linearization method.

Both these approaches will be illustrated below during the analysis of model effective Hamiltonians invariant with respect to a symmetry group (see secs. 8 and 9).

5.4. The linearization method

In this subsection, we explain how the linearization method works. For notational simplicity we denote the off-diagonal components of the Hamiltonian by $X + iY$. Then the transition function given in (56) is expressed as $\Phi = \varepsilon\,(X + iY)/\sqrt{X^2 + Y^2}$. A straightforward calculation shows that

$$\Phi^{-1} d\Phi = i \frac{X dY - Y dX}{X^2 + Y^2}. \tag{65}$$

We can relate this equation with the formula for the index of a vector field. We take (x, y) as local coordinates of the north hemisphere of S^2, for example. There are several choices of hemispheres, of course. Then we can view $\boldsymbol{W} = (X, Y)$ as a vector field defined locally on the domain $\{(x, y);\, x^2 + y^2 < \rho^2\}$ of $\mathbb{R}^2$ and the exceptional points in the north hemisphere as singular points of this vector fields, *i.e.*, as zeros of $\boldsymbol{W} = (X, Y)$. Suppose that we have a small circle $\Gamma(\varepsilon)$ of radius $\varepsilon > 0$ centered at an exceptional point and that the circle encloses no other exceptional points. We can normalize the vector field $\boldsymbol{W}$ to be $\boldsymbol{w}$ in a vicinity of but outside of the present exceptional point and denote by $\boldsymbol{v}$ the vector field $\boldsymbol{w}$ rotated by $\pi/2$ counterclockwise;

$$\boldsymbol{w} = \frac{1}{\sqrt{X^2 + Y^2}} \begin{pmatrix} X \\ Y \end{pmatrix}, \quad \boldsymbol{v} = \frac{1}{\sqrt{X^2 + Y^2}} \begin{pmatrix} -Y \\ X \end{pmatrix}. \tag{66}$$

Then, the one-form $\Phi^{-1}d\Phi$ is rewritten as

$$\Phi^{-1}d\Phi = i\boldsymbol{v}\cdot d\boldsymbol{w}, \tag{67}$$

so that we obtain

$$\frac{1}{2\pi i}\int_{\Gamma(\varepsilon)}\Phi^{-1}d\Phi = \frac{1}{2\pi}\int_{\Gamma(\varepsilon)}\boldsymbol{v}\cdot d\boldsymbol{w}. \tag{68}$$

If we make ε tend to zero, the right-hand side of the above equation gives the definition of the index of the vector field $\boldsymbol{W}$ at the singularity in question,

$$\mathrm{ind}(\boldsymbol{W}) = \lim_{\varepsilon\to 0}\frac{1}{2\pi}\int_{\Gamma(\varepsilon)}\boldsymbol{v}\cdot d\boldsymbol{w} = \lim_{\varepsilon\to 0}\frac{1}{2\pi i}\int_{\Gamma(\varepsilon)}\Phi^{-1}d\Phi. \tag{69}$$

In the process of $\varepsilon\to 0$, we see that the linear approximation of $\boldsymbol{W}$ is sufficient for calculating the index of $\boldsymbol{W}$. Taking the local coordinates (x,y), we get the linear approximation of $\boldsymbol{W}$ in the vicinity of the exceptional point in question,

$$\begin{pmatrix}\frac{\partial X}{\partial x} & \frac{\partial X}{\partial y}\\ \frac{\partial Y}{\partial x} & \frac{\partial Y}{\partial y}\end{pmatrix}\begin{pmatrix}\xi_1\\ \xi_2\end{pmatrix}, \tag{70}$$

where (ξ_1,ξ_2) are the Cartesian coordinates whose origin is located at the exceptional points in question and where the coefficient matrix is evaluated at the exceptional point. For the index of a linear vector field $\boldsymbol{W}=A\boldsymbol{\xi}$, we have the formula

$$\mathrm{ind}(A\boldsymbol{\xi}) = \begin{cases} 1 & \text{if} \quad \det A>0,\\ -1 & \text{if} \quad \det A<0,\end{cases} \tag{71}$$

which is easily proved by calculating the defining contour integral. It is to be noted here that this formula is applicable only if $\det A\neq 0$. Thus it turns out that if we evaluate the determinant of the coefficient matrix in (70) we find the index or the winding number at the exceptional point in question. It is to be noted further that the orientation of the circle surrounding the exceptional point and the orientation of the local coordinate system adopted should be taken into account, since these orientations affect the sign of the determinant. For example, if we take the south hemisphere, the local coordinate system (x,y) is negatively oriented against the sphere. The positive oriented local coordinate system should be (y,x), which means that the coefficient matrix to be considered is

$$\begin{pmatrix}\frac{\partial X}{\partial y} & \frac{\partial X}{\partial x}\\ \frac{\partial Y}{\partial y} & \frac{\partial Y}{\partial x}\end{pmatrix}. \tag{72}$$

Further, as in the case of the small circles shown in Fig. 3, if the small circle concerned is clockwise oriented, the index in question should be reversed from those given in (71).

In closing this section, we have to make a remark on the locally-defined vector field $\boldsymbol{W} = (X, Y)$. For the purpose of evaluating a contour integral along a small circle, we took $\boldsymbol{W}$ as a vector field locally-defined on a hemisphere. However, the $\boldsymbol{W}$ cannot be extended so as to be a globally defined vector field on the two-sphere. In order that $\boldsymbol{W}$ be defined globally, it should be subject to a transformation rule according to the coordinate change in the intersection of local charts, say, in the intersection of the hemisphere with $z > 0$ and that with $x > 0$, where z and x are considered as height functions for the respective hemisphere, and the local coordinates adopted are (x, y) and (y, z), respectively. However, the $\boldsymbol{W}$ is not subject to such a transformation rule. Further, if the $\boldsymbol{W}$ were defined on the two-sphere, the sum of the indices would be two, the Euler number of the two-sphere. However, the Chern numbers we will obtain in our examples are not restricted to two. This implies also that the $\boldsymbol{W}$ is not globally defined on the two-sphere.

6. Iso-Chern diagrams

6.1. Iso-Chern domains

So far we have studied generic effective 2×2 Hermitian matrix Hamiltonians defined on S^2 and possessing nondegenerate eigenvalues. Now we turn to the discussion of families of Hamiltonians which depend as well on some control parameters $(d_1, d_2, \ldots)$. This means that degeneration of eigenvalues may occur for some control parameter values and we need to start our analysis by finding the stratification of the control parameter space with the condition of eigenvalue degeneration. The whole space of parameters should be split into the union of a subset of "regular" values of parameters (corresponding to the absence of degenerate eigenvalues) and a subset formed by degeneracy points, *i.e.*, "singular" values of parameters (corresponding to the presence of degenerate eigenvalues). The subset of degeneracy points can include in general an isolated points, lines, surfaces, ... As a whole, the set of regular points in the control parameter space is split generically into connected domains in such a way that any two points within one connected domain can be connected by a parameter dependent continuous path going only through "regular" points in the parameter space. Any such domain can be named an "iso-Chern" domain because Chern numbers for two eigen-line

bundles should be the same for all parameter values belonging to the same domain.

For simplicity, we treat traceless Hermitian matrices only in what follows. To find the boundaries of iso-Chern domains, we need to solve the equation:

$$\det \begin{pmatrix} a_{11} & a_{12}+ib_{12} \\ a_{12}-ib_{12} & -a_{11} \end{pmatrix} = 0, \tag{73}$$

which is equivalent (assuming that a_{11}, a_{12}, and b_{12} are real) to the system of three equations

$$a_{11} = 0; \quad a_{12} = 0; \quad b_{12} = 0. \tag{74}$$

In order to make explicit the dependence of matrix elements on control parameters $d_1, \ldots, d_k$ and on parameters characterizing the point of the base space S^2, given by $\boldsymbol{x}^2 = x^2+y^2+z^2 = \rho^2$ equation, we can rewrite the system (74) defining the degeneracy points as

$$a_{11}(\boldsymbol{x}; d_j) = 0, \quad a_{12}(\boldsymbol{x}; d_j) = 0, \quad b_{12}(\boldsymbol{x}; d_j) = 0, \quad \boldsymbol{x}^2 = \rho^2, \quad j = 1, \cdots, k.$$

These equations mean that degeneracy points are special case of "exceptional" points. Namely, an exceptional point determined by $a_{12}(\boldsymbol{x}; d_j) = b_{12}(\boldsymbol{x}; d_j) = 0$ become a degeneracy point if the diagonal matrix element $a_{11}(\boldsymbol{x}; d_j)$ takes zero value at the exceptional point. As soon as the codimension of degeneracy points of generic Hermitian complex matrix is three and the base space has dimension 2, the codimension of degeneracy points in the control parameter space is one. Consequently, the degeneracy points split the control parameter space into connected domains. Within each connected domain the eigenvalues remain non-degenerate and the corresponding eigen-line bundles are topologically invariant, *i.e.*, have the same Chern numbers. This explains why the diagram representing the splitting of the control parameter space into connected domains by subsets associated with Hamiltonians possessing degenerate eigenvalues is named an iso-Chern diagram. We note here that we speak of degeneracy points from two different points of view; one is assigned to the control parameter space, and the other to the sphere. The exceptional points are also spoken about in two ways; one is assigned to the control parameter space and the other to the sphere.

Though the boundary of an iso-Chern domain in the control parameter space consist of degeneracy points, the number of corresponding degeneracy points on S^2 may vary piecewise-constantly on the boundary. In an analogous

manner, the number of exceptional points in the iso-Chern domain may vary from place to place. In spite of this fact, the Chern number which is evaluated by taking into account the corresponding exceptional points on the sphere should be the same throughout the iso-Chern domain in question. We will show this fact with an concrete example in section 9. No matter how many are the exceptional points concerned, the calculation of Chern numbers for one chosen point of control parameter values is sufficient for each connected domains of the iso-Chern diagram.

6.2. Elementary transformations of the Hamiltonian

Suppose that we have distinct eigenvalues $\lambda_1 > \lambda_2$ and the associated normalized eigenvectors $\boldsymbol{u}_1$ and $\boldsymbol{u}_2$, respectively;

$$H\boldsymbol{u}_1 = \lambda_1\boldsymbol{u}_1, \quad H\boldsymbol{u}_2 = \lambda_2\boldsymbol{u}_2, \tag{75}$$

where the eigenvectors are defined on a suitable domain of the sphere. We denote the associated eigen-line bundles by L_1 and L_2, where L_1 and L_2 are associated with the larger eigenvalue and with the smaller one, respectively. If we associate the complex plane $\mathbb{C}^2$ at each point of the sphere, we have a trivial bundle over the sphere, which decomposes into the direct sum $L_1 \oplus L_2$. The sum of respective Chern numbers is zero, accordingly.

We now discuss a simple scaling of the Hamiltonian. If we multiply the Hamiltonian by a non-zero real number μ, the Hamiltonian μH has eigenvalues $\mu\lambda_1$ and $\mu\lambda_2$, but the associated normalized eigenvectors remains to be $\boldsymbol{u}_1$ and $\boldsymbol{u}_2$. If $\mu > 0$, the ordering of the eigenvalues is invariant, $\mu\lambda_1 > \mu\lambda_2$, and the associated normalized eigenvectors are $\boldsymbol{u}_1$ and $\boldsymbol{u}_2$, respectively. This implies that the Chern number which is evaluated through the local connection forms $\omega_\pm = \boldsymbol{u}_\pm^\dagger d\boldsymbol{u}_\pm$ remains to be the same value, where $\boldsymbol{u}_\pm$ is a short form of $\boldsymbol{u}_{1\pm}$ or $\boldsymbol{u}_{2\pm}$ (see (58)). However, if $\mu < 0$, the ordering of the eigenvalues is reversed; $\mu\lambda_1 < \mu\lambda_2$. Then we may exchange the normalized eigenvectors and associate $\boldsymbol{u}_1$ to $\mu\lambda_2$ and $\boldsymbol{u}_2$ to $\mu\lambda_1$. This implies that the roles of the eigen-line bundles L_1 and L_2 are exchanged and accordingly the Chern numbers are exchanged. This fact can be interpreted as follows: If μ varies continuously from the positive half of $\mathbb{R}$ to the negative half, it must pass the origin, at which the direct sum $L_1 \oplus L_2$ breaks down. When μ gets into the negative half of $\mathbb{R}$, the direct sum is reconstructed, but the roles of L_1 and L_2 are exchanged together with the Chern numbers.

If the matrix elements depend homogeneous-linearly on the parameters d_j, the above observation can be described in terms of iso-Chern diagrams as

follows: Trivial scaling of all terms of the Hamiltonian by the same positive factor naturally transforms regular point of the control parameter space into regular point. All such regular points should belong to the same "iso-Chern" domain of the control parameter space. At the same time the simultaneous scaling of all terms of the Hamiltonian by a negative factor transforms regular point of parameter space into another regular point of the parameter space, but corresponding points are not obliged to belong to the same connected (iso-Chern) domain of the parameter space. This is due to the fact that the zero value of the scaling factor can result in a singular parameter value.

Each connected regular domain of iso-Chern diagram is characterized by Chern numbers associated with eigen-line bundles for positive and negative eigenvalues. Trivial scaling by (-1) of the Hamiltonian cannot naturally change the set of two Chern numbers for two eigen-line bundles for any regular domain, but if these two Chern numbers are not zero and different by sign, the scaling by (-1) of the Hamiltonian will interchange the Chern numbers for positive and negative eigen-line bundles. Thus this scaling transforms Hamiltonian from one iso-Chern domain to another one.

As an extension of trivial scaling, we are interested in the complex conjugation of the Hamiltonian. By complex conjugation, Eq. (75) are transformed into

$$\overline{H}\overline{\boldsymbol{u}}_1 = \lambda_1\overline{\boldsymbol{u}}_1, \quad \overline{H}\overline{\boldsymbol{u}}_2 = \lambda_2\overline{\boldsymbol{u}}_2. \tag{76}$$

If H is complex conjugated, the eigenvalues are the same, and the ordering of the eigenvalues is unchanged; $\lambda_1 > \lambda_2$. Then, the eigen-line bundle associated with λ_1 is endowed with the local connection form $\overline{\omega}_1 = \overline{\boldsymbol{u}}_1^\dagger d\overline{\boldsymbol{u}}_1$, where $\omega_1 = \boldsymbol{u}_1^\dagger d\boldsymbol{u}_1$. Since the connection form takes its value in the Lie algebra $u(1)$, we see that $\overline{\omega}_1 = -\omega_1$, so that one has the curvature form $\overline{\Omega}_1 = -\Omega_1$ for L_1. This implies that the Chern number changes in the sign under the transformation $H \mapsto \overline{H}$.

If we multiply Eq. (76) by -1, and if we use the fact that $-\lambda_1 = \lambda_2$, which is the case for traceless Hermitian 2×2 matrices, then we obtain

$$-\overline{H}\overline{\boldsymbol{u}}_1 = \lambda_2\overline{\boldsymbol{u}}_1, \quad -\overline{H}\overline{\boldsymbol{u}}_2 = \lambda_1\overline{\boldsymbol{u}}_2. \tag{77}$$

The local connection form for L_1 is then given by $\overline{\omega}_2 = \overline{\boldsymbol{u}}_2^\dagger d\overline{\boldsymbol{u}}_2$, which is equal to $-\omega_2$. Since the Chern number evaluated by ω_2 is -1 times that evaluated by ω_1, it turns out that the Chern number in question is kept unchanged under the transformation $H \mapsto -\overline{H}$.

The change in Chern numbers under the transformations $H \mapsto \overline{H}$ and $H \mapsto -\overline{H}$ will make a pattern in the distribution of Chern numbers on the iso-Chern diagram. An interesting question related with iso-Chern diagrams is the description of typical boundaries and associated modifications of Chern numbers especially in the presence of symmetry. We will return to this question later in this article when studying concrete examples.

7. Semi-quantum Hamiltonians invariant by symmetry

Let us return to semi-quantum models and view classical and quantum variables as spanning typically some representation of the dynamic symmetry group. In addition, any continuous or finite subgroup of this dynamic symmetry group may be considered as an invariance group of the problem. Very natural examples of dynamic symmetry groups appearing in molecular problems are given by unitary groups accompanied with invariance groups which are continuous or finite subgroups of an associated orthogonal group. As finite symmetry groups, we take point symmetry groups which are used as symmetry groups for equilibrium configuration of molecules. We extend as well geometrical transformations by adding time reversal which is typically assumed to be a symmetry operation in the case of isolated molecules in the absence of magnetic field. According to Eugene Wigner [46], a symmetry operation S for a Hamiltonian in quantum mechanics is represented either by a unitary operator, $S = U$, or an anti-unitary operator, $S = UK$, where U is unitary, and K denotes complex conjugation. We note here that the time reversal is anti-unitary.

7.1. Symmetry groups and their action on classical and quantum variables

Let us treat the simplest model problem constructed from two angular momenta $\boldsymbol{N}$ and $\boldsymbol{S}$ from the viewpoint of possible invariance groups, where $\boldsymbol{N}$ and $\boldsymbol{S}$ are looked upon as classical and quantum variables, respectively. In the context of the semi-quantum models, rotation-vibration interaction will be spoken about in association of $\boldsymbol{N}$ and $\boldsymbol{S}$ with rotational and vibrational variables, respectively. As is already shown, the classical variables are viewed as those on the sphere $S^2(\rho)$ of radius $\rho > 0$. By appropriate scaling transformation we can put $\rho = 1$. This is the case if the elements of the Hamiltonian defined on the sphere take the form of polynomials of classical variables, and if the coefficients undergo due changes. In this section, $\boldsymbol{N}$ or $\boldsymbol{x}$ is used without distinction for the description of the classical variables.

Let G be a group which is supposed to be an invariance group and to act both on the classical and quantum variables. Our task is to specify how it acts on them as an invariance group. The G action on classical variables is viewed as a subgroup of $O(3)$, either compact or finite with its natural action in $\mathbb{R}^3$ spanned by $\boldsymbol{x}$ (or $\boldsymbol{N}$) variables. From the viewpoint of a representation of G in $\mathbb{R}^3$, the representation, which we denote by $\Gamma_{\rm rot}$, can be reducible or irreducible, depending on the group G. We denote the action of G on classical variables by $\boldsymbol{x} \mapsto g\boldsymbol{x}$ with $\boldsymbol{x} \in S^2(\rho)$ and $g \in G$, if $\Gamma_{\rm rot}$ is specified. In the case of $G = SU(2)$, we have the action of $SO(3)$, as is shown in (21). Since we take a position of semi-quantum models, the inverse notation such as A^{-1} in (21) is needless to use. Further, we note also that a choice of basis vectors is in our hands when realizing $\Gamma_{\rm rot}$ in $\mathbb{R}^3$. In contrast with this, the action of G on the quantum variables is treated through a unitary representation, $\Gamma_{\rm vib} = (V, D)$, of G, where V is a representation space and D is a map of G to $U(V)$, the space of unitary matrices acting on V. For the sake of simplicity, we restrict V to $\dim V = 2$ with an application to two-level models in mind, and the representation is either reducible or irreducible. Put in detail, depending on the choice of physical models, the representation is isomorphic either to the direct sum of two one-dimensional irreducible representations, to a pair of complex conjugate representations, or to one two-dimensional irreducible representation.

Then, G acts also on Hermitian matrices by adjoint action. The procedure for this is performed through the Schwinger representation of angular momenta in terms of the two-dimensional isotropic harmonic oscillator. Let a_α and $a_\alpha^\dagger$ be annihilation and creation operators, which are subject to the commutation relations,

$$[a_\alpha, a_\beta] = 0, \quad [a_\alpha^\dagger, a_\beta^\dagger] = 0, \quad [a_\alpha, a_\beta^\dagger] = \delta_{\alpha\beta}, \quad \alpha, \beta = 1, 2. \tag{78}$$

The operators $a_\alpha^\dagger a_\beta$, $\alpha, \beta = 1, 2$, form a basis of the space of quadratic Hermitian operators,

$$\sum_{\alpha,\beta} c_{\alpha\beta} a_\alpha^\dagger a_\beta, \quad C := (c_{\alpha\beta}) : \ 2 \times 2 \text{ Hermitian matrices}. \tag{79}$$

If C's are $S_k, k = 1, 2, 3$, the associated operators are referred to as vibrational angular momenta, where the S_k are the basis of the representation space for $su(2)$ with $S = \frac{1}{2}$.

Let $U(g)$ and $D(g)$ denote a unitary operator and a matrix expression, respectively. Then, the transformations of the operators a_α and $a_\alpha^\dagger$ are put in the form

$$U(g)a_\alpha^\dagger U(g)^{-1} = \sum_\beta D(g)_{\beta\alpha} a_\beta^\dagger, \quad U(g)a_\alpha U(g)^{-1} = \sum_\beta \overline{D(g)}_{\beta\alpha} a_\beta, \tag{80}$$

where the overline denotes the complex conjugate. Accordingly, the quadratic operator is subject to the transformation

$$U(g)\sum_{\alpha,\beta} c_{\alpha\beta} a_\alpha^\dagger a_\beta U(g)^{-1} = \sum_{\alpha,\beta} (D(g)CD(g)^{-1})_{\alpha\beta} a_\alpha^\dagger a_\beta. \tag{81}$$

This shows that the G acts on Hermitian matrices by adjoint action. Put another way, the quantum variables S_k, if viewed as traceless Hermitian matrices, are subject to adjoint transformations.

So far we have specified the action of G on the classical and quantum variables. We now describe the time reversal. In view of the origin of the classical variables $\boldsymbol{x}$ (or $\boldsymbol{N}$) as angular momenta and of the fact that the direction of a momentum is reversed by time reversal, we think of time reversal as the transformation

$$\boldsymbol{x} \mapsto -\boldsymbol{x}, \quad (S_1, S_2, S_3) \mapsto (S_1, -S_2, S_3). \tag{82}$$

Here we note that S_k serve only as basis matrices for 2×2 traceless Hermitian matrices and bear no physical meaning such as spin angular momenta. Indices $1, 2, 3$ are used instead of more standard x, y, z indices, since we prefer in the following applications to associate Cartesian indices (x, y, z) with symmetry elements acting on rotational variables according to conventions used in physical literature on point symmetry group applications.

Now we can describe the condition for Hamiltonians to be of rotational-vibrational invariance. Let $H(\boldsymbol{x})$ denote a 2×2 Hermitian matrix depending on $\boldsymbol{x} \in S^2(\rho)$, which is thought of as a Hamiltonian for a two-level model. Then, the $H(\boldsymbol{x})$ is invariant under the G action, if and only if

$$D(g)^{-1} H(g\boldsymbol{x}) D(g) = H(\boldsymbol{x}), \quad g \in G. \tag{83}$$

We here expand $H(\boldsymbol{x})$ in the form $H(\boldsymbol{x}) = \sum_k f_k(\boldsymbol{x}) S_k$. Note here that higher degrees of operators S_k do not appear because of two-level approximation.

Like (16), the adjoint action of G is expressed as

$$D(g)^{-1}S_kD(g) = \sum_j a_{kj}(g)S_j, \tag{84}$$

where $(a_{kj}(g))$ is the 3×3 matrix representation of G as a subgroup of $SO(3)$. Hence, the condition (83) gives rise to

$$f_k(g\boldsymbol{x}) = \sum_j a_{kj}(g)f_j(\boldsymbol{x}), \tag{85}$$

which means that the vector-valued function $f_k(\boldsymbol{x})$ is equivariant with respect to G. Note that Eq. (30) is a special one of the above equation. The matrix representation $(a_{kj}(g))$ is determined through the decomposition of the tensor product representation $\Gamma_{\rm vib}\otimes\Gamma_{\rm vib}$ into the sum of irreducible representations, if the representation $\Gamma_{\rm vib}$ is real, as is expected from (84). We will meet with such a case for $G = D_3$ in Sec. 7.3.

If we take the time reversal symmetry (82) into account, we obtain, for a Hamiltonian admitting time reversal symmetry, the conditions

$$f_1(-\boldsymbol{x}) = f_1(\boldsymbol{x}), \quad f_2(-\boldsymbol{x}) = -f_2(\boldsymbol{x}), \quad f_3(-\boldsymbol{x}) = f_3(\boldsymbol{x}). \tag{86}$$

Now our task is to find functions subject to (85). For this purpose, the invariant-tensor approach could give a guide. From three elementary rotational variables, we can construct tensors of each needed symmetry type in terms of polynomial series by using the integrity basis approach widely used in the theory of invariants [27]. The degree of rotational tensors can be arbitrary. All tensors of even degree are invariant with respect to time reversal, whereas tensors of odd degree change the sign under time reversal. Let us denote rotational tensors of degree Ω by $R^{\Omega(n,\Gamma)}$, where n is the multiplicity index counting tensors of the same representation Γ and the same degree Ω, and by $V^{\Gamma,\alpha}$ vibrational tensors belonging to the representation Γ, where the index $\alpha = \pm$ is added to specify symmetry properties with respect to time reversal. To get all rotation-vibration invariant Hamiltonian, we need to couple vibrational angular momenta with rotational tensors into totally symmetric (of Γ_0 type) rotation-vibration tensors

$$\left(V^{\Gamma,\alpha}\otimes R^{\Omega(n,\Gamma)}\right)^{\Gamma_0}. \tag{87}$$

For real representations, the construction of invariants is possible only if rotation and vibration tensors transform according to the same irreducible

representation (see (85)). In order to respect the time reversal symmetry, the vibrational tensors of $\alpha = +$ type should be coupled with rotational tensors of even degree, whereas vibrational tensors of $\alpha = -$ type should be coupled with rotational tensors of odd degree.

In what follows, we choose G to be $SO(2)$ as a continuous subgroup and D_3 as a finite subgroup and determine invariant Hamiltonians in the respective cases.

7.2. $SO(2)$ symmetry models

Let us start with an abelien group $SO(2)$ as an invariance group of the problem. All irreps of $SO(2)$ are one-dimensional. We denote them by (m) with m being any integer. In such a case, the rotational variables N_k transform according to the representation $(0)\oplus(-1)\oplus(1)$. We assume that N_z belongs to (0) and $N_x \pm iN_y$ to (± 1) representations (see (14)). Then, $SO(2)$ acts on $\mathbb{R}^3$ as a rotation about the z-axis. Under this action, all invariants can be put in the form $P(z, x^2+y^2)$ and all covariants of type $(\pm m)$ in the form $P(z, x^2+y^2)(x \pm iy)^m$. (Note that $\boldsymbol{x}$ is used instead of $\boldsymbol{N}$ for notation simplicity.) If we restrict our analysis to the sphere $x^2+y^2+z^2 = \rho^2$, all invariants can be written as $P(z)$ polynomials of one variable. General covariants of type $(\pm m)$ have the form $P(z)(x \pm iy)^m$ (see (34)).

Since we are interested in the two-level quantum state model, we need to specify the symmetry of operators S_k for the two-level model. We can specify it phenomenologically in several different ways. Put another way, our task here is to choose a representation $\Gamma_{\text{vib}} = (V, D)$ of $SO(2)$. Though a physically reasonable choice is a representation $(m) \oplus (-m)$, we here choose a representation $(m) \oplus (n)$ for the sake of computational generality. Then our unitary matrix acting on V is written as

$$D(g_t) = \mathrm{diag}(e^{imt}, e^{int}), \quad g_t \in SO(2), \tag{88}$$

where m and n are integers. We now put together (83) and (88) to obtain the conditions for entries $h_{k\ell}(\boldsymbol{x})$ of $H(\boldsymbol{x})$,

$$h_{11}(g_t\boldsymbol{x}) = h_{11}(\boldsymbol{x}), \quad h_{22}(g_t\boldsymbol{x}) = h_{22}(\boldsymbol{x}), \tag{89a}$$

$$h_{12}(g_t\boldsymbol{x}) = e^{i(n-m)t}h_{12}(\boldsymbol{x}), \quad h_{21}(g_t\boldsymbol{x}) = e^{-i(n-m)t}h_{21}(\boldsymbol{x}). \tag{89b}$$

It then turns out that without the restriction of $\boldsymbol{x}$ to $S^2(\rho)$, a general solution matrix has the form

$$\begin{pmatrix} f_{11}(z, x^2+y^2) & f_{12}(z, x^2+y^2)(x+iy)^{n-m} \\ f_{12}(z, x^2+y^2)(x-iy)^{n-m} & -f_{11}(z, x^2+y^2) \end{pmatrix} + f_0(z, x^2+y^2)\mathbf{I}. \tag{90}$$

The term proportional to the identity matrix is not important at all. Consequently only rotational tensors of (0) and $\pm(m-n)$ types appear in the Hamiltonian. If we set $n=-m$ and exclude the term proportional to the identity matrix, and if we restrict solutions of (89) to polynomials and pose the condition of $\boldsymbol{x}\in S^2(\rho)$, we obtain

$$\begin{pmatrix} f_{11}(\cos\theta) & f_{12}(\cos\theta)\ \sin^K\theta\ \exp(iK\phi) \\ f_{12}(\cos\theta)\ \sin^K\theta\ \exp(-iK\phi) & -f_{11}(\cos\theta) \end{pmatrix} \tag{91}$$

with $K=-2m$ and f_{ij} being any real polynomial.

The exponent $K=-2m$ seems to be restricted to even numbers. However, if we take another choice of representation for $SO(2)$, we can show that K is allowed to be odd. We regard $SO(2)$ as a subgroup $U(1)$ of $SU(2)$, and in place of (88), we choose to takes

$$D(g_t)=\mathrm{diag}(e^{\frac{1}{2}imt},e^{-\frac{1}{2}imt}), \tag{92}$$

which is a double cover of (88) with $n=-m$. Eqs. (83) and (92) are put together to provide (91) with $K=-m$.

To compare the present result with (36a), we have to note that if $D(g_t)$ is chosen as

$$D(g_t)=\mathrm{diag}(e^{-\frac{1}{2}imt},e^{\frac{1}{2}imt}) \tag{93}$$

in place of (92), we can obtain (36a) with a bit different notation of functions.

If $m=n=0$, we have two quantum states which are both invariant, that is, belong both to (0) representation. In such a case, all matrix elements should be invariant as well

$$\begin{pmatrix} f_{11}(z,x^2+y^2) & f_{12}(z,x^2+y^2) \\ f_{21}(z,x^2+y^2) & -f_{11}(z,x^2+y^2) \end{pmatrix} + f_0(z,x^2+y^2)\mathbf{I}, \tag{94}$$

where f_{12} and f_{21} are complex conjugate, of course. In the absence of time reversal symmetry, the non-diagonal elements are supposed to be generically complex. If restricted on a two-sphere, this matrix reads

$$\begin{pmatrix} f_{11}(z) & f_{12}(z) \\ f_{21}(z) & -f_{11}(z) \end{pmatrix} + f_0(z)\mathbf{I}. \tag{95}$$

If we additionally suppose that the system is time reversal invariant, the matrix (95) takes the form

$$\begin{pmatrix} f_{11}(z^2) & f_{12}(z^2)+izg_{12}(z^2) \\ f_{12}(z^2)-izg_{12}(z^2) & -f_{11}(z^2) \end{pmatrix} + f_0(z^2)\mathbf{I}.$$

7.3. D_3 symmetry models

Let us consider now the problem with finite symmetry group D_3 and with two vibrational states spanning two-dimensional irreducible representation of D_3. Group D_3 is shown in figure 4 together with its natural action on the two-dimensional sphere. Group D_3 includes one axis C_3 of the third order and three axes C_2 of second order.

The D_3 action on the classical and quantum variables are subject to $\Gamma_{\rm rot} = E \oplus A_2$ and $\Gamma_{\rm vib} = E$, respectively. Note that $\Gamma_{\rm rot}$ is realized as a subgroup of $SO(3)$. The decomposition of the direct product of two E representations ($\Gamma_{\rm vib} = E$) takes the form

$$E \otimes E = A_1 \oplus E \oplus \{A_2\}, \tag{96}$$

where the $\{A_2\}$ indicates the antisymmetric part of the square of representation. Then, we choose $(a_{ij}(g))$ in (84) to belong to $E \oplus \{A_2\}$, since the space of traceless Hermitian matrices carries the representation $E \oplus A_2$ through adjoint action. The space spanned by the identity matrix carries the A_1 representation.

The 2×2 rotation-vibration invariant Hamiltonian in this case can be put in the form

$$\begin{pmatrix} (N(\boldsymbol{x}))_1^E & (N(\boldsymbol{x}))_2^E - i\,(N(\boldsymbol{x}))^{A_2} \\ (N(\boldsymbol{x}))_2^E + i\,(N(\boldsymbol{x}))^{A_2} & -(N(\boldsymbol{x}))_1^E \end{pmatrix} + N(\boldsymbol{x})^{A_1}\mathbf{I}, \tag{97}$$

where $(N(\boldsymbol{x}))_\alpha^\Gamma$ denote components of tensor operator transforming according to the irreducible representation Γ. For the two-dimensional E representation, there are two components with $\alpha = 1, 2$. For one-dimensional A_2 representation, there is only one component for which the subscript is not indicated. Here we note that the space spanned by S_3 and S_1 carries the E representation and the space span by S_2 is the representation space for A_2.

To write out the Hamiltonian (97), we need to construct the rotational tensors of types E, A_2, and generally of A_1 type, although the invariant rotational tensors enter only in the trivial scalar diagonal part of the matrix (97).

General expression for rotational tensors of symmetry type A_1, A_2, and E, constructed from the initial rotational representation $\Gamma_{\rm rot} = A_2 \oplus E$ can

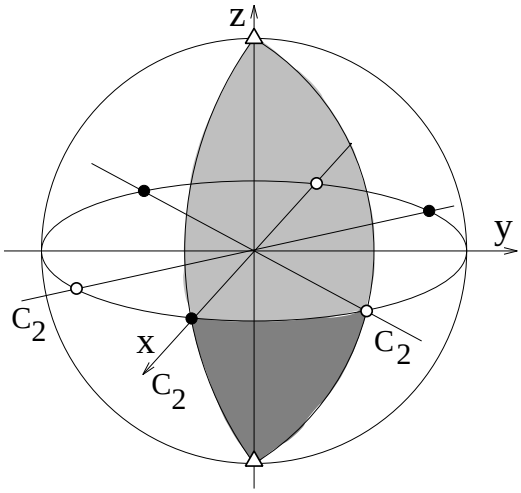

Figure 4: D_3 group and its action on the sphere. z axis is the C_3 symmetry axis. Three C_2 axes belong to xy plane. Two intersection points of C_3 axis and the sphere form two-point orbit with C_3 stabilizer. Six points of intersection of three C_2 axes with the sphere form two three-point orbits with stabilizer C_2. The choice of the "elementary cell" for the D_3 group action on the sphere is shown by a hatched sector (to be compared with the representation of the orbits in Figure 5).

be written using integrity basis approach (see [27], Table 5);

$$
\begin{aligned}
{}^{D_3}P^{A_1} &= P_0\left(N_x^2+N_y^2, N_y(3N_x^2-N_y^2)\right) \\
&\quad +N_zN_x(N_x^2-3N_y^2)P_4\left(N_x^2+N_y^2, N_y(3N_x^2-N_y^2)\right), \qquad (98)\\
{}^{D_3}P^{A_2} &= N_zP_1\left(N_x^2+N_y^2, N_y(3N_x^2-N_y^2)\right) \\
&\quad +N_x(N_x^2-3N_y^2)P_3\left(N_x^2+N_y^2, N_y(3N_x^2-N_y^2)\right), \qquad (99)\\
{}^{D_3}P^{E} &= (N^E\otimes N^E)^E\ P_2\left(N_x^2+N_y^2, N_y(3N_x^2-N_y^2)\right) \\
&\quad +(N^E\otimes N^E\otimes N^E)^E\ P_{3e}\left(N_x^2+N_y^2, N_y(3N_x^2-N_y^2)\right), \qquad (100)
\end{aligned}
$$

where the z-axis is chosen along C_3 symmetry axis and the x-axis coincides with one of C_2 symmetry axes of D_3 group, and P_i are arbitrary polynomials of its variables, and where $N^E=\begin{pmatrix} N_x^E \\ N_y^E \end{pmatrix}$, and the notations $(N^E\otimes N^E)^E$ and $(N^E\otimes N^E\otimes N^E)^E$ denote E type tensors from the decomposition of the product of two or three E type tensors N^E.

Additional symmetry with respect to time reversal requires that real part

of matrix elements should be of even degree whereas imaginary part of off-diagonal element should be of odd degree. The totally symmetric part of Hamiltonian can be omitted.

The analysis of effective Hamiltonian composed of terms of degree not higher than three in elementary rotational variables, which will be analysed in section 9, is found explicitly as follows: If we keep only terms of degree not higher than three under the convention of the choice of symmetry axes, we obtain the following two-term expression for A_2 tensor of odd degree,

$$(N(\boldsymbol{x}))^{A_2} = a_1 z + a_3 y(3x^2 - y^2). \tag{101}$$

The E tensor proves to take the form

$$(N(\boldsymbol{x}))^E_\alpha = a_{2e}(E \otimes E)^E_\alpha + a_{2a}(A_2 \otimes E)^E_\alpha. \tag{102}$$

Two tensors of degree two are written below explicitly in terms of x, y, z components of elementary initial tensors

$$(E \otimes E)^E = \begin{pmatrix} \frac{1}{2}(y^2 - x^2) \\ xy \end{pmatrix}, \tag{103}$$

$$(A_2 \otimes E)^E = \begin{pmatrix} \frac{1}{\sqrt{2}}(-zy) \\ \frac{1}{\sqrt{2}}(zx) \end{pmatrix}. \tag{104}$$

Since the numerical coefficients are not important, we can multiply both components of each tensor by a non-zero factor in order to remove the denominator. Under such a choice we can write the linear combination of two degree-two-tensors of type E as

$$a_{2e}\,(E \otimes E)^E + a_{2a}\,(A_2 \otimes E)^E = a_{2e} \begin{pmatrix} y^2 - x^2 \\ 2xy \end{pmatrix} + a_{2a} \begin{pmatrix} -zy \\ zx \end{pmatrix}. \tag{105}$$

Putting (101) and (105) together, we obtain a complete rotation-vibration invariant Hamiltonian whose terms are of degree less than four as follows:

$$h_{11} = a_{2e}(y^2 - x^2) + a_{2a}(-zy), \tag{106a}$$

$$\Re h_{12} = a_{2e} 2xy + a_{2a} zx, \tag{106b}$$

$$\Im h_{12} = a_1 z + a_3 y(3x^2 - y^2). \tag{106c}$$

7.4. Symmetry and degeneracy points

The eigenvalues and the eigenvectors of invariant Hamiltonians $H(\boldsymbol{x})$ are of our main concern in the following sections. In particular, degeneracy of eigenvalues is important as we have already pointed out in section 6. Since $H(\boldsymbol{x})$ is a 2×2 Hermitian matrix, the discriminant of the eigenvalue equation for $H(\boldsymbol{x})$ is given by $\mathcal{D}(\boldsymbol{x}) = (\mathrm{tr}H(\boldsymbol{x}))^2 - 4 \det H(\boldsymbol{x})$ and is invariant under the G action (see (83)); $\mathcal{D}(g\boldsymbol{x}) = \mathcal{D}(\boldsymbol{x})$. (Note that for our $SO(2)$ symmetry models and D_3 symmetry models we have $\mathrm{tr}H(\boldsymbol{x}) = 0$.) Hence we see that if $\mathcal{D}(\boldsymbol{x}) = 0$ then $\mathcal{D}(g\boldsymbol{x}) = 0$, which implies that if a point $\boldsymbol{x}$ is a degeneracy point then the orbit of G through $\boldsymbol{x}$ is a set of degeneracy points. A generic orbit is a finite set or a curve, according to whether G is finite or continuous. Figure 5 shows the space of orbits for $SO(2)$ group possessing one continuous parameter and for D_3 finite group. For a continuous group with one parameter the space of orbits of the group action on 2D-manifold is generically one-dimensional because each generic orbit is itself a continuous curve (circle in the case of $SO(2)$ group action on two-dimensional sphere).

From a more detailed point of view, orbits are classified according to their stabilizers. For the $SO(2)$ natural action on the S^2 sphere there are two types of orbits: generic orbits with trivial stabilizer C_1 which are circles and one-point orbits with stabilizer $SO(2)$ corresponding to the north and south poles of the sphere. For the D_3 action on the sphere there are three different types of orbits. One orbit with stabilizer C_3 consists of two points coinciding with the C_3 axis positions on the sphere. There are two three-point orbits with stabilizer C_2 formed by intersection points of C_2 axes with sphere. All other points on the sphere form generic orbits with stabilizer C_1. Each such orbit consists of six points.

For the analysis of D_3 invariant objects it is sufficient to look at an "elementary cell" on the sphere (dashed area on the figure 4) representing orbits of the D_3 action. In order to characterize orbits it is possible to use invariant polynomials (see figure 5). We use two main "denominator" invariant polynomials, θ_2 and θ_2, and one "numerator" polynomial φ defined, respectively, by

$$\theta_2 = z^2, \quad \theta_3 = x(x^2 - 3y^2), \quad \varphi = zy(3x^2 - y^2), \tag{107}$$

where these invariants are related by

$$\varphi^2 = \left((1 - \theta_2)^3 - \theta_3^2\right) \theta_2). \tag{108}$$

According to general approach of invariant theory, to characterize orbits we need the value of θ_2 and θ_3 and the sign of φ. The geometrical representation

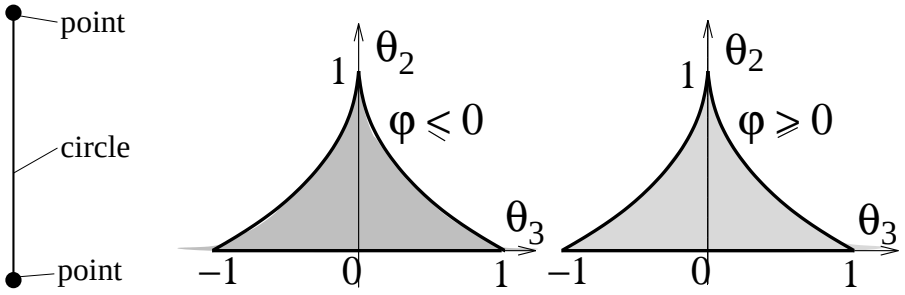

Figure 5: Left : Space of orbits for $SO(2)$ group action on the sphere. There are two one-point orbits with stabilizer C_∞ and continuity of generic circular orbits with stabilizer C_1. Right : Space of orbits for D_3 group action on the sphere. Space of orbits is represented in invariant polynomial coordinates $\theta_2 = z^2, \theta_3 = x(x^2 - 3y^2)$. Two parts corresponds to orbits with different sign of auxiliary invariant $\phi = zy(3x^2 - y^2)$. Corresponding points on the boundary of $\phi \geq 0$ and $\phi \leq 0$ parts should be identified. Orbit with stabilizer C_3 has $\theta_3 = 0, \theta_2 = 1$ coordinates. Two orbits with stabilizer C_2 have coordinates $\theta_3 = \pm 1, \theta_2 = 0$

of the space of orbits in (θ_2, θ_3) variables consists of two regions (see Fig. 5) bounded by curve $\varphi^2 = 0$ and corresponding to $\varphi \geq 0$ and to $\varphi \leq 0$ with identification of respective points on the boundary.

Another point to make in advance concerns exceptional points, which are determined as zeros of the off-diagonal element. In contrast with degeneracy points, the exceptional points do not form an orbit of the symmetry group in general. However, if the symmetry of vibrational part is the direct sum of one-dimensional representations, say, $\Gamma_{\text{vib}} = A_1 \oplus A_2$, then the exceptional points form an orbit of the symmetry group action. This is because the invariance condition in this case provides $\varepsilon h_{12}(g\boldsymbol{x}) = h_{12}(\boldsymbol{x})$ for the off-diagonal element, where $\varepsilon = \pm 1$, which implies that if $h_{12}(\boldsymbol{x}) = 0$ then $h_{12}(g\boldsymbol{x}) = 0$. Further, in the case of $SO(2)$ symmetry, Eq. (89) implies as well that if $h_{12}(\boldsymbol{x}) = 0$ then $h_{12}(g_t\boldsymbol{x}) = 0$.

8. SO(2) invariant Hamiltonian

In this section, we apply the method for Chern number calculation studied in section 5 to problems with axial symmetry.

8.1. Chern numbers in the presence of weighted $SO(2)$ symmetry

As is seen from (91) together with a remark stated after (92), the matrix admitting weighted $SO(2)$ symmetry takes the form

$$\begin{pmatrix} f_{11}(\cos\theta) & f_{12}(\cos\theta)\ \sin^K\theta\ \exp(iK\phi) \\ f_{12}(\cos\theta)\ \sin^K\theta\ \exp(-iK\phi) & -f_{11}(\cos\theta) \end{pmatrix}, \tag{109}$$

where K and f_{ij} are an integer and any real polynomial, respectively.

The application of our method to (109) will provide the following:

Proposition 1. The matrix (109) has two eigenvalues, positive and negative, with no degeneracy points, if f_{11} and $\sin^K\theta f_{12}$ do not share zeros. For $K \neq 0$, the complex line bundle associated with each eigenvalue is defined over the two-sphere S^2, which is characterized by the first Chern number. The Chern number is equal to 0 for two line bundles or to $\pm K$ with the sum over two bundles being 0, depending on whether the number of zeros of the diagonal element, counted with their multiplicities, is even or odd.

Before starting the proof of the proposition, we make a comment on the degeneracy of eigenvalues. For the matrix (109), the eigenvalues

$$\lambda_{1,2} = \pm\sqrt{f_{11}^2(\cos\theta) + f_{12}^2(\cos\theta)\ \sin^{2K}\theta} \tag{110}$$

can be taken as non-degenerate because two functions of one variables cannot go through zero simultaneously in general. Hence generality is not much lost with the assumption on zeros of f_{11} and $f_{12}\sin^K\theta$. However, for one-parameter family of such matrices the formation of degenerate points is possible and so we can expect a change in the Chern numbers when going from one generic matrix to another.

We now proceed to the proof of Proposition 1, following the analysis of a general two state model dealt with in Sec. 5. Let us now suppose that λ_1 is positive and λ_2 is negative. For the matrix (109), Eqs. (41) and (42) take the form

$$(f_{11} - \lambda_1)C_1^{\rm up} + f_{12}\sin^K\theta\exp(iK\phi)C_2^{\rm up} = 0, \tag{111}$$

and

$$f_{12}\sin^K\theta\exp(-iK\phi)C_1^{\rm down} + (-f_{11} - \lambda_1)C_2^{\rm down} = 0, \tag{112}$$

respectively. The solution to (111) yields the normalized eigenvector

$$\begin{pmatrix} C_1^{\rm up} \\ C_2^{\rm up} \end{pmatrix} = \frac{1}{\sqrt{(\lambda_1 - f_{11})^2 + f_{12}^2 \sin^{2K}\theta}} \begin{pmatrix} f_{12}\sin^K\theta \exp(iK\phi) \\ \lambda_1 - f_{11} \end{pmatrix}, \quad (113)$$

which is a specialization of (43). This eigenvector is defined everywhere on the sphere except at the points where the expression under the square root becomes zero. From (48), this happens if $f_{12}\sin^K\theta = 0$ and if at the same time $f_{11} > 0$. The off-diagonal element always goes through zero at $\theta = 0, \pi$ (these two points correspond to the north and the south poles of the sphere), and equally at zeros of $f_{12}(\cos\theta)$. Each such zero other than the north and the south poles corresponds to a circle on the sphere due to the symmetry group action. Again by the generality arguments the zeros of f_{11} do not coincide with the zeros of f_{12} in general. We have here to point out that the exceptional points are discrete in a generic case (see Fig.2b), but the exceptional circles appear in the present case, which are orbits by $SO(2)$ symmetry group action, as is stated in the last sentence of Sec. 7.

The sphere is divided into zones with constant sign of the diagonal element f_{11}. Note that we are interested only in zeros located at $\theta \neq 0, \pi$. If the number of zeros counted with multiplicity is even, the south and the north poles of the sphere belong to the regions with the same sign of f_{11}. If the number of zeros is odd, the sign of f_{11} at the north pole is opposite to that at the south pole. In this sense, a single zero of multiplicity two is equivalent to a pair of zeros of multiplicity one. We can deform f_{11}, as long as the assumption of Prop. 1 holds, *i.e.*, unless f_{11} and $f_{12}\sin^K\theta$ share zeros, in such a way that a pair of zeros of multiplicity one get together to form a single zero of multiplicity two and then the zero disappears, and also deform f_{11} conversely. In this process, the change in the number of zeros is two. In general, if we deform f_{11} to make the number of its zeros increase/decrease by two, the sign of f_{11} at the both poles is kept the same as before, where the deformation should be made so as to keep the $SO(2)$ symmetry.

For the description of the eigenvector given by (113), the singularities of the norm in (113) include all filled points and solid lines representing circles determined by $f_{12}\sin^K\theta = 0$ and located within the zone of positive values of f_{11} limited by dash lines. These singularities should be removed from the sphere in order to get the domain $U_{\rm up}$. In a similar way, by removing from the sphere all singularities determined by $f_{12}\sin^K\theta = 0$ and $f_{11} < 0$, we get the domain $U_{\rm down}$. See Figure 7 for the cases where the numbers of zeros of

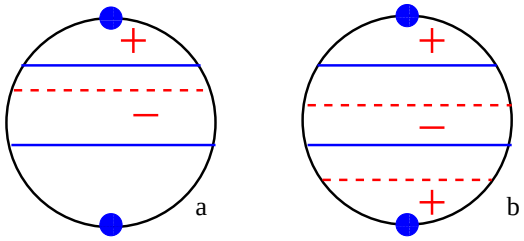

Figure 6: Location of zeros of diagonal and non-diagonal elements of the matrix. Filled points - zeros of $\sin\theta$ factor of non-diagonal element. Solid lines - zeros of f_{12} factor. Dash lines - zeros of diagonal element f_{11}. Plus and minus signs indicate the sign of f_{11} diagonal element in the region. Sub-figure a corresponds to the situation when two filled points belong to zones with different sign of f_{11}. Sub-figure b corresponds to the situation when two filled points belong to zones with the same sign of f_{11}.

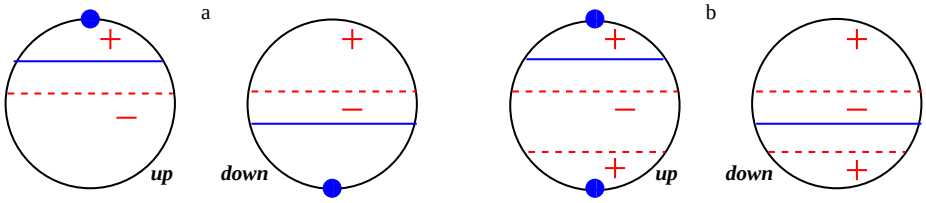

Figure 7: a - Singularities on domains *up* and *down* for an example shown in figure 6a, with odd number of zeros of diagonal element. b - Singularities on domains *up* and *down* for an example shown in figure 6b, with even number of zeros of diagonal element.

multiplicity one are one and two with the assumption that $f_{11}(1) > 0$ and $f_{11}(-1) < 0$ for Fig. 7a and $f_{11}(1) > 0$ and $f_{11}(-1) > 0$ for Fig. 7b. From the definition, the domain U_{down}, for example, can include both poles, only one (north or south), and even no poles.

Suppose we are given the situation represented by Figure 8. There are two solid circles associated with zero of non-diagonal element, two filled points, and one double dash circle associated with a zero of f_{11} of multiplicity two.

In this case, the domain U_{up} is obtained from the sphere by removing all circles and points mentioned above, but the domain U_{down} is the whole sphere with no exceptional circles and points.

For notational convenience, we denote by U_+ and U_- the domains U_{up} and U_{down}, respectively. Namely, the U_+ denotes the domain obtained from the sphere by removing all zeros of off-diagonal element which belong to

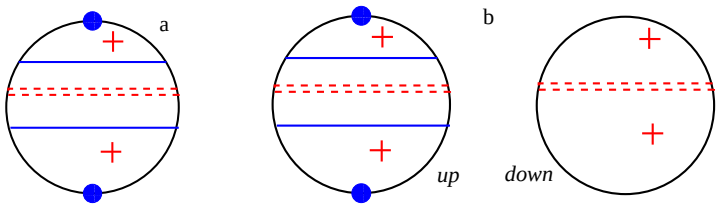

Figure 8: *a* - Example of location of zeros of diagonal and non-diagonal elements in the case of one double zero of diagonal element (shown by double dash line). *b* -Singularities on domains *up* and *down* for an example shown in subfigure *a*.

the region of positive value of the diagonal element f_{11}, and the U_- denotes the domain obtained from the sphere by removing all zeros of off-diagonal element which belong to the region of negative value of f_{11}.

The eigenvectors defined on these two domains are proportional on the intersection $U_+ \cap U_-$. The coefficient of proportionality is a complex phase, $\exp(iK\phi)$, as is seen from (54) with $a_{12} + ib_{12} = f_{12} \sin^K \theta \exp(iK\phi)$ and $\varepsilon = \mathrm{sgn}(\lambda_1 - a_{22}) = 1$. This coefficient is defined on the intersection of domains even in the case of domains composed of several disjoint components (namely in cases when diagonal and/or off-diagonal elements have several zeros).

Now we can follow the calculation done in the section 5 on the basis of the Stokes theorem. Since $\Phi = e^{iK\phi}$ in the present case, the relation (59) takes the form

$$\omega_+ = iKd\phi + \omega_- \quad \text{on} \quad U_+ \cap U_-. \tag{114}$$

The global curvature form Ω on the whole S^2 is defined like (60). A way to integrate the curvature and calculate the Chern number is to make more specific choice of parts into which we split the sphere.

In the example shown in Figures 6*a* and Figure 7*a* (the number of zeros of f_{11} is one), we need to split the sphere into only two regions, as is shown in Figure 9. In the example shown in Figures 6*b* and Figure 7*b* (the number of zeros of f_{11} is two), we need to split the sphere into three regions, as is shown in Figure 10.

First we consider the case where the number of zeros of f_{11} is one, where the zero is of multiplicity one (or odd). Let C denote a circle which is in $U_+ \cap U_-$ and separates the sphere into two, as is shown in Figure 9. Let S^2_+ and S^2_- denote the regions included in U_+ and U_-, respectively (the lower and the upper hatched semi-spheres shown in Figure 9 on the spheres

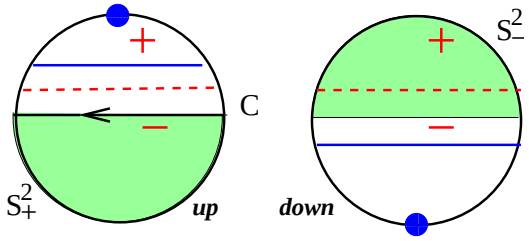

Figure 9: Choice of the splitting of the whole sphere into two regions of integration for an example given in Figure 6*a*. The choice of charts follows that shown in Figure 7*a*. the arrow indicate the direction of contour integral after application of Stokes theorem to surface integral of the curvature form.

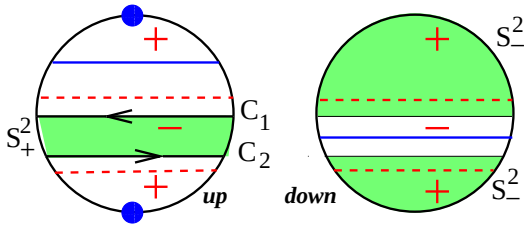

Figure 10: Choice of the splitting of the whole sphere into three regions of integration for an example given in figure 6*b*. The choice of charts follows that shown in figure 7*b*. Arrows indicate the direction of contour integral after application of Stokes theorem to surface integral of the curvature form.

representing "up" and "down" domains, respectively). Note that the local connection forms ω_+ and ω_- have no singularity in S^2_+ and S^2_-, respectively. According to our rule, adopted in Sec. 5.3, of choosing the orientation of curves separating S^2_+ and S^2_-, the orientation of C is given in such a way that the coordinate ϕ varies from 2π to 0, which is shown in the left figure of Fig. 9. Then, the integration of the transition rule (114) is expressed as

$$\int_C \omega_+ = iK \int_C d\phi + \int_C \omega_-, \tag{115}$$

and then the Stokes theorem applies to provide

$$\int_{S^2} \Omega = \int_{S^2_+} d\omega_+ + \int_{S^2_-} d\omega_- = \int_C \omega_+ + \int_{-C} \omega_- = iK \int_C d\phi, \tag{116}$$

which results in the Chern number

$$\frac{i}{2\pi} \int_{S^2} \Omega = K. \tag{117}$$

We note here that we have assumed that $f_{11}(1) > 0$ and $f_{11}(-1) < 0$. If the sign of f_{11} at $z = \pm 1$ is opposite, *i.e.*, $f_{11}(1) < 0$ and $f_{11}(-1) > 0$, then the right-hand side of the above equation changes the sign, *i.e.*, we obtain the Chern number $-K$.

We turn to the case where the number of zeros of f_{11} is two, but the multiplicity of each zero is one (or odd). Let C_1 and C_2 denote circles which are in $U_+ \cap U_-$ and separate the sphere into three regions, as is shown in Figure 10. The respective orientations of the circles are indicated by the arrows put on them in the left figure. Let S^2_+ and S^2_- denote the regions which are included in U_+ and U_-, respectively, where S^2_+ is a cylinder-like region with boundary C_1 and C_2 and S^2_- consists of two disjoint subsets (the left and the right hatched regions shown in Figure 10b, respectively). Then the integration with the Stokes theorem provides

$$\int_{S^2} \Omega = \int_{S^2_+} d\omega_+ + \int_{S^2_-} d\omega_- = \int_{C_1+C_2} \omega_+ - \omega_- = iK \int_{C_1+C_2} d\phi = 0, \tag{118}$$

which shows that the Chern number is zero. We note that the last equality of the above equation is due to the orientation of C_1 and of C_2.

In the case of a multiplicity-two zero, the domain U_- is the whole sphere, as was alredy explained, so that ω_- is defined globally. Then the Stokes theorem provides

$$\int_{S^2} \Omega = \int_{S^2} d\omega_- = 0. \tag{119}$$

If the number of zeros of f_{11} is three with multiplicity one for each zero, we take three circles C_k, $k = 1, 2, 3$, to separate the sphere into four regions. However, we can form S^2_+ and S^2_- by gathering two of those regions so that the local connection forms ω_+ and ω_- may be well defined on S^2_+ and S^2_-, respectively. Then, the three circles form boundaries of S^2_+ and S^2_-. In a similar manner to the above, the Stokes theorem applies to yield

$$\begin{aligned}\int_{S^2} \Omega &= \int_{S^2_+} d\omega_+ + \int_{S^2_-} d\omega_- \\ &= \int_{C_1+C_2+C_3} \omega_+ + \int_{-(C_1+C_2+C_2)} \omega_- \\ &= \int_{C_1+C_2+C_3} iKd\phi \ = \ \int_{C_3} iKd\phi,\end{aligned} \tag{120}$$

where the last equality of the above equation is due to the orientation of the circles, and where C_3 is the boundary of the saucer-shape region like the left figure of Figure 9. On account of the orientation of C_3, we obtain the Chern number

$$\frac{i}{2\pi}\int_{S^2} \Omega = K. \tag{121}$$

In the case where the number of zeros is three counted with multiplicity and where they are one multiplicity-two zero and a multiplicity-one zero, we have only to draw a circle which divide the sphere into two, S^2_+ and S^2_-, so that ω_+ and ω_- may be well defined on S^2_+ and S^2_-, respectively. The argument for (120) applies with a slight modification to result in (121).

In a similar manner, we can treat the case of bigger numbers of zeros of f_{11}. A point to make here is the parity of the number of circles and the orientation of the circles. Thus we find that the Chern number is zero or K under the assumption that $f_{11}(1) > 0$, according to whether the number of circles counted with multiplicity is even or odd. If $f_{11}(1) < 0$, then the Chern number becomes zero or $-K$.

So far we have worked with the line bundle associated with the positive eigenvalue. A similar treatment will run in parallel for the negative eigenvalue, and the Chern number of the line bundle associated with the negative

eigenvalue will be found to be zero or $\pm K$, depending on whether the Chern number for the positive eigenvalue is zero or $\mp K$. This completes the proof.

8.2. Characteristic number for real symmetric matrices

If the two-by-two matrix of the effective two level Hamiltonian can be chosen real, the associated vector bundles are real line bundles. The transition rule (56) becomes

$$\boldsymbol{u}_+ = \pm \boldsymbol{u}_-, \quad \pm 1 \in \mathbf{Z}_2, \tag{122}$$

where $\boldsymbol{u}_\pm$ are real eigenvectors. The transformation rule (59) for local connection forms becomes

$$\omega_+ = \omega_- \quad \text{on} \quad U_+ \cap U_-, \tag{123}$$

which implies that the connection form ω is defined globally on S^2. The curvature from $\Omega = d\omega$ is defined globally as well, so that the Stokes theorem provides

$$\int_{S^2} \Omega = \int_{S^2} d\omega = 0. \tag{124}$$

Thus the characteristic number for any real symmetric matrix is zero.

9. D_3 invariant Hamiltonian for E vibrational state

Now in this section we concentrate on one concrete example of effective rotation-vibration Hamiltonian for two vibrational states which transform according to two-dimensional irreducible representation E of D_3 group supposed to be an invariance symmetry group of equilibrium configuration of a molecule. Restricting the tensorial polynomials to not higher than third degree in elementary rotational tensors denoted for simplicity by (x, y, z) and choosing a coordinate system with the z axis along C_3 symmetry axis of D_3 group and with the x axis along one of C_2 symmetry axes (see Fig. 4), we have obtained a model Hamiltonian with entries given in (106). If we choose four phenomenological coefficients a_1, a_2, b_1, b_2 for notational convenience in place of those used in (106), the model Hamiltonian in this section takes the following 2×2 matrix form,

$$H(\boldsymbol{x}) = \begin{pmatrix} b_1(y^2 - x^2) + b_2 zy & 2b_1 yx - b_2 zx - i(a_1 z + a_2 y(y^2 - 3x^2)) \\ 2b_1 yx - b_2 zx + i(a_1 z + a_2 y(y^2 - 3x^2)) & -b_1(y^2 - x^2) - b_2 zy \end{pmatrix}. \tag{125}$$

The pairs of parameters (a_1, a_2) and (b_1, b_2) are associated with rotational tensors transforming according to the A_2 and the E representations of D_3 group, respectively. Since we are concerned with vibrational angular momenta $S_k, k = 1, 2, 3$, transforming according to $E \oplus A_2$ representation of D_3, we assume that $(a_1, a_2) \neq (0, 0)$ and $(b_1, b_2) \neq (0, 0)$, and hence the parameter space is expressed as $\dot{\mathbb{R}}^2 \times \dot{\mathbb{R}}^2$, where $\dot{\mathbb{R}}^2 = \mathbb{R}^2 - \{0\}$.

We apply the general method of section 5 to describe the eigen-line bundles formed by eigenspaces of Hamiltonian (125). If $\det H(\boldsymbol{x}) \neq 0$, the eigenvalues of the Hamiltonian H are distinct. We denote them by $\lambda_+ > 0$ and $\lambda_- < 0$ and note that they are related by $-\lambda_+ = \lambda_-$. Further, we denote by $\boldsymbol{u}_\pm$ the normalized eigenvectors associated with $\lambda_\pm$, respectively. These eigenvectors $\boldsymbol{u}_\pm$ are not generically defined globally on the two-sphere without singularity. We call such a singularity an exceptional point. However, for each eigenvalue, assuming the absence of degeneracies, we can obtain locally-defined normalized eigenvectors on suitably chosen domains U_{up} and U_{down}. These eigenvectors are patched together on the intersection $U_{\text{up}} \cap U_{\text{down}}$ by a transformation rule. Then we can form the eigen-line bundle associated with each eigenvalue, which we denote by $L^\pm$ according to the eigenvalues $\lambda_\pm$. The whole bundle structure associated with the Hamiltonian is expressed as $L^+ \oplus L^-$, a direct sum. If $\det H(\boldsymbol{x}) = 0$, the eigenvalues are degenerate, and hence there is no natural way to define a line bundle over a sphere S^2 associated with the degenerate eigenvalue. We call the points determined by $\det H(\boldsymbol{x}) = 0$ on S^2 degeneracy points. The set of parameters a_1, a_2, b_1, b_2 corresponding to Hamiltonians possessing degeneracy points on the S^2 sphere defines the boundaries of the iso-Chern domains in the space of parameters a_1, a_2, b_1, b_2 as it is described in section 6 and allows us to construct the iso-Chern diagram.

9.1. Reduction of the parameter space

It is easy to see that under the constraint condition $\boldsymbol{x} \in S^2(1)$, one has

$$\det H(\boldsymbol{x}) = 0 \;\Leftrightarrow\; \begin{cases} b_1(y^2 - x^2) + b_2 zy = 0, \\ x(2b_1 y - b_2 z) = 0, \\ a_1 z + a_2 y(y^2 - 3x^2) = 0. \end{cases} \tag{126}$$

We note here that we can set the radius of the two-dimensional sphere to be $\rho = 1$ by a suitable scaling. The above condition (126) is invariant under the

parameter transformation

$$(a_1, a_2) \mapsto (\lambda a_1, \lambda a_2), \quad (b_1, b_2) \mapsto (\mu b_1, \mu b_2), \tag{127}$$

where λ and μ are real non-zero numbers. Note that the parameters λ and μ are allowed to be negative. The transformation (127) defines an equivalence relation on the parameter space $\dot{\mathbb{R}}^2 \times \dot{\mathbb{R}}^2$, and the quotient space by this equivalence relation becomes $\mathbb{R}P^1 \times \mathbb{R}P^1$, where $\mathbb{R}P^1$ denotes the real projective space of one dimension. Thus, we may conclude that the original parameter space $\dot{\mathbb{R}}^2 \times \dot{\mathbb{R}}^2$ projects to $\mathbb{R}P^1 \times \mathbb{R}P^1$ on account of the scale invariance of the degeneracy condition $\det(H) = 0$ (126).

However, as we have already observed in Sec. 6, under the transformation (127) with $\lambda = \mu = -1$, the Hamiltonian transforms like $H \to -H$, and though the whole bundle structure is also the same as before, that is, $L^+ \oplus L^-$, the roles of L^+ and L^- are exchanged together with the Chern numbers. Then, it turns out that if we are interested in the eigen-line bundle associated with the positive or negative eigenvalue, the scaling transformation (127) with $\lambda < 0$ and $\mu < 0$ is not allowed, but restricted to the case of $\lambda > 0$ and $\mu > 0$. Hence, the reduced parameter space proves to be $T^2 = S^1 \times S^1$, a quadruple covering of $\mathbb{R}P^1 \times \mathbb{R}P^1$, where each factor of $S^1 \times S^1$ is determined by either of

$$a_1^2 + a_2^2 = 1, \quad b_1^2 + b_2^2 = 1. \tag{128}$$

In what follows, we refer to $S^1 \times S^1$ and $\mathbb{R}P^1 \times \mathbb{R}P^1$ as the reduced parameter space and the over-reduced parameter space, respectively. Though $\mathbb{R}P^1 \cong S^1$, we will distinguish $S^1 \times S^1$ from $\mathbb{R}P^1 \times \mathbb{R}P^1$ for the reason stated above.

9.2. Degeneracy set and iso-Chern domains

Though the control parameters (a_1, a_2, b_1, b_2) are subject to the constraint conditions (128), we are to find those values which correspond to the existence of points $\boldsymbol{x} \in S^2(1)$ determined by the condition $\det H(\boldsymbol{x}) = 0$ without reference to (128) for the sake of another purpose.

(1) In the case of $a_1 \neq 0$, $a_2 = 0$, the equations we have to solve are

$$b_1(y^2 - x^2) + b_2 zy = 0, \quad x(2b_1 y - b_2 z) = 0, \quad a_1 z = 0. \tag{129}$$

Since $a_1 \neq 0$, one has $z = 0$ from the third equation of (129). If $b_1 \neq 0$ further, then the first and the second equations of (129) provide $y^2 = x^2$ and $yx = 0$. If $y = 0$ in this case, one has $x = 0$, a contradiction to the

constraint. If $x = 0$ in this case, the same result comes out. Thus, we have found that in the case of $a_1 \neq 0$, $a_2 = 0$, $b_1 \neq 0$ no degeneracy point occurs. If $b_1 = 0$, then Eq. (129) becomes $b_2 zy = 0, b_2 xz = 0, a_1 z = 0$. Since $a_1 \neq 0$ and $b_2 \neq 0$, these equations hold for $z = 0$. From the constraint condition $x^2 + y^2 + z^2 = 1$, in the case of $a_1 \neq 0$, $a_2 = 0$, $b_1 = 0$, $b_2 \neq 0$, the degeneracy points form a circle

$$x^2 + y^2 = 1, \tag{130}$$

which consists of infinity of orbits of the D_3 group action on S^2. More exactly, there are two orbits with C_2 stabilizer and infinity of generic orbits with C_1 stabilizer.

(2) If $b_1 \neq 0$, $b_2 = 0$, then the equations to be solved are

$$y^2 - x^2 = 0, \quad yx = 0, \quad a_1 z + a_2 y(y^2 - 3x^2) = 0. \tag{131}$$

From the second equation of (131), one has (i) $y = 0$ and (ii) $x = 0$.

(i) In the case of $y = 0$, the first equation of (131) gives $x = 0$. Then, the third equation of (131) becomes $a_1 z = 0$. If $a_1 \neq 0$, one has $z = 0$, a contradiction to the constraint. If $a_1 = 0$, the third equation of (131) is satisfied, and then one has $z = \pm 1$ from the constraint condition.

(ii) In the case of $x = 0$, the first equation of (131) provides $y = 0$, and hence the third equation becomes $a_1 z = 0$. If $a_1 \neq 0$, then $z = 0$, the same contradiction occurring. If $a_1 = 0$, one has $z = \pm 1$ from the constraint.
Thus we have found that in the case of $a_1 \neq 0$, $b_1 \neq 0$, $b_2 = 0$, there are no degeneracy points, and that in the case of $a_1 = 0$, $b_1 \neq 0$, $b_2 = 0$, there are two degeneracy points expressed as

$$\begin{pmatrix} 0 \\ 0 \\ \pm 1 \end{pmatrix} \tag{132}$$

and forming one orbit of the D_3 action with stabilizer C_3.

(3) Now we consider the case where all the parameters a_j, b_j are non-zero. From the second equation of (126), we obtain (i) $x = 0$ and (ii) $b_2 z = 2b_1 y$.

(i) When $x = 0$, the first equation of (126) becomes $y(b_1 y + b_2 z) = 0$, which results in $y = 0$ or $b_1 y + b_2 z = 0$. If $y = 0$, then the third equation of (126) becomes $a_1 z = 0$, which implies that $z = 0$, contradicting to $x^2 + y^2 + z^2 = 1$.

Hence, $y \neq 0$ in this case. If $b_1 y + b_2 z = 0$, then the third equation of (126) becomes $y(a_2 y^2 - (a_1 b_1)/b_2) = 0$. Since $y \neq 0$, one has $y^2 = a_1 b_1 / a_2 b_2$. Hence, a condition for $H(\boldsymbol{x})$ to have degenerate eigenvalues is

$$0 < \frac{a_1 b_1}{a_2 b_2} \leq 1. \tag{133}$$

In this case, we have solutions $y = \pm\sqrt{a_1 b_1 / a_2 b_2}$, and then $z = \mp(b_1/b_2)\sqrt{a_1 b_1 / a_2 b_2}$. Thus, the degeneracy points in this case are

$$\begin{pmatrix} 0 \\ \sqrt{\frac{a_1 b_1}{a_2 b_2}} \\ -\frac{b_1}{b_2}\sqrt{\frac{a_1 b_1}{a_2 b_2}} \end{pmatrix}, \quad \begin{pmatrix} 0 \\ -\sqrt{\frac{a_1 b_1}{a_2 b_2}} \\ \frac{b_1}{b_2}\sqrt{\frac{a_1 b_1}{a_2 b_2}} \end{pmatrix}. \tag{134}$$

Since these degeneracy points should be on the sphere $S^2(1)$, the parameters (a_1, a_2, b_1, b_2) should be subject to the condition,

$$\frac{a_1 b_1}{a_2 b_2} + \frac{a_1 b_1^3}{a_2 b_2^3} = \frac{a_1 b_1}{a_2 b_2}\left(1 + \frac{b_1^2}{b_2^2}\right) = 1. \tag{135}$$

(ii) When $b_2 z = 2 b_1 y$, the first equation of (126) becomes $b_1(3y^2 - x^2) = 0$, so that $x = \pm\sqrt{3} y$. Then the third equation of (126) is expressed as $2 b_1 a_1 y / b_2 - 8 a_2 y^3 = 0$. If $y = 0$, then $z = x = 0$, a contradiction to the constraint, so that $y \neq 0$. Hence, one has $y^2 = a_1 b_1 / 4 a_2 b_2$. Thus we obtain another condition for $H(\boldsymbol{x})$ to have degenerate eigenvalues,

$$0 < \frac{a_1 b_1}{a_2 b_2} \leq 4. \tag{136}$$

If this is the case, we have solutions $y = \pm(1/2)\sqrt{a_1 b_1 / a_2 b_2}$, and then $z = \pm(b_1/b_2)\sqrt{a_1 b_1 / a_2 b_2}$, $x = \pm\sqrt{3} y$. The degeneracy points we have obtained here are

$$\begin{pmatrix} \pm\frac{\sqrt{3}}{2}\sqrt{\frac{a_1 b_1}{a_2 b_2}} \\ \frac{1}{2}\sqrt{\frac{a_1 b_1}{a_2 b_2}} \\ \frac{b_1}{b_2}\sqrt{\frac{a_1 b_1}{a_2 b_2}} \end{pmatrix}, \quad \begin{pmatrix} \mp\frac{\sqrt{3}}{2}\sqrt{\frac{a_1 b_1}{a_2 b_2}} \\ -\frac{1}{2}\sqrt{\frac{a_1 b_1}{a_2 b_2}} \\ -\frac{b_1}{b_2}\sqrt{\frac{a_1 b_1}{a_2 b_2}} \end{pmatrix}. \tag{137}$$

These degeneracy points should be on the sphere $S^2(1)$, so that the parameters are subject to a constraint, which is shown to be the same as (135).

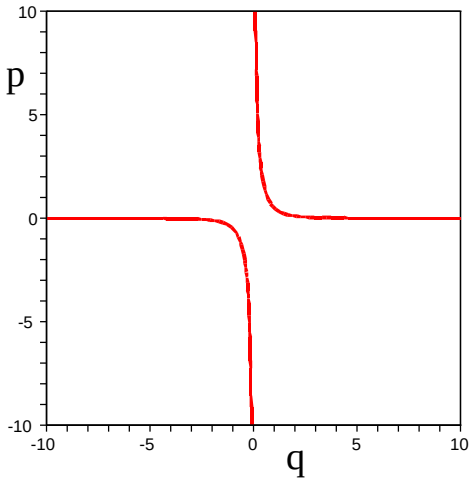

Figure 11: A degeneracy curve in the space of reduced control parameters $p = a_1/a_2$, $q = b_1/b_2$ given by relation $pq(1+q^2) = 1$.

The above expression of the condition for degeneracy points suggests us to introduce parameters

$$p = \frac{a_1}{a_2}, \quad q = \frac{b_1}{b_2}, \tag{138}$$

which are looked upon as local coordinates of $\mathbb{R}P^1 \times \mathbb{R}P^1$. Later, we will introduce local coordinates of $S^1 \times S^1$. In terms of these parameters, the constraint (135) is expressed as

$$pq(1+q^2) = 1, \tag{139}$$

from which we find that the quantity $pq = a_1 b_1 / a_2 b_2$ ranges as follows,

$$0 < pq = \frac{1}{1+q^2} < 1, \tag{140}$$

which satisfy the inequalities (133) and (136).

The graph of (139) is shown in Figure 11.

It then turns out that the Hamiltonian with non-zero parameters (a_1, a_2, b_1, b_2) has degenerate eigenvalues if and only if the constraint (139) holds among the parameters. If the parameters are subject to this constraint, there are

six degeneracy points given in (134) and (137), which are rewritten below in terms of p and q parameters. Two subsets of three points each

$$\left\{ \begin{pmatrix} 0 \\ \sqrt{pq} \\ -q\sqrt{pq} \end{pmatrix}, \quad \begin{pmatrix} \frac{\sqrt{3}}{2}\sqrt{pq} \\ -\frac{1}{2}\sqrt{pq} \\ -q\sqrt{pq} \end{pmatrix}, \quad \begin{pmatrix} -\frac{\sqrt{3}}{2}\sqrt{pq} \\ -\frac{1}{2}\sqrt{pq} \\ -q\sqrt{pq} \end{pmatrix} \right\}, \tag{141}$$

and

$$\left\{ \begin{pmatrix} 0 \\ -\sqrt{pq} \\ q\sqrt{pq} \end{pmatrix}, \quad \begin{pmatrix} -\frac{\sqrt{3}}{2}\sqrt{pq} \\ \frac{1}{2}\sqrt{pq} \\ q\sqrt{pq} \end{pmatrix}, \quad \begin{pmatrix} \frac{\sqrt{3}}{2}\sqrt{pq} \\ \frac{1}{2}\sqrt{pq} \\ q\sqrt{pq} \end{pmatrix} \right\}, \tag{142}$$

form triangles on the plane $z = -q\sqrt{pq}$ and $z = q\sqrt{pq}$, respectively. Each of these triangles corresponds to an orbit of the subgroup C_3 of D_3. Alltogether these six points form a generic orbit of D_3 group.

Up to now we have analyzed the case of $a_1 \neq 0, b_1 \neq 0$. Let us be reminded here that the solutions for degeneracy points (and for exceptional points below) do not depend on the sign of a_1 and b_1 parameters. We proceed now to consider the cases where one of the parameters a_1 or b_1 vanishes.

(4) In the case of $a_1 = 0$, $a_2 \neq 0$, we have to solve the equations

$$b_1(y^2 - x^2) + b_2 zy = 0, \quad x(2b_1 y - b_2 z) = 0, \quad a_2 y(y^2 - 3x^2) = 0 \tag{143}$$

to find degeneracy points. From the last equation of (143), we obtain (i) $y = 0$ and (ii) $y^2 - 3x^2 = 0$.

(i) If $y = 0$, then the first equation of (143) provides $b_1 x^2 = 0$. If further $b_1 \neq 0$, then one has $x = 0$, so that $z = \pm 1$.

(ii) We turn to the case of $y^2 = 3x^2$. If $x = 0$ in this case, then one has $y = 0$, so that $z = \pm 1$. If $x \neq 0$, the second equation of (143) provides $2b_1 y = b_2 z$, and thereby the first equation of (143) becomes $b_1 x^2 = 0$. If further $b_1 \neq 0$, one has $x = 0$, a contradiction to the assumption that $x \neq 0$. The case of $b_1 = 0$ will be dealt with in below. So far we have found that in the case of $a_1 = 0$, $a_2 \neq 0$, $b_1 \neq 0$ there are two degeneracy points expressed as

$$\begin{pmatrix} 0 \\ 0 \\ \pm 1 \end{pmatrix}, \tag{144}$$

which form an orbit of D_3 with stabilizer C_3. If $b_1 = 0$ in addition to $a_1 = 0$, the equations (143) reduce to

$$b_2 zy = 0, \quad b_2 xz = 0, \quad a_2 y(y^2 - 3x^2) = 0. \tag{145}$$

If $b_2 \neq 0$, one has two cases (i) $z = 0$ and (ii) $z \neq 0$, $(x, y) = (0, 0)$ from the first and the second equations of (145).

(i) If $z = 0$ and if $y \neq 0$ further, the third equation of (145) provides $y^2 - 3x^2 = 0$, so that $y = \pm\sqrt{3}x$. In this case, one obtains, from the constraint condition, $1 = 4x^2$, which is solved by $x = \pm\frac{1}{2}$, and thereby $y = \pm\frac{\sqrt{3}}{2}$. If $y = z = 0$, then one has $x = \pm 1$ because of the constraint.

(ii) If $z \neq 0$ and $(x, y) = (0, 0)$, then one has $z = \pm 1$ on account of the constraint. Thus, we have found that in the case of $a_1 = 0$, $a_2 \neq 0$, $b_1 = 0$, $b_2 \neq 0$ there are eight degeneracy points expressed as

$$\begin{pmatrix} 0 \\ 0 \\ \pm 1 \end{pmatrix}, \quad \begin{pmatrix} \pm 1 \\ 0 \\ 0 \end{pmatrix}, \quad \begin{pmatrix} \pm\frac{1}{2} \\ \frac{\sqrt{3}}{2} \\ 0 \end{pmatrix}, \quad \begin{pmatrix} \pm\frac{1}{2} \\ \frac{-\sqrt{3}}{2} \\ 0 \end{pmatrix}. \tag{146}$$

These eight points are broken into three orbits of D_3,

$$\left\{ \begin{pmatrix} \frac{1}{2} \\ \frac{\sqrt{3}}{2} \\ 0 \end{pmatrix}, \begin{pmatrix} \frac{1}{2} \\ -\frac{\sqrt{3}}{2} \\ 0 \end{pmatrix}, \begin{pmatrix} -1 \\ 0 \\ 0 \end{pmatrix} \right\}, \quad \left\{ \begin{pmatrix} -\frac{1}{2} \\ \frac{\sqrt{3}}{2} \\ 0 \end{pmatrix}, \begin{pmatrix} -\frac{1}{2} \\ -\frac{\sqrt{3}}{2} \\ 0 \end{pmatrix}, \begin{pmatrix} 1 \\ 0 \\ 0 \end{pmatrix} \right\}, \quad \left\{ \begin{pmatrix} 0 \\ 0 \\ \pm 1 \end{pmatrix} \right\}. \tag{147}$$

Two three-point orbits have stibilizer C_2, whereas the last two-point orbit has stabilizer C_3.

(5) If $b_1 = 0$, $b_2 \neq 0$, the equations we have to solve are

$$b_2 zy = 0, \quad b_2 zx = 0, \quad a_1 z + a_2 y(y^2 - 3x^2) = 0. \tag{148}$$

From the first and the second equations of (148), one has two cases, (i) $z = 0$ and (ii) $z \neq 0$, $(x, y) = 0$.

(i) If $z = 0$, the third equation of (148) becomes $a_2 y(y^2 - 3x^2) = 0$. If $a_2 \neq 0$ in this case, one obtains $y(y^2 - 3x^2) = 0$, and thereby $y = 0$, $y^2 - 3x^2 = 0$. In the case of $y = 0$, one has $x = \pm 1$. In the case of $y^2 = 3x^2$, one has $y = \pm\sqrt{3}x$, and thereby the constraint condition becomes $1 = 4x^2$, so that $x = \pm\frac{1}{2}$ and $y = \pm\frac{\sqrt{3}}{2}$. If $a_2 = 0$, then the third equation of (148) becomes $a_1 z = 0$. Since $a_1 \neq 0$, one has $z = 0$. Then the first and the second equation (148) are satisfied. This means that in the case of $a_1 \neq 0, a_2 = 0, b_1 = 0, b_2 \neq 0$ the circle $y^2 + x^2 = 1$ is a degeneracy set, which we have obtained in (130).

(ii) If $z \neq 0$, $(x, y) = (0, 0)$, then the third equation of (148) provides $a_1 z = 0$. If $a_1 \neq 0$ in this case, one has $z = 0$, a contradiction to the

constraint. If $a_1 = 0$, the third equation of (148) is satisfied and then one has $z = \pm 1$. Thus we have found that in the case of $a_2 \neq 0$, $b_1 = 0$, $b_2 \neq 0$ there are six degeneracy points expressed as

$$\begin{pmatrix} \pm 1 \\ 0 \\ 0 \end{pmatrix}, \quad \begin{pmatrix} \pm\frac{1}{2} \\ \frac{\sqrt{3}}{2} \\ 0 \end{pmatrix}, \quad \begin{pmatrix} \pm\frac{1}{2} \\ -\frac{\sqrt{3}}{2} \\ 0 \end{pmatrix}, \tag{149}$$

and if $a_1 = 0$ in addition, two degeneracy points appear further;

$$\begin{pmatrix} 0 \\ 0 \\ \pm 1 \end{pmatrix}. \tag{150}$$

That is, if $a_1 = 0$, $a_2 \neq 0$, $b_1 = 0$, $b_2 \neq 0$, there are eight degeneracy points, forming one C_3 and two C_2 orbits which are already given by (146). If $a_1 \neq 0, a_2 = 0, b_1 = 0, b_2 \neq 0$, then there appears a degeneracy curve already found in (130).

The above observation of degeneracy points can be described in the q-p plane, where (q, p) are defined, if $a_2 \neq 0$ and $b_2 \neq 0$, by (138), where (p, q) are viewed as local coordinates of the over-reduced parameter space $\mathbb{R}P^1 \times \mathbb{R}P^1$. The degeneracy curves on the q-p plane are $pq(1+q^2) = 1$, $p = 0$, and $q = 0$, where the lines $p = 0$ and $q = 0$ correspond to parameters of type $(0, a_2, b_1, b_2)$ and $(a_1, a_2, 0, b_2)$, respectively. For the parameters corresponding to the curve $qp(1 + q^2) = 1$, the Hamiltonian has six degeneracy points (one six-point generic orbit with stabilizer C_1 of D_3 action on the sphere), which are given in (141) and (142). For the parameters corresponding to the line $q = 0$ except for the origin $(p, q) = (0, 0)$, the Hamiltonian has six degeneracy points (two three-point orbits with stabilizer C_2), which are given in (149). For the parameters corresponding to the line $p = 0$ except for the origin $(p, q) = (0, 0)$, the Hamiltonian has two degeneracy points (two-point orbit with stabilizer C_3), which are given in (144) or (132). For the origin $(p, q) = (0, 0)$, the Hamiltonian has eight degeneracy points (two three-point orbits with stabilizer C_2 and one two-point orbit with stabilizer C_3), which are given in (146). We have obtained another degeneracy points which cannot be described in the q-p plane. In fact, for parameters with $a_2 = 0$ and $b_1 = 0$, we have a degeneracy circle, which is given in (130).

Since the degeneracy points form orbits of group D_3, they are mapped to the orbits space. For the degeneracy points (141) and (142), the invariant

polynomials defined in (107) take the values $\theta_3 = 0$, $\theta_2 = 1 - pq$, $\varphi = q(pq)^2$. This allows us to plot easily the positions of corresponding degeneracy points on the orbit space in the polynomial coordinates. For the degeneracy points with stabilizers C_2 and C_3, both given in (147), one has $(\theta_2, \theta_3) = (0, \pm 1)$ and $(\theta_2, \theta_3) = (1, 0)$, respectively. The circle of degeneracy points (130) is represented on the space of orbits as $\theta_2 = 0$ boundary interval. The images of these degeneracy points are shown in Figure 12.

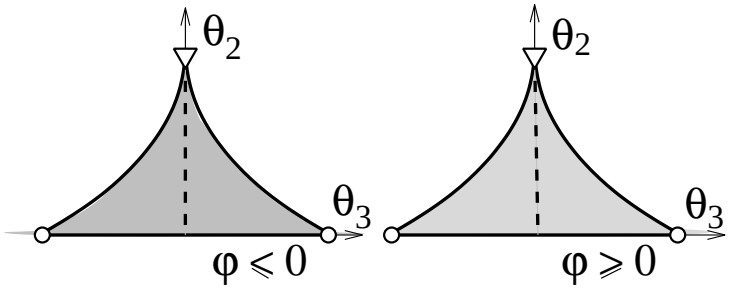

Figure 12: Degeneracy points on the space of orbits. Dash line corresponds to six-point degeneracy orbits with C_1 stabilizer. Two-point orbit with C_3 stabilizer is represented by a triangle. Two three-point orbits with C_2 stabilizer are shown by circles. Note that the respective points on the boundary of $\varphi \leq 0$ and $\varphi \geq 0$ domains should be identified. (See figure 5.)

In order to describe completely the degeneracy set, we choose to use the reduced parameter space $T^2 = S^1 \times S^1$, which is a quadruple covering of $\mathbb{R}P^1 \times \mathbb{R}P^1$. We introduce in the reduced parameter space the local coordinates (ϕ_1, ϕ_2) determined by

$$a_1 = \cos\phi_1, \quad a_2 = \sin\phi_1, \quad b_1 = \cos\phi_2, \quad b_2 = \sin\phi_2. \tag{151}$$

The degeneracy curve $pq(1 + q^2) = 1$ can be expressed in terms of these parameters. Since $p = \cos\phi_1 / \sin\phi_1$, $q = \cos\phi_2 / \sin\phi_2$, we find that ϕ_1 and ϕ_2 are related by

$$\cos\phi_1 \cos\phi_2 = \sin\phi_1 \sin^3\phi_2. \tag{152}$$

We have another exceptional curves, which are described as $p = 0$ and $q = 0$. These curves can be expressed also as $\phi_1 = \pm\frac{\pi}{2}$ and $\phi_2 = \pm\frac{\pi}{2}$, respectively. Note that the parameters $(a_1, 0, 0, b_2) \neq 0$ are mapped to $(\phi_1, \phi_2) = (0, \pm\frac{\pi}{2}), (\pm\pi, \pm\frac{\pi}{2})$, where $\phi_1 = \pi$ and $\phi_1 = -\pi$ are identified, of course. Figure 13 shows the degeneracy set, which forms all boundaries

of the iso-Chern domains in the reduced parameter space $S^1 \times S^1$ for the Hamiltonian (125).

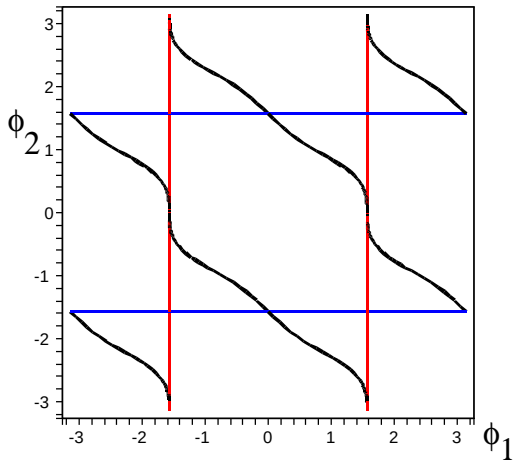

Figure 13: Degeneracy set for Hamiltonian (125) in the space (ϕ_1, ϕ_2) of control parameters. Black curve : degeneracy on six-point generic orbit with C_1 stabilizer. Blue horizontal lines : degeneracy on two three-point orbits with stabilizer C_2. Red vertical lines : degeneracy on one two-point orbit with stabilizer C_3. For intersection points of the horizontal and vertical lines, three orbits of degeneracy points are present : two three-point orbits with stabilizer C_2 and one two-point orbit with stabilizer C_3. The intersection points of black curve and red vertical line one six-point generic orbit with C_1 stabilizer and one two-point orbit with stabilizer C_3 are fused together to form one C_3 orbit with multiple zero. Further, to the intersection points between the curves and the horizontal lines, there corresponds a degeneracy circle consisting of an infinity of D_3 orbits.

In order to complete the construction of the iso-Chern diagram for the Hamiltonian (125), we need to calculate Chern numbers for any representative point from each connected iso-Chern domain. For this purpose, the elementary transformation of the Hamiltonian and the accompanying change in Chern numbers, or a distribution rule of Chern numbers works well, which were discussed in Sec. 6. To see this in the present situation, Figure 14 is of great help. What we have to do is to evaluate Chern numbers assigned to three subregions of the region I. The Chern numbers to be assigned on other subregions are determined from those three by using the distribution rule of Chern numbers.

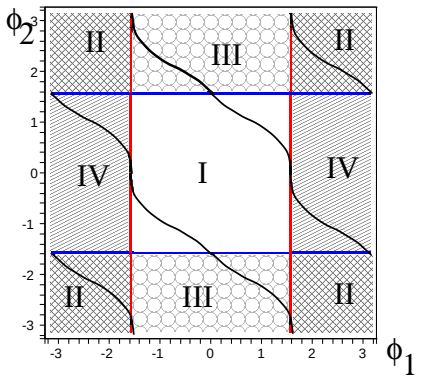

Figure 14: Representation of T^2 space of reduced parameters (ϕ_1, ϕ_2) as a four-fold covering of a space of parameters characterizing system of equations for degeneracy and exceptional points. Four regions I, II, III, IV correspond to identical solutions for degeneracy and for exceptional points. If region I is associated with Hamiltonian H, region II corresponds to $-H$, region IV to $\bar{H}$ which is complex conjugate of H, and region III to $-\bar{H}$.

9.3. Chern numbers and iso-Chern diagram

Detailed calculations for Chern numbers are given in the appendix by using as an example the closed path (**1**) represented in Figure 15. They are done through the explicit calculation of all exceptional points. Winding numbers for exceptional points are found by the linearization method. The present subsection gives short summary of these calculations of Chern numbers and discusses the so obtained complete iso-Chern diagram for D_3-model Hamiltonian (125) depending on four parameters.

In order to see better what kind of change in Chern numbers could be observed for families of Hamiltonians depending on control parameters, we show in Figure 15 the evolution of Chern numbers along different closed paths chosen on the reduced parameter space.

9.3.1. A local coordinate system on the two-torus

Since the parameters (ϕ_1, ϕ_2) on the torus are not convenient for the calculation of Chern numbers for eigen-line bundles for Hamltonian (125), we choose to use another coordinate system defined in the following. In the (a_1, a_2)-plane, we draw a unit circle centered at the origin along with tangent lines to the circle at $(1, 0), (0, -1), (-1, 0), (0, 1)$. These lines serve

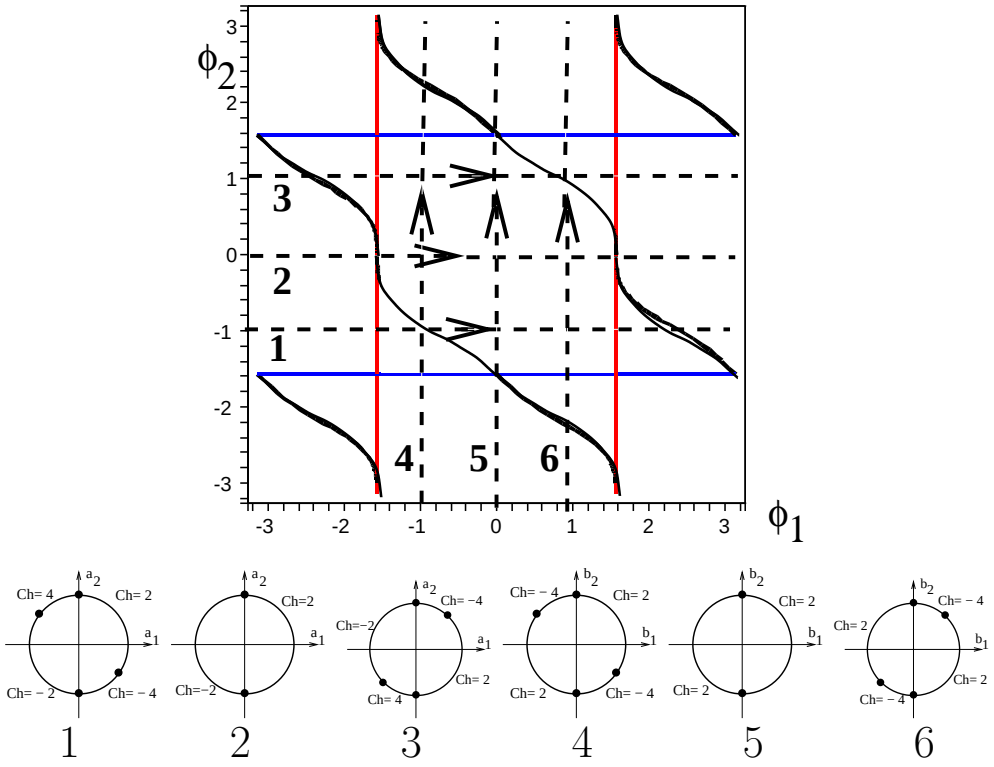

Figure 15: The space of reduced parameters (ϕ_1, ϕ_2) for a model D_3 invariant Hamiltonian (125). The space is a two-dimensional torus represented as a square with identification of points on opposite boundaries. Dash lines 1,2,3,4,5,6 correspond to six closed paths in the space of reduced parameters (ϕ_1, ϕ_2). The evolution of Chern numbers along these closed paths is shown in subfigures $1 - 6$.

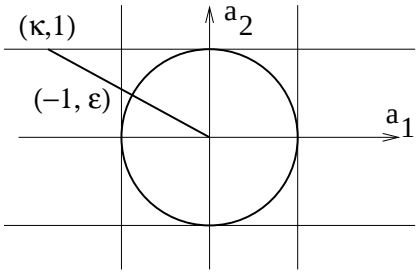

Figure 16: Local coordinate patches (A).

as coordinate patches of the circle. For a given point of a chosen tangent line, we draw the line segment which connect the point to the center of the circle. Then, the intersection point of the line segment with the circle is uniquely determined. In this manner, the tangent line and a half of the circle are in one-to-one correspondence. In order to find the transformation of local coordinates, we take, say, the tangent lines to $(-1, 0)$ and to $(0, 1)$, which are expressed as $(-1, \varepsilon)$ and $(\kappa, 1)$, respectively, where $\varepsilon, \kappa \in \mathbb{R}$. Then, the ε and the κ serve as local coordinates of the circle. The tangent lines $(-1, \varepsilon)$ and $(1, \kappa)$ cover the left and the upper halves of the circle, respectively (see Fig. 16). In the intersection of the left and the upper halves of the circle, two local coordinates are related by

$$\frac{1}{\sqrt{1+\kappa^2}}(\kappa, 1) = \frac{1}{\sqrt{1+\varepsilon^2}}(-1, \varepsilon), \tag{153}$$

from which we find that the coordinate transformation between κ and ε is given by

$$\kappa\varepsilon = -1, \quad \varepsilon > 0, \ \kappa < 0. \tag{154}$$

Other tangent lines also serve as coordinate patches for the circle, and coordinate transformations are found in the same manner as above.

In a similar manner, we can define local coordinates on the unit circle in the (b_1, b_2)-plane. In the (b_1, b_2)-plane, like Fig. (17), we draw a unit circle centered at the origin together with tangent lines to the circle at $(1, 0), (0, -1), (-1, 0), (0, 1)$. In order to find the transformation of local coordinates, we take, say, the tangent lines to $(1, 0)$ and to $(0, 1)$, which are expressed as $(1, \varepsilon)$ and $(\kappa, 1)$, respectively, where $\varepsilon, \kappa \in \mathbb{R}$. Then, the ε and the κ serve as local coordinates of the circle. The tangent lines $(1, \varepsilon)$ and

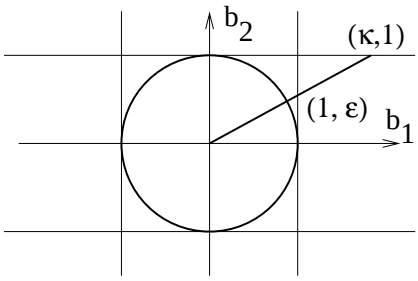

Figure 17: Local coordinate patches (B).

$(1, \kappa)$ cover the right and the upper halves of the circle, respectively (see Fig. 17). In the intersection of the right and the upper halves of the circle, two local coordinates are related by

$$\frac{1}{\sqrt{1+\kappa^2}}(\kappa, 1) = \frac{1}{\sqrt{1+\varepsilon^2}}(1, \varepsilon), \tag{155}$$

from which we find the coordinate transformation between κ and ε

$$\kappa\varepsilon = 1, \quad \varepsilon > 0,\ \kappa > 0. \tag{156}$$

The local coordinate patches

$$\{(1, \lambda_1)\},\ \{(\lambda_2, 1)\},\ \{(-1, \lambda_3)\},\ \{(\lambda_4, -1)\} \tag{157}$$

assigned to S^1 in the (a_1, a_2)-plane and

$$\{(1, \mu_1)\},\ \{(\mu_2, 1)\},\ \{(-1, \mu_3)\},\ \{(\mu_4, -1)\} \tag{158}$$

assigned to S^1 in the (b_1, b_2)-plane are put together to form the products, $\{(1, \lambda_1)\} \times \{(\mu_2, 1)\}$, $\{(\lambda_2, 1)\} \times \{(-1, \mu_3)\}$ *etc.*, as a local coordinate system of the two-torus.

9.3.2. Exceptional points and Chern numbers along a closed path (**1**)

In what follows, we give the results of the evaluation of positions of exceptional points and the values of Chern numbers along the closed path (**1**) on the two-torus which is shown in Fig. 15, leaving the calculations in Appendix. Table 1 gives a summary of the result of calculation for Chern numbers. The parameters ε and κ in the first and the second row are local coordinates attached to the left and the upper halves of the closed path (**1**), respectively.

Table 1: Evolution of exceptional points, sign of diagonal matrix element, and corresponding Chern numbers for closed path (**1**). Parameters ε and κ are related to ϕ_1, ϕ_2 as $\phi_1 = \pi - \arctan\varepsilon$, $\phi_2 = \pi/2 - \arctan\kappa$. Positions of exceptional points on the sphere are shown in Figure 18. The details of calculations are given in the Appendix.

	$\varepsilon \le -\frac{100}{27}$	$-\frac{100}{27} < \varepsilon < \frac{4}{9}$	$\frac{4}{9} \le \varepsilon < \frac{26}{27}$	$\varepsilon = \frac{26}{27}$	$\frac{26}{27} < \varepsilon$			
		$\kappa < -\frac{9}{4}$	$-\frac{9}{4} \le \kappa < -\frac{27}{26}$	$\kappa = -\frac{27}{26}$	$-\frac{27}{26} < \kappa < 0$	$\kappa = 0$	$0 < \kappa < \frac{27}{100}$	$\frac{27}{100} < \kappa$
$\boldsymbol{e}_\pm$	+	+	+	0	−	0	+	+
$\boldsymbol{n}_\pm$	−	−	−	−	−	−	−	−
$\boldsymbol{a}_\pm, \boldsymbol{b}_\pm$	+	(*empty*)	−	0	+	+	+	(*empty*)
Chern number	−2	−2	−2	*not defined*	4	*not defined*	2	2

On the overlapped interval of respective parameters, the coordinate change (154) is used to identify corresponding subintervals with each other. These two parameters are put together to cover three quarters of the circle (**1**). In the bottom row of Table 1, along this three-quarter circle, the Chern numbers are given for the eigen-line bundle associated with a positive eigenvalue of Hamiltonian (125). Though this table does not cover all Chern numbers along the closed path (**1**), we can determine the other Chern numbers, as is shown in subfigure 15.1, by using a shift law for Chern numbers, which we will explain in the following subsection. (In Appendix, the missing quarter of the circle (**1**) is treated by the method similar to the shift law touched upon above.) The third row of Table 1 gives exceptional points denoted by $\boldsymbol{e}_\pm, \boldsymbol{n}_\pm$, $\boldsymbol{a}_\pm$, and $\boldsymbol{b}_\pm$ together with signs which indicate that each of them is positive or negative exceptional point. When the parameter takes special values, the number zero is placed at due positions of the row, which means that the exceptional points in question become degeneracy points at each of those moments. For example, if $\varepsilon = 26/27$ or $\kappa = -27/26$, the $\boldsymbol{e}_\pm$, $\boldsymbol{a}_\pm$, and $\boldsymbol{b}_\pm$ become degeneracy points, and thereby no Chern numbers are defined.

From the expression of these exceptional points given in Appendix, we observe that there are three types of exceptional points. The exceptional points $\boldsymbol{n}_\pm$ are independent of the parameter modifications. They are fixed at $(x = \pm 1, y = 0, z = 0)$ points of the sphere. Second pair of exceptional points, namely $\boldsymbol{e}_\pm$, is located on the great circle $x = 0$ of the sphere. These two points remain always antipodal to each other. They exist for all values of parameters and go along the great circle when the parameters follow the path (**1**). Finally, the quadruple $(\boldsymbol{a}_\pm, \boldsymbol{b}_\pm)$ of exceptional points exist only for some

subset of parameter values corresponding to path (**1**). These four exceptional points appear through a bifurcation at $\boldsymbol{n}_\pm$ points and then annihilate in pairs when arriving at $x = 0$ plane. All positions of these exceptional points at different values of parameters are plotted in Figure 18. Figure 18 represents the sphere as projections of two hemispheres $z \geq 0$ and $z \leq 0$ on the plane $z = 0$. All the positions of $\boldsymbol{a}_\pm, \boldsymbol{b}_\pm$ points form ellipsoidal curves.

Figure 18 remains qualitatively the same even if the position of the path (**1**) moves to another values of ϕ_2 parameter. As soon as ϕ_2 approaches $\phi_2 = -\pi/2$ the interval of ϕ_1 values for which the quadruple of exceptional points $\boldsymbol{a}_\pm, \boldsymbol{b}_\pm$ exists shrinks to $\phi_1 = 0$ and the whole circle of exceptional points defined by $z = 0$ exists for $\phi_1 = 0$, $\phi_2 = -\pi/2$ point in the parameter space. However, this circle should be referred to as a degeneracy curve, as we see from (130). We note here that degeneracy points are special ones of exceptional points. If, on another way, ϕ_2 approaches $\phi_2 = 0$, the set of exceptional points approaches the circle $y = 0$ and for the $\phi_1 = -\pi/2$, $\phi_2 = 0$ point in the parameter space we get the whole circle of exceptional points defined on the sphere by $x^2 + z^2 = 1$, but two points $z = \pm 1$ of this circle should be referred to as degeneracy points.

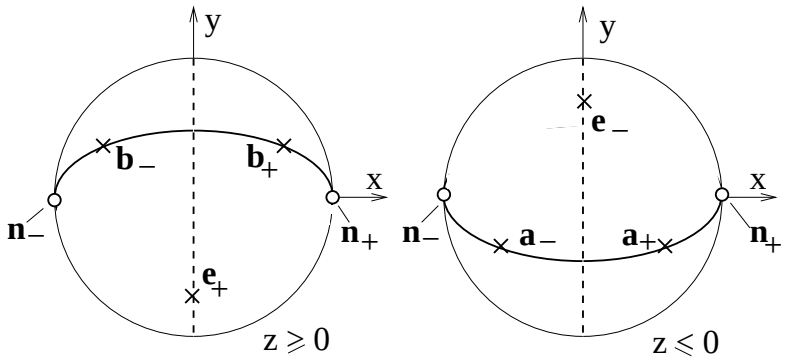

Figure 18: Positions of exceptional points on the sphere along the closed path **1** represented in Fig. 15. The sphere is shown through projections of its north ($z \geq 0$) and south ($z \leq 0$) hemispheres on the plane $\{x, y\}$. The $\boldsymbol{n}_+$ and $\boldsymbol{n}_-$ as exceptional points are fixed and present for all points along the path **1**. Positions of $\boldsymbol{e}_+$ and $\boldsymbol{e}_-$ exceptional points are shown by dash line. The $\boldsymbol{e}_+ = -\boldsymbol{e}_-$ move along the great circle. Projections of the points $\boldsymbol{a}_\pm, \boldsymbol{b}_\pm$ on the $\{x, y\}$ plane move along ellipsoidal curve shown by solid line. These four points appears by bifurcating from $\boldsymbol{n}_\pm$ points at $\kappa = -9/4$ and disappears through bifurcation at $\kappa = 27/100$ at $x = 0$ point of the solid curve.

9.3.3. The iso-Chern diagram

We here give a shift law for Chern numbers on the iso-Chern diagram, using the results in Sec. 6.2. From the point of view of the Hamiltonian (125) the transformation $(a_1, a_2, b_1, b_2) \mapsto (-a_1, -a_2, b_1, b_2)$ corresponds to modification $H \mapsto \bar{H}$, where $\bar{H}$ is a complex conjugate to H. The transformation $(a_1, a_2, b_1, b_2) \mapsto (-a_1, -a_2, -b_1, -b_2)$ corresponds to modification $H \mapsto -H$, and the transformation $(a_1, a_2, b_1, b_2) \mapsto (a_1, a_2, -b_1, -b_2)$ corresponds to modification $H \mapsto -\bar{H}$ (see Figure 14). On the other hand, the transformations $(a_1, a_2) \mapsto (-a_1, -a_2)$ and $(b_1, b_2) \mapsto (-b_1, -b_2)$ correspond to the transformations $\phi_1 \mapsto \phi_1 \pm \pi$ and $\phi_2 \mapsto \phi_2 \pm \pi$ on the two-torus, respectively. From the results obtained in Sec. 6.2, it follows that according as the shift operations on the torus

$$(\phi_1, \phi_2) \mapsto (\phi_1 \pm \pi, \phi_2) \quad \text{or} \quad (\phi_1, \phi_2) \mapsto (\phi_1, \phi_2 \pm \pi), \tag{159}$$

the Chern number assigned to (ϕ_1, ϕ_2) undergoes a change in sign or is kept unchanged. This gives a shift law for Chern numbers on our iso-Chern diagram. Using this law, we can determine the Chern numbers along the whole closed curve (**1**), as is shown in subfigure 15.1. Further, since the curve (**1**) passes the lower left and center subregions of the region I, we can determine Chern numbers on the iso-Chern domains to which the lower left and the central subregions of the region I are shifted by the transformations (159). However, the curve (**1**) does not pass the upper right subregion, and hence in order to complete the iso-Chern diagram, we have to find the Chern number to be assigned to the upper right subregion of the region I in Fig. 14. For this purpose, we choose the closed curve (**3**) in Fig. 15 for the Chern number evaluation. Like Table 1, after a straightforward calculation, which we do not give here, we obtain the following table as the result of the evaluation of Chern numbers along the upper half of the closed curve (**3**).

From Table 2, we see that the Chern number to be assigned to the upper right subregion of the region I is -4. Now we can make out the iso-Chern diagram by using the above-shown shift law together with the Chern numbers so far obtained.

Proposition 2. For the D_3 invariant Hamiltonian (125), the reduced parameter space is the two torus on which the iso-Chern diagram for the eigen-line bundle associated with positive eigenvalue is described as is shown in Fig. 19. The iso-Chern diagram for the eigen-line bundle associated with negative eigenvalue is obtained by opposing the sign of the Chern number assigned to each iso-Chern domain.

Table 2: Evolution of exceptional points, signs of the diagonal matrix element, and corresponding Chern numbers for the upper half of the closed path (**3**).

	$\kappa < -\frac{27}{100}$	$-\frac{27}{100} \le \kappa < 0$	$\kappa = 0$	$0 < \kappa < \frac{27}{26}$	$\kappa = \frac{27}{26}$	$\frac{27}{26} < \kappa \le \frac{9}{4}$	$\frac{9}{4} < \kappa$
$\boldsymbol{e}_\pm$	$-$	$-$	0	$+$	0	$-$	$-$
$\boldsymbol{n}_\pm$	$+$	$+$	$+$	$+$	$+$	$+$	$+$
$\boldsymbol{a}_\pm, \boldsymbol{b}_\pm$	$(empty)$	$-$	$-$	$-$	0	$+$	$(empty)$
Chern number	-2	-2	$not\ defined$	-4	$not\ defined$	2	2

(160)

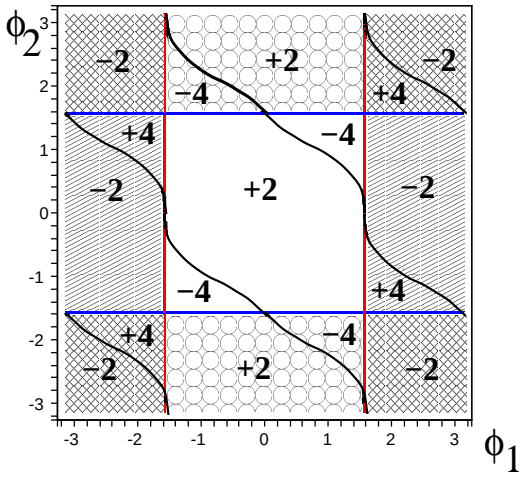

Figure 19: Complete iso-Chern diagram for D_3 invariant Hamiltonian (125). In each iso-Chern domain the Chern number for eigen-line bundle with positive eigenvalue is indicated. Chern number for eigen-line bundle associated with negative eigenvalue has opposite sign.

10. Conclusion

We have analysed in this paper the consequences imposed by symmetry on the possible values of topological Chern numbers for energy bands and on their allowed modifications. The analysis is made essentially in the semi-quantum model which has a finite number of quantum states describing quantum subsystem which is supposed to be in interaction with classical subsystem described by classical variables defined over classical phase space with prescribed topology. An important assumption is the two level approximation leading within the semi quantum model to effective Hamiltonian linear in $SU(2)$ generators, and the $S^2 \sim \mathbb{C}P^1$ topology of the classical phase space corresponding to physical example of rotational structure for two vibrational states.

Under these assumptions after giving the symmetry group of the problem (which defines in its turn the action on quantum states and on classical variables) we have obtained that only some special integers (depending on the symmetry group) could appear as Chern numbers for individual eigenline bands. The results for the $SO(2)$ and D_3 symmetry Hamiltonian models are given in Propositions 1 and 2, respectively.

Here in conclusion, we try to formulate several important generalizations and possible further steps in the study of qualitative description of bands and their rearrangements.

It is necessary to find mathematical justification for selection rules for possible Chern numbers in the presence of symmetry which follows from the purely group theoretical analysis of band decompositions for quantum molecular problems formulated in [48, 47, 24] in terms of the numbers of states in bands. Combining these selection rules with the correspondence between Chern numbers for semi-quantum model and exact numbers of quantum states for corresponding purely quantum problem [13, 14, 15] leads to results confirmed by explicit calculation of Chern numbers on concrete examples in the present paper. In particular, for D_3 invariant model with two quantum states transforming according to two-dimensional E-type representation the direct application of group theoretical selection rules [48, 47] gives the following restrictions on the possible values of Chern numbers: $\mathrm{Ch} = \pm 2 \bmod 6$. We have found for four-parameter model ± 2 and ± 4 as possible values. Adding higher degree terms (namely fourth degree in elementary rotational variables) in the Hamltonian enables us to find iso-Chern domains in the parameter

Table 3: Codimension of eigenvalue degeneracies for complex Hermitian matrices under the absence of symmetry.

Degeneracy	$\lambda_i = \lambda_j$	$\lambda_i = \lambda_j$ $\lambda_k = \lambda_l$	$\lambda_i = \lambda_j = \lambda_k$	$\lambda_i = \lambda_j$ $\lambda_k = \lambda_l$ $\lambda_m = \lambda_n$	$\lambda_i = \lambda_j$ $\lambda_k = \lambda_l = \lambda_m$
Codimension	3	6	8	9	11

space with Chern numbers ± 8. Nevertheless the systematic proof of this selection rule remains an open problem.

One of the possible ways to generalize the model is to consider several quantum states but to keep the dimension and the topology of the classical phase space unchanged. In order to preserve under such generalization the generic character of the model we need to include in the model nonlinear terms in $SU(2)$ generators. The constructed $N \times N$ matrix of N-state model in such a case will have exactly the same codimension of degeneracies as two-state problem taking into account the symmetry of quantum states. In a generic way the rearrangement of bands can take place for one-parameter families of Hamiltonians at isolated values of control parameter.

Another possible way of a generalization is to go to models with classical subsystems being described by phase space of higher dimension (and naturally of different topology). In this case the complex dimension of a base space is larger than 1 and new effects appear if the number of quantum states taken into account is sufficiently large.

The most important new feature is the appearance of non-decomposable bands associated with several quantum states. The appearance of such bands follows directly from the comparison of codimension of degeneracy points listed in table 3 with the dimension of base space. In order to characterize bands topologically for higher dimensional base spaces the first Chern class is insufficient and higher Chern classes appear naturally. Example of such three-state model over classical phase space with $\mathbb{C}P^2$ topology was studed in [16]. The study of symmetry effects for such multi-state problems with non-trivial topology of highly-dimensional classical phase space is completely open problem.

Appendix A. Calculation of Chern numbers for D_3 model Hamiltonian

We calculate in this appendix the Chern numbers along a closed path defined by $(a_1, a_2) = (\cos\phi_1, \sin\phi_1)$ and $(b_1, b_2) = (\frac{2}{\sqrt{13}}, -\frac{3}{\sqrt{13}})$ in the parameter space. This path is denoted by **1** in Figure 15. For the sake of simplicity in the notation, we choose to take the local coordinates defined in (157) and (158). With a bit change of parameters, we then treat the Hamiltonian (125) in terms of the parameters

$$a_1 = -1, \quad a_2 = \varepsilon, \quad b_1 = 1, \quad b_2 = -\frac{3}{2}. \tag{A.1}$$

The equations for exceptional points in this case are given by

$$x(2y + \frac{3}{2}z) = 0, \quad z - \varepsilon y(y^2 - 3x^2) = 0. \tag{A.2}$$

From the first equation of (A.2) we see that there are two cases: (i) $x = 0$ and (ii) $2y + \frac{3}{2}z = 0$.
(i) If $x = 0$, then the second equation of (A.2) becomes $z = \varepsilon y^3$. Then, the constraint condition yields the equation $1 = y^2(1 + \varepsilon^2 y^4)$, which is solved by $\pm\alpha$, where α is determined uniquely as the only real solution of $\alpha(1+\varepsilon^2\alpha^2) = 1$, since the function $f(s) = s(1+\varepsilon^2 s^2)$ is monotone increasing in s. We note also that the α depends on the parameter ε. Thus, we have obtained the exceptional points

$$\boldsymbol{e}_+ := \begin{pmatrix} 0 \\ \alpha^{1/2} \\ \varepsilon\alpha^{3/2} \end{pmatrix}, \quad \boldsymbol{e}_- := \begin{pmatrix} 0 \\ -\alpha^{1/2} \\ -\varepsilon\alpha^{3/2} \end{pmatrix}. \tag{A.3}$$

(ii) If $2y + \frac{3}{2}z = 0$, then the second equation of (A.2) becomes $-\frac{4}{3}y - \varepsilon y(y^2 - 3x^2) = 0$. If $y = 0$, then $z = 0$, so that $x = \pm 1$ because of the constraint condition. Thus we have obtained the exceptional points,

$$\boldsymbol{n}_\pm := \begin{pmatrix} \pm 1 \\ 0 \\ 0 \end{pmatrix}. \tag{A.4}$$

If $y \neq 0$, then the second equation of (A.2) reduces to $-\frac{4}{3} = \varepsilon(y^2 - 3x^2)$. In this case, the constraint condition provides $\frac{28}{9}y^2 = 1 - \frac{4}{9\varepsilon}$. If $\varepsilon > \frac{4}{9}$, then the

right-hand side of this equation is positive, and we have non-zero solutions $y = \pm\frac{3}{2\sqrt{7}}\sqrt{1-\frac{4}{9\varepsilon}}$, so that $z = \mp\frac{2}{\sqrt{7}}\sqrt{1-\frac{1}{\varepsilon}\frac{4}{9}}$. Then, the constraint condition provides the equation for x, $x^2 = \frac{3}{28}+\frac{1}{\varepsilon}\frac{25}{63}$, which is solved by $x = \pm\sqrt{\frac{3}{28}+\frac{1}{\varepsilon}\frac{25}{63}}$ if $-\frac{100}{27} < \varepsilon$. From the above results, it follows that if $-\frac{100}{27} < \varepsilon < \frac{4}{9}$, there are no real solutions of the present type, but for $\varepsilon \le -\frac{100}{27}$ or $\varepsilon \ge \frac{4}{9}$, we have the exceptional points,

$$\boldsymbol{a}_\pm := \begin{pmatrix} \pm\sqrt{\frac{3}{28}+\frac{1}{\varepsilon}\frac{25}{63}} \\ \frac{3}{2\sqrt{7}}\sqrt{1-\frac{4}{9\varepsilon}} \\ -\frac{2}{\sqrt{7}}\sqrt{1-\frac{4}{9\varepsilon}} \end{pmatrix}, \quad \boldsymbol{b}_\pm := \begin{pmatrix} \pm\sqrt{\frac{3}{28}+\frac{1}{\varepsilon}\frac{25}{63}} \\ -\frac{3}{2\sqrt{7}}\sqrt{1-\frac{4}{9\varepsilon}} \\ \frac{2}{\sqrt{7}}\sqrt{1-\frac{4}{9\varepsilon}} \end{pmatrix} \qquad \text{(A.5)}$$
$$\text{for} \quad \varepsilon \le -\tfrac{100}{27} \quad \text{or} \quad \varepsilon \ge \tfrac{4}{9}.$$

In particular, if $\varepsilon = \frac{4}{9}$, the exceptional points $\boldsymbol{a}_\pm$ and $\boldsymbol{b}_\pm$ coincide with each other and equal $\boldsymbol{n}_\pm$.

The next task for us to do is to determine $U_{\rm up}$ and $U_{\rm down}$. To this end, we examine the sign of the values of

$$F = y^2 - x^2 - \frac{3}{2}zy \qquad \text{(A.6)}$$

for the exceptional points obtained, where F is the left upper element of the Hamiltonian matrix. An exceptional point is assigned to $U_{\rm up}$ or $U_{\rm down}$, according to whether $F > 0$ or $F < 0$ for that point.

First we take up (A.3). We then need to find the sign of $F(\boldsymbol{e}_\pm) = \alpha - \frac{3}{2}\varepsilon\alpha^2$. To this end, we set $f(s) = s(1+\varepsilon^2 s^2)$ and $g(s) = s - \frac{3}{2}\varepsilon s^2$. Our task becomes to find the sign of $g(\alpha)$. By the definition of α, one has $f(\alpha) = 1$. It is easy to see that $g(0) = g(\frac{2}{3\varepsilon}) = 0$. Now we have $f(\frac{2}{3\varepsilon}) = \frac{26}{27}\frac{1}{\varepsilon}$. First we consider the case of $\varepsilon > 0$. If $f(\frac{2}{3\varepsilon}) > 1 = f(\alpha)$, then $\alpha < \frac{2}{3\varepsilon}$. This is because the function $f(s)$ is monotone increasing. Since $g(s) > 0$ for $0 < s < \frac{2}{3\varepsilon}$, we see that $g(\alpha) = \alpha - \frac{3}{2}\varepsilon\alpha^2 > 0$ for $< \alpha < \frac{2}{3\varepsilon}$. It turn out that if $\frac{26}{27}\frac{1}{\varepsilon} > 1$ or $\varepsilon < \frac{26}{27}$, then $g(\alpha) > 0$. Contrarily, if $\varepsilon > \frac{26}{27}$, then $f(\frac{2}{3\varepsilon}) < 1 = f(\alpha)$, so that we verify that $\frac{2}{3\varepsilon} < \alpha$. Since $g(s) < 0$ for $s > \frac{2}{3\varepsilon}$, we find that $g(\alpha) = \alpha - \frac{3}{2}\varepsilon\alpha^2 < 0$ if $\varepsilon > \frac{26}{27}$. In the case of $\varepsilon < 0$, we see easily that $g(s) < 0$ for $s > 0$, so that $g(\alpha) = \alpha - \frac{3}{2}\varepsilon\alpha^2 < 0$.

We turn to the exceptional points (A.5). For $\boldsymbol{a}_\pm$ and $\boldsymbol{b}_\pm$, we obtain $F(\boldsymbol{a}_\pm) = F(\boldsymbol{b}_\pm) = \frac{6}{7\varepsilon}(\varepsilon - \frac{26}{27})$, and for $\boldsymbol{n}_\pm$ we have $F(\boldsymbol{n}_\pm) = -1 < 0$.

In a summary, the sign of the value of $F = y^2 - x^2 - \frac{3}{2}zy$ for each of the exceptional points and for all studied intervals of ε-parameter values is listed up in the table 1 given in the main text, section 9.

It is to be noted that $F(\boldsymbol{e}_\pm) = F(\boldsymbol{a}_\pm) = F(\boldsymbol{b}_\pm) = 0$ at $\varepsilon = \frac{26}{27}$. This means that the points $\boldsymbol{e}_\pm$, $\boldsymbol{a}_\pm$, $\boldsymbol{b}_\pm$ become degeneracy points at the moment of $\varepsilon = \frac{26}{27}$. This can be also verified as follows: For $\varepsilon = \frac{26}{27}$, the reduced parameters take the values $p = a_1/a_2 = -\frac{27}{26}$ and $q = b_1/b_1 = -\frac{2}{3}$, which satisfy $pq(1+q^2) = 1$. This implies that the line $(p, q) = (-\frac{1}{\varepsilon}, -\frac{2}{3})$ with the parameter ε crosses the degeneracy curve $pq(1+q^2) = 1$ at $(-\frac{27}{26}, -\frac{2}{3})$. In addition, we note also that at the moment of $\varepsilon = \frac{26}{27}$, the six degeneracy points $\boldsymbol{e}_\pm$, $\boldsymbol{a}_\pm$, $\boldsymbol{b}_\pm$ are expressed as

$$\boldsymbol{e}_+ = \begin{pmatrix} 0 \\ \frac{3}{\sqrt{13}} \\ \frac{2}{\sqrt{13}} \end{pmatrix}, \ \boldsymbol{e}_- = \begin{pmatrix} 0 \\ -\frac{3}{\sqrt{13}} \\ -\frac{2}{\sqrt{13}} \end{pmatrix}, \ \boldsymbol{a}_\pm = \begin{pmatrix} \pm\frac{3}{2}\sqrt{\frac{3}{13}} \\ \frac{3}{2\sqrt{13}} \\ -\frac{2}{\sqrt{13}} \end{pmatrix}, \ \boldsymbol{b}_\pm = \begin{pmatrix} \pm\frac{3}{2}\sqrt{\frac{3}{13}} \\ -\frac{3}{2\sqrt{13}} \\ \frac{2}{\sqrt{13}} \end{pmatrix}. \tag{A.7}$$

The set of three points $\{\boldsymbol{e}_+, \boldsymbol{b}_\pm\}$ and that of $\{\boldsymbol{e}_+, \boldsymbol{a}_\pm\}$ form triangles, respectively. Each triple corresponds to one orbit of the C_3 subgroup of the D_3 group with trivial stabilizer. All six points together form one six-point orbit of the symmetry group D_3 with trivial stabilizer.

According to the sign of F for the exceptional points, we find the following four types of domains;

$$U_{\rm up} = S^2 - \{\boldsymbol{e}_\pm, \boldsymbol{a}_\pm, \boldsymbol{b}_\pm\}, \quad U_{\rm down} = S^2 - \{\boldsymbol{n}_\pm\} \quad \text{for } \varepsilon \le -\frac{100}{27}, \tag{A.8}$$

$$U_{\rm up} = S^2 - \{\boldsymbol{e}_\pm\}, \quad U_{\rm down} = S^2 - \{\boldsymbol{n}_\pm\} \quad \text{for } -\frac{100}{27} < \varepsilon < \frac{4}{9}, \tag{A.9}$$

$$U_{\rm up} = S^2 - \{\boldsymbol{e}_\pm\}, \ U_{\rm down} = S^2 - \{\boldsymbol{n}_\pm, \boldsymbol{a}_\pm, \boldsymbol{b}_\pm\} \quad \text{for } \frac{4}{9} \le \varepsilon < \frac{26}{27}, \tag{A.10}$$

$$U_{\rm up} = S^2 - \{\boldsymbol{a}_\pm, \boldsymbol{b}_\pm\}, \quad U_{\rm down} = S^2 - \{\boldsymbol{n}_\pm, \boldsymbol{e}_\pm\} \quad \text{for } \varepsilon > \frac{26}{27}. \tag{A.11}$$

To evaluate the Chern number, we take the linearization method explained in Sec. 6.2. Let $X = a_{12}$ and $Y = b_{12}$, the real and the imaginary parts of the upper off-diagonal element of the Hamiltonian matrix;

$$X = x(2y + \frac{3}{2}z), \quad Y = z - \varepsilon y(y^2 - 3x^2). \tag{A.12}$$

Note that the transition function on $U_{\rm up} \cap U_{\rm down}$ is expressed as $\Phi = \epsilon(X + iY)/\sqrt{X^2+Y^2}$ with $\epsilon = \pm 1$.

In the case of $\varepsilon \leq -\frac{100}{27}$, we draw two circles C_1 and C_2 on the levels $x = \pm h$ with $\sqrt{\frac{3}{28}} < h < 1$, respectively. The circles divide the sphere into three regions. We denote by S^2_+ the union of the regions which contain either of $\boldsymbol{n}_\pm$, and by S^2_- the region which contains the equator. The orientation of C_1 and that of C_2 are in keeping with the orientation of S^2_+. We take (y, z) as local coordinates and view x as a height function. Then, the first-order derivatives of X, Y with respect to (y, z) are

$$\frac{\partial X}{\partial y} = -\frac{y}{x}(2y + \frac{3}{2}z) + 2x, \quad \frac{\partial X}{\partial z} = -\frac{z}{x}(2y + \frac{3}{2}z) + \frac{3}{2}x, \tag{A.13a}$$

$$\frac{\partial Y}{\partial y} = 3\varepsilon(-3y^2 + x^2), \quad \frac{\partial Y}{\partial z} = 1 - 6\varepsilon yz. \tag{A.13b}$$

Then, the determinant of the coefficient matrix of the linearlized vector is evaluated at $\boldsymbol{n}_\pm$ as

$$\det \begin{pmatrix} \frac{\partial X}{\partial y} & \frac{\partial X}{\partial z} \\ \frac{\partial Y}{\partial y} & \frac{\partial Y}{\partial z} \end{pmatrix} = \begin{vmatrix} 2x & \frac{3}{2}x \\ 3\varepsilon & 1 \end{vmatrix} = 2x(1 - \frac{9}{4}\varepsilon), \tag{A.14}$$

where x denotes the x-component of $\boldsymbol{n}_\pm$. Since $\varepsilon \leq -\frac{100}{27}$, the right-hand side of the above equation is positive or negative, according as $x = 1$ or $x = -1$. Hence, the winding number of C_1 for $\boldsymbol{n}_+$ is $+1$. Since the local coordinate system (y, z) is negatively oriented against the orientation of the hemisphere with $x < 0$, the winding number of C_2 for $\boldsymbol{n}_-$ is $+1$ as well. Thus, the sum of the winding numbers is $+2$, so that the Chern number is -2.

We now consider the case of $-\frac{100}{27} < \varepsilon < \frac{4}{9}$. Since no degeneracy points appear as ε passes the number $\varepsilon = -\frac{100}{27}$, the Chern number should remain to be the same though the points $\boldsymbol{a}_\pm$ and $\boldsymbol{b}_\pm$ disappear. We verify this fact by evaluating the Chern number. We draw two circles C_1 and C_2 on the levels $x = \pm h$ with $0 < h < 1$, respectively. The circles divide the sphere into three regions. As in the case of $\varepsilon \leq -\frac{100}{27}$, we denote by S^2_+ the union of the regions which contain either of $\boldsymbol{n}_\pm$, and by S^2_- the region which contains the equator. The orientation of C_1 and that of C_2 are in keeping with the orientation of S^2_+. We take the linearization method as well. Taking (y, z) as local coordinates, we obtain the same determinant evaluated at $\boldsymbol{n}_\pm$ as in the case of $\varepsilon < -\frac{100}{27}$. Since $-\frac{100}{27} < \varepsilon < \frac{4}{9}$, the sign of the right-hand side

of (A.14) is the same as in the case of $\varepsilon \leq -\frac{100}{27}$, so that the same reasoning can be made to result in the same Chern number -2.

We turn to the case of $\frac{4}{9} \leq \varepsilon < \frac{26}{27}$. We draw two circles C_1 and C_2 which are located on the levels $x = \pm h$, where $0 < h < \frac{3}{2}\sqrt{\frac{3}{13}}$. Here, we note that $\frac{3}{2}\sqrt{\frac{3}{13}} < \sqrt{\frac{3}{28} + \frac{1}{\varepsilon}\frac{25}{63}}$ for $\frac{4}{9} < \varepsilon < \frac{26}{27}$. The circles divide the sphere into three regions. We use the notation S^2_+ and S^2_- in a similar manner to the above. The S^2_+ is the union of the two regions which contains either the exceptional points $\boldsymbol{a}_+, \boldsymbol{b}_+, \boldsymbol{n}_+$ or $\boldsymbol{a}_-, \boldsymbol{b}_-, \boldsymbol{n}_-$. The S^2_- is the region containing the equator. We take (z, x) as local coordinates in view of the position of $\boldsymbol{e}_\pm$ and look on y as a height function. The first-order derivatives of X, Y with respect to z, x are

$$\frac{\partial X}{\partial z} = -2\frac{xz}{y} + \frac{3}{2}x, \quad \frac{\partial X}{\partial x} = 2y + \frac{3}{2}z - 2\frac{x^2}{y}, \tag{A.15a}$$

$$\frac{\partial Y}{\partial z} = 1 + 3\varepsilon yz - 3\varepsilon\frac{zx^2}{y}, \quad \frac{\partial Y}{\partial x} = 9\varepsilon yx - 3\varepsilon\frac{x^3}{y}. \tag{A.15b}$$

For the exceptional points $\boldsymbol{e}_\pm$ given in (A.3), we have

$$\det\begin{pmatrix} \frac{\partial X}{\partial z} & \frac{\partial X}{\partial x} \\ \frac{\partial Y}{\partial z} & \frac{\partial Y}{\partial x} \end{pmatrix} = \begin{vmatrix} 0 & 2\alpha^{1/2} + \frac{3}{2}\varepsilon\alpha^{3/2} \\ 1 + 3\varepsilon^2\alpha^2 & 0 \end{vmatrix} < 0, \tag{A.16}$$

and

$$\det\begin{pmatrix} \frac{\partial X}{\partial z} & \frac{\partial X}{\partial x} \\ \frac{\partial Y}{\partial z} & \frac{\partial Y}{\partial x} \end{pmatrix} = \begin{vmatrix} 0 & -2\alpha^{1/2} - \frac{3}{2}\varepsilon\alpha^{3/2} \\ 1 + 3\varepsilon^2\alpha^2 & 0 \end{vmatrix} > 0, \tag{A.17}$$

respectively. The local coordinate system (z, x) is positively oriented on the hemisphere with $y > 0$ in which $\boldsymbol{e}_+$ is included, but negatively oriented on the hemisphere with $y < 0$ in which $\boldsymbol{e}_-$ is included. However, the orientation of small circles centered at respective exceptional points are clockwise. Thus, we observe that the winding numbers associated with $\boldsymbol{e}_\pm$ are both 1 and summed up to be 2. The Chern number is then -2 in this case. Thus, we have verified that the Chern number is the same as in the case of $\varepsilon < \frac{4}{9}$.

We proceed to the case of $\varepsilon > \frac{26}{27}$. We draw two circles C_1 and C_2 in a bit different manner from that in the above two cases. The circles C_1 and C_2 enclose the exceptional points $\boldsymbol{a}_\pm$ in the hemisphere with $y > 0$ and $\boldsymbol{b}_\pm$ in the hemisphere with $y < 0$, respectively. The circles divide the sphere into three regions. We denote by S^2_+ the middle of the three and by S^2_- the union

of the remaining two. The region S^2_+ then contains the exceptional points $\boldsymbol{n}_\pm$ and $\boldsymbol{e}_\pm$ and the S^2_- contains $\boldsymbol{a}_\pm$ and $\boldsymbol{b}_\pm$. In view of the positions of the exceptional points $\boldsymbol{a}_\pm$ and $\boldsymbol{b}_\pm$, we take (z, x) as local coordinates and look on y as a height function. From (A.15) we verify that the determinant of the coefficient matrix of the linearized vector is evaluated at $\boldsymbol{a}_\pm$ and $\boldsymbol{b}_\pm$ as

$$\det \begin{pmatrix} \frac{\partial X}{\partial z} & \frac{\partial X}{\partial x} \\ \frac{\partial Y}{\partial z} & \frac{\partial Y}{\partial x} \end{pmatrix} = \begin{vmatrix} -2\frac{z}{y}x + \frac{3}{2}x & 2y + \frac{3}{2}z - 2\frac{x^2}{y} \\ 1 + 3\varepsilon yz - 3\varepsilon\frac{z}{y}x^2 & 9\varepsilon yx - 3\varepsilon\frac{x^3}{y} \end{vmatrix} = \frac{x^2}{y}(9\varepsilon - 4), \quad \text{(A.18)}$$

where y and x are y- and x-components of $\boldsymbol{a}_\pm$ or $\boldsymbol{b}_\pm$. Since $\varepsilon > \frac{4}{9}$, the right-hand side of the above equation is positive or negative according to whether the y-component of $\boldsymbol{a}_\pm$ or $\boldsymbol{b}_\pm$ is positive or negative. Since the y-component of $\boldsymbol{a}_\pm$ is positive and that of $\boldsymbol{b}_\pm$ is negative, we find that the determinant is positive for $\boldsymbol{a}_\pm$ and negative for $\boldsymbol{b}_\pm$. Since the orientation of small circles centered at $\boldsymbol{a}_\pm$ is negative, the winding numbers for $\boldsymbol{a}_\pm$ are both -1. Taking into account the fact that the (z, x)-coordinate system is negatively oriented against the sphere in the neighborhood of $\boldsymbol{b}_\pm$, we observe that the total winding number is -4, so that the Chern number is 4.

In a summary, we have extended the table of signs of $F = y^2 - x^2 - \frac{3}{2}zy$ for the exceptional points by calculating corresponding Chern numbers (see table 1 of section 9).

We are interested in what happens to the exceptional points in the limit as $\varepsilon \to \infty$. We first consider the exceptional points $\boldsymbol{e}_\pm$ given in (A.3). If $\varepsilon \to \infty$, then the α as a real solution to $1 = s + \varepsilon^2 s^3$ tends to 0. Since the relation $1 = \alpha + \varepsilon^2\alpha^3$ is preserved in the process of $\varepsilon \to \infty$, we observe that $\varepsilon^2\alpha^3 \to 1$. It then follows from (A.3) that

$$\boldsymbol{e}_\pm \to \begin{pmatrix} 0 \\ 0 \\ \pm 1 \end{pmatrix} \quad \text{as } \varepsilon \to \infty. \qquad \text{(A.19)}$$

For these limit points, we see that $F = y^2 - x^2 - \frac{3}{2}zy = 0$, which implies that the above points (A.19) become degeneracy points as $\varepsilon \to \infty$. This can be verified also by letting $\alpha \to 0$ in the expression $\alpha - \frac{3}{2}\varepsilon\alpha^2$. In fact, we obtain $\alpha - \frac{3}{2}\varepsilon\alpha^2 = \alpha - \frac{3}{2}\varepsilon\alpha^{3/2}\alpha^{1/2} \to 0$ as $\varepsilon \to \infty$. Note also that the points $\boldsymbol{e}_\pm$ given in (A.19) form two-point orbit of the group D_3 with stabilizer C_3.

We turn to the exceptional points $\boldsymbol{a}_\pm, \boldsymbol{b}_\pm$ given in (A.5). If we make

$\varepsilon \to \infty$ in (A.5), we obtain

$$\boldsymbol{a}_\pm \to \begin{pmatrix} \pm\frac{\sqrt{3}}{2\sqrt{7}} \\ \frac{3}{2\sqrt{7}} \\ -\frac{2}{\sqrt{7}} \end{pmatrix}, \quad \boldsymbol{b}_\pm \to \begin{pmatrix} \pm\frac{\sqrt{3}}{2\sqrt{7}} \\ -\frac{3}{2\sqrt{7}} \\ \frac{2}{\sqrt{7}} \end{pmatrix}. \tag{A.20}$$

Since we have $F(\boldsymbol{a}_\pm) = F(\boldsymbol{b}_\pm) = \frac{6}{7} - \frac{1}{\varepsilon}\frac{6\cdot 26}{7\cdot 27}$ for generic $\boldsymbol{a}_\pm$, $\boldsymbol{b}_\pm$, we verify that $F(\boldsymbol{a}_\pm) = F(\boldsymbol{b}_\pm) \to \frac{6}{7}$ as $\varepsilon \to \infty$. This implies that $\boldsymbol{a}_\pm$ and $\boldsymbol{b}_\pm$ remain to be exceptional points if $\varepsilon \to \infty$. The exceptional points $\boldsymbol{n}_\pm$ are independent of ε and remain to be exceptional points if $\varepsilon \to \infty$.

We are to observe what happens to the exceptional points if $\varepsilon \to -\infty$. We first consider the exceptional points $\boldsymbol{e}_\pm$. If $\varepsilon \to -\infty$, then α tends to 0 in the same manner as in the case of $\varepsilon \to \infty$. However, in the case of $\varepsilon \to -\infty$, the $\boldsymbol{e}_\pm$ converge to

$$\boldsymbol{e}_+ \to \begin{pmatrix} 0 \\ 0 \\ -1 \end{pmatrix}, \quad \boldsymbol{e}_- \to \begin{pmatrix} 0 \\ 0 \\ 1 \end{pmatrix}, \tag{A.21}$$

respectively, in contrast with (A.19). Similar to the case of $\varepsilon \to \infty$, the limit points (A.21) are degeneracy points. Like (A.20), if $\varepsilon \to -\infty$, we obtain the limit points

$$\boldsymbol{a}_\pm \to \begin{pmatrix} \pm\frac{\sqrt{3}}{2\sqrt{7}} \\ \frac{3}{2\sqrt{7}} \\ -\frac{2}{\sqrt{7}} \end{pmatrix}, \quad \boldsymbol{b}_\pm \to \begin{pmatrix} \pm\frac{\sqrt{3}}{2\sqrt{7}} \\ -\frac{3}{2\sqrt{7}} \\ \frac{2}{\sqrt{7}} \end{pmatrix}, \tag{A.22}$$

which are exceptional points. This is verified in the same manner as in the case of $\varepsilon \to \infty$. The exceptional points $\boldsymbol{n}_\pm$ are independent of ε and remain to be exceptional points if $\varepsilon \to -\infty$. The degeneracy points (A.21) form a two-point orbit of D_3 group with stabilizer C_3.

We note here that the operations $\varepsilon \to \pm\infty$ correspond to $\phi_1 \to \frac{\pi}{2}$ and $\phi_1 \to \frac{3\pi}{2}$, respectively. Put another way, the parameter ε cover the left half of the unit circle in the (a_1, a_2)-plane (see figure 16).

We turn to the upper half of the unit circle. In other words, we now consider the Hamiltonian with the parameters

$$a_1 = \kappa, \quad a_2 = 1, \quad b_1 = 1, \quad b_2 = -\frac{3}{2}. \tag{A.23}$$

The equations for exceptional points are given by

$$x(2y + \frac{3}{2}z) = 0, \quad \kappa z + y(y^2 - 3x^2) = 0. \tag{A.24}$$

From the first equation of (A.24), we have two cases (i) $x = 0$ and (ii) $2y + \frac{3}{2}z = 0$.
(i) If $x = 0$, the second equation of (A.24) becomes $\kappa z + y^3 = 0$. Then, the constraint condition provides $1 = y^2(1 + \frac{1}{\kappa^2}y^4)$, if $\kappa \neq 0$. We will treat the case of $\kappa = 0$ separately after finishing the case of $\kappa \neq 0$. Since the function $f(s) = s(1 + \frac{1}{\kappa^2}s^2)$ is monotone increasing in s, we have a unique real positive solution α determined by $1 = \alpha(1 + \frac{1}{\kappa^2}\alpha^2)$. Solutions to the equation $1 = y^2(1 + \frac{1}{\kappa^2}y^4)$ are then given by $y = \pm\alpha^{1/2}$. Thus we have obtained the exceptional points with the vanishing x-components. For the reason to be explained later, we denote the exceptional points $\boldsymbol{e}_\pm$ obtained above by

$$\boldsymbol{e}_- := \begin{pmatrix} 0 \\ \alpha^{1/2} \\ -\frac{1}{\kappa}\alpha^{3/2} \end{pmatrix}, \quad \boldsymbol{e}_+ := \begin{pmatrix} 0 \\ -\alpha^{1/2} \\ \frac{1}{\kappa}\alpha^{3/2} \end{pmatrix}, \quad \kappa > 0, \tag{A.25}$$

$$\boldsymbol{e}_+ := \begin{pmatrix} 0 \\ \alpha^{1/2} \\ -\frac{1}{\kappa}\alpha^{3/2} \end{pmatrix}, \quad \boldsymbol{e}_- := \begin{pmatrix} 0 \\ -\alpha^{1/2} \\ \frac{1}{\kappa}\alpha^{3/2} \end{pmatrix}, \quad \kappa < 0. \tag{A.26}$$

(ii) If $z = -\frac{4}{3}y$, then the second equation of (A.24) becomes $-\frac{4}{3}\kappa y + y(y^2 - 3x^2) = 0$. The $y = 0$ is a solution to this equation. Then, we have $z = 0$, so that $x = \pm 1$ because of the constraint condition. Thus, we have found the exceptional points

$$\boldsymbol{n}_\pm := \begin{pmatrix} \pm 1 \\ 0 \\ 0 \end{pmatrix}. \tag{A.27}$$

If $y \neq 0$, then we have $-\frac{4}{3}\kappa + y^2 - 3x^2 = 0$. This equation and the constraint condition are put together to provide the equation $1 = \frac{100}{27}\kappa + \frac{84}{9}x^2$, and then $x^2 = \frac{9}{84}(1 - \frac{100}{27}\kappa)$. The right-hand side of this equation is in the range $0 \leq \frac{9}{84}(1 - \frac{100}{27}\kappa) \leq 1$ if and only if $-\frac{9}{4} \leq \kappa \leq \frac{27}{100}$. If $-\frac{9}{4} \leq \kappa \leq \frac{27}{100}$, we obtain the solutions $x = \pm\frac{3}{2\sqrt{21}}\sqrt{1 - \frac{100}{27}\kappa}$. Then, $y^2 = \frac{4}{3}\kappa + 3x^2$ is solved by $y = \pm\frac{1}{\sqrt{7}}\sqrt{\kappa + \frac{9}{4}}$, so that $z = \mp\frac{4}{3\sqrt{7}}\sqrt{\kappa + \frac{9}{4}}$. Thus, we have found the

exceptional points

$$\boldsymbol{a}_\pm := \begin{pmatrix} \pm\frac{3}{2\sqrt{21}}\sqrt{1-\frac{100}{27}\kappa} \\ \frac{1}{\sqrt{7}}\sqrt{\kappa+\frac{9}{4}} \\ -\frac{4}{3\sqrt{7}}\sqrt{\kappa+\frac{9}{4}} \end{pmatrix}, \quad \boldsymbol{b}_\pm := \begin{pmatrix} \pm\frac{3}{2\sqrt{21}}\sqrt{1-\frac{100}{27}\kappa} \\ -\frac{1}{\sqrt{7}}\sqrt{\kappa+\frac{9}{4}} \\ \frac{4}{3\sqrt{7}}\sqrt{\kappa+\frac{9}{4}} \end{pmatrix} \tag{A.28}$$
$$\text{for} \quad -\tfrac{9}{4} \le \kappa \le \tfrac{27}{100}.$$

We now explain the reason why we have chosen the definitions (A.25) and (A.26), where the suffices $\pm$ look exchanged, if the sigh of κ is ignored. We can prove the validity of the definition (A.26) from the viewpoint of the parameter change (154). In terms of the parameter ε, the exceptional points $\boldsymbol{e}_\pm$ are defined in (A.3) with the α determined by $1 = \alpha(1+\varepsilon^2\alpha^2)$. Let us be reminded of the fact that the parameter change (154) is valid for $\varepsilon > 0$ and $\kappa < 0$. In (A.25), α is determined by the equation $1 = \alpha(1 + \frac{1}{\kappa^2}\alpha^2)$, which is put into $1 = \alpha(1+\varepsilon^2\alpha^2)$ if $\kappa = -1/\varepsilon$ is taken into account. With these in mind, we can observe that the exceptional points (A.3) in the case of $\varepsilon > 0$ are exactly the same as (A.26) in the case of $\kappa < 0$.

We further verify that although the exceptional points $\boldsymbol{e}_\pm$ look discontinuous at $\kappa = 0$, they are continuous in a neighborhood of $\kappa = 0$. To this end, we first note that if $\kappa \to 0$ then $\alpha \to 0$. Since the relation $1 = \alpha + \frac{1}{\kappa^2}\alpha^3$ is preserved in the process of $\kappa \to 0$, it follows that $\frac{1}{\kappa^2}\alpha^3 \to 1$ as $\kappa \to 0$. On account of this, we find from (A.25) that

$$\boldsymbol{e}_\pm \to \begin{pmatrix} 0 \\ 0 \\ \pm 1 \end{pmatrix} \quad \text{as } \kappa \downarrow 0. \tag{A.29}$$

In the case of $\kappa < 0$, from the definition (A.26), the limit points of $\boldsymbol{e}_\pm$ as $\kappa \to 0$ with $\kappa < 0$ prove to be

$$\boldsymbol{e}_\pm \to \begin{pmatrix} 0 \\ 0 \\ \pm 1 \end{pmatrix}, \quad \kappa \uparrow 0. \tag{A.30}$$

Eqs. (A.29) and (A.30) are put together to show that the exceptional points $\boldsymbol{e}_\pm$ defined by (A.25) and (A.26) depend continuously on κ in a neighborhood of $\kappa = 0$.

We note further that if $\kappa < 0$, the exceptional points $\boldsymbol{a}_\pm$ and $\boldsymbol{b}_\pm$ defined in (A.28) are transformed into those defined in (A.5) with $\varepsilon \geq \frac{4}{9}$.

If $\kappa = 0$, Eqs. (A.24) become

$$x(2y + \frac{3}{2}z) = 0, \quad y(y^2 - 3x^2) = 0. \tag{A.31}$$

From the first equation of the above, we have two cases, (i) $x = 0$ and (ii) $2y + \frac{3}{2}z = 0$.
(i) If $x = 0$, then the second equation becomes $y^3 = 0$, so that $y = 0$. Then, the constraint condition provides $z = \pm 1$.
(ii) If $2y + \frac{3}{2}z = 0$, the second equation of the above is rewritten as $-\frac{3}{4}z(\frac{9}{16}z^2 - 3x^2) = 0$. If $z = 0$, then one has $y = 0$, so that the constraint condition provides $x = \pm 1$. If $z \neq 0$, then the present equation reduces to $\frac{9}{16}z^2 - 3x^2 = 0$. This and the constraint condition are put together to give $1 = \frac{7}{4}z^2$, so that $z = \pm\frac{2}{\sqrt{7}}$ and $y = \mp\frac{3}{2\sqrt{7}}$, and thereby $x = \pm\frac{\sqrt{3}}{2\sqrt{7}}$. Thus, for $\kappa = 0$, we have found the exceptional points

$$\begin{pmatrix} 0 \\ 0 \\ \pm 1 \end{pmatrix}, \quad \begin{pmatrix} \pm 1 \\ 0 \\ 0 \end{pmatrix}, \quad \begin{pmatrix} \pm\frac{\sqrt{3}}{2\sqrt{7}} \\ \frac{3}{2\sqrt{7}} \\ -\frac{2}{\sqrt{7}} \end{pmatrix}, \quad \begin{pmatrix} \pm\frac{\sqrt{3}}{2\sqrt{7}} \\ -\frac{3}{2\sqrt{7}} \\ \frac{2}{\sqrt{7}} \end{pmatrix}. \tag{A.32}$$

We note that the leftmost exceptional points among the above are limit points of $\boldsymbol{e}_\pm$ as $\kappa \to 0$, as is seen in (A.29) and (A.30). The second one is the same as $\boldsymbol{n}_\pm$. The third and the last ones are the limit points of $\boldsymbol{a}_\pm$ and $\boldsymbol{b}_\pm$, respectively. In fact, if $\kappa \to 0$, the exceptional points $\boldsymbol{a}_\pm$ and $\boldsymbol{b}_\pm$ given in (A.28) tend to

$$\boldsymbol{a}_\pm \to \begin{pmatrix} \pm\frac{3}{2\sqrt{21}} \\ \frac{3}{2\sqrt{7}} \\ -\frac{2}{\sqrt{7}} \end{pmatrix}, \quad \boldsymbol{b}_\pm \to \begin{pmatrix} \pm\frac{3}{2\sqrt{21}} \\ -\frac{3}{2\sqrt{7}} \\ \frac{2}{\sqrt{7}} \end{pmatrix}, \tag{A.33}$$

respectively.

So far we have obtained all the exceptional points, our next task is to examine the sign of the value of $F = y^2 - x^2 - \frac{3}{2}zy$ for each of the exceptional points obtained. For $\boldsymbol{a}_\pm$ and $\boldsymbol{b}_\pm$, we obtain $F(\boldsymbol{a}_\pm) = F(\boldsymbol{b}_\pm) = \frac{6}{7}(1 + \frac{26}{27}\kappa)$, which is positive for $\kappa > 0$. For $\boldsymbol{e}_\pm$, one has $F(\boldsymbol{e}_\pm) = \alpha + \frac{3}{2\kappa}\alpha^2 > 0$ for $\kappa > 0$. For $\boldsymbol{n}_\pm$, one has $F(\boldsymbol{n}_\pm) = -1 < 0$. In the case of $\kappa = 0$, a straightforward calculation shows that $F(\boldsymbol{e}_\pm) = 0$, $F(\boldsymbol{n}_\pm) < 0$, $F(\boldsymbol{a}_\pm) = F(\boldsymbol{b}_\pm) > 0$. In the

case of $\kappa < 0$, we need not to examine the sign of the value of F, since we can find the sign by applying the parameter change $\kappa = -1/\varepsilon$ to the results in the case of $\varepsilon > 0$. The summary of our results is given in the table 1 in section 9, where the correspondence between results obtained by using ε and κ parameters is explicitely demonstrated.

It is to be noted here that the exceptional points $\boldsymbol{e}_\pm$ become degeneracy points at the moment of $\kappa = 0$, which we have already shown when we studied the limit points of $\boldsymbol{e}_\pm$ as $\varepsilon \to \infty$.

In what follows, we study the case of $\kappa > 0$. The domains $U_{\rm up}$ and $U_{\rm down}$ are now determined according to the sign of F for the exceptional points as follows:

$$U_{\rm up} = S^2 - \{\boldsymbol{a}_\pm, \boldsymbol{b}_\pm, \boldsymbol{e}_\pm\}, \quad U_{\rm down} = S^2 - \{\boldsymbol{n}_\pm\} \quad \text{for } 0 < \kappa \leq \frac{27}{100}, \tag{A.34}$$

$$U_{\rm up} = S^2 - \{\boldsymbol{e}_\pm\}, \quad U_{\rm down} = S^2 - \{\boldsymbol{n}_\pm\} \quad \text{for } \frac{27}{100} < \kappa. \tag{A.35}$$

To evaluate the Chern number, we take the linearization method. Let

$$X = x(2y + \frac{3}{2}z), \quad Y = -\kappa z - y(y^2 - 3x^2). \tag{A.36}$$

In the case of $0 < \kappa \leq \frac{27}{100}$, we draw two circles C_1 and C_2 on the levels $x = \pm h$, where $\frac{3}{2\sqrt{21}} < h < 1$. These circles divide the sphere into three regions. We denote by S^2_+ the union of regions containing either of $\boldsymbol{e}_\pm$, and by S^2_- the region containing the equator. The orientations of the circles are in keeping with that of S^2_+. We take (y, z) as local coordinates and view x as a height function. Then the first-order derivatives of X and Y are given by

$$\frac{\partial X}{\partial y} = -\frac{y}{x}(2y + \frac{3}{2}z) + 2x, \quad \frac{\partial X}{\partial z} = -\frac{z}{x}(2y + \frac{3}{2}z) + \frac{3}{2}x, \tag{A.37a}$$

$$\frac{\partial Y}{\partial y} = -9y^2 + 3x^2, \quad \frac{\partial Y}{\partial z} = -\kappa - 6yz. \tag{A.37b}$$

The determinant of the coefficient matrix of the linearized vector is evaluated at $\boldsymbol{n}_\pm$ as

$$\det \begin{pmatrix} \frac{\partial X}{\partial y} & \frac{\partial X}{\partial z} \\ \frac{\partial Y}{\partial y} & \frac{\partial Y}{\partial z} \end{pmatrix} = \begin{vmatrix} 2x & \frac{3}{2} \\ 3x & -\kappa \end{vmatrix} = -2x(\kappa + \frac{9}{4}), \tag{A.38}$$

where x is the x-components of $\boldsymbol{n}_\pm$. If $\kappa > 0$, the right-hand side of the above equation is negative or positive according to whether $x = 1$ or $x = -1$.

Thus, the winding number associated with $\boldsymbol{n}_\pm$ are both -1 on account of the orientation of the coordinate system (y, z) against the north and the south hemispheres. It follows that the Chern number is 2.

In the case of $\frac{27}{100} < \kappa$, we draw two circles C_1 and C_2 on the levels $x = \pm h$, where $0 < h < 1$. The regions S^2_+ and S^2_- are defined in a similar manner as above. The Chern number is also evaluated in the same manner as above to result in 2.

The summary of the results can be seen again in the table 1 in section 9.

If we set $\kappa \to \infty$, then from the definition of α we obtain $\alpha \to 1$, and thereby from (A.29)

$$\boldsymbol{e}_\pm \to \begin{pmatrix} 0 \\ \mp 1 \\ 0 \end{pmatrix}. \tag{A.39}$$

For these limit points, the function $F = y^2 - x^2 - \frac{3}{2}zy$ has the value $1 > 0$, so that they remain to be exceptional points. The exceptional points $\boldsymbol{n}_\pm$ remains to be fixed, since they are independent of κ.

We move on to the right half circle in the (a_1, a_2)-plane. The tangent line to the circle at $(1, 0)$, which is a coordinate patch of the half cycle in question, is expressed as $(1, -\varepsilon)$, which is the inversion of the tangent line $(-1, \varepsilon)$ at $(-1, 0)$, where $\varepsilon \in \mathbb{R}$. The present parametrization of the tangent line carries the advantage that we need not to perform another calculation to find exceptional points. This is because the equation for exceptional points for the parameter

$$a_1 = 1, \quad a_2 = -\varepsilon, \quad b_1 = 1, \quad b_2 = -\frac{3}{2} \tag{A.40}$$

are given by

$$x(2y + \frac{3}{2}z) = 0, \quad z - \varepsilon y(y^2 - 3x^2) = 0, \tag{A.41}$$

which are the same as in the case of $(a_1, a_2) = (-1, \varepsilon)$. Then, we have the same exceptional points as those obtained in the case of $(a_1, a_2) = (-1, \varepsilon)$. And the domains U_{up} and U_{down} prove to be the same. However, the Chern numbers are not the same, since the quantities X and Y are not the same. They are given by

$$X = x(2y + \frac{3}{2}z), \quad Y = -z + \varepsilon y(y^2 - 3x^2), \tag{A.42}$$

We note that Y is changed in the sign in comparison with (A.12). This modification is due to the transformation $H \to \bar{H}$ of Hamiltonian to its complex conjugate as shown in Figure 14. If we are reminded of the fact that Chern numbers can be evaluated through the sign of the determinant of the coefficient matrix of the linearized vector, we can observe that the Chern number is reversed in the sign under the transformation $(X, Y) \to (X, -Y)$. Thus, we have for the case of $(a_1, a_2) = (1, -\varepsilon)$ the following table

	$\varepsilon \leq -\frac{100}{27}$	$-\frac{100}{27} < \varepsilon < \frac{4}{9}$	$\frac{4}{9} \leq \varepsilon < \frac{26}{27}$	$\varepsilon = \frac{26}{27}$	$\frac{26}{27} < \varepsilon$
$\boldsymbol{e}_\pm$	$+$	$+$	$+$	0	$-$
$\boldsymbol{n}_\pm$	$-$	$-$	$-$	$-$	$-$
$\boldsymbol{a}_\pm, \boldsymbol{b}_\pm$	$+$	$(empty)$	$-$	0	$+$
Chern number	2	2	2	*not defined*	-4

which is completely similar to the appropriate part of Table 1 dealing with $(a_1, a_2) = (-1, \varepsilon)$. The only formal difference is the inversed sign of the Chern number for the same eigen-line bundle associated with positive eigenvalue of the model Hamiltonian (125).

It is to be noted here that the coordinate patches with $\varepsilon < 0$ and with $\varepsilon > 0$ cover the upper right quarter and the lower right quarter of the circle, respectively.

In the same manner, we can inverse the sign of $(\kappa, 1)$ to obtain the tangent line, $(-\kappa, -1)$, to the circle at $(0, -1)$. By the same reasoning as above, we can obtain the following table for the case of $(a_1, a_2) = (-\kappa, -1)$:

	$\kappa < -\frac{9}{4}$	$-\frac{9}{4} \leq \kappa < -\frac{27}{26}$	$-\frac{27}{26}$	$-\frac{27}{26} < \kappa < 0$	0	$0 < \kappa < \frac{27}{100}$	$\frac{27}{100} < \kappa$
$\boldsymbol{e}_\pm$	$+$	$+$	0	$-$	0	$+$	$+$
$\boldsymbol{n}_\pm$	$-$	$-$	$-$	$-$	$-$	$-$	$-$
$\boldsymbol{a}_\pm, \boldsymbol{b}_\pm$	$(empty)$	$-$	0	$+$	$+$	$+$	$(empty)$
Chern number	2	2	*not defined*	-4	*not defined*	-2	-2

This table again coincides with the appropriate part of Table 1 dealing with $(a_1, a_2) = (\kappa, 1)$ case except for the sign of Chern numbers, which are inversed.

Thus, we have found all Chern numbers along the closed path determined by $(a_1, a_2) = (\cos\phi_1, \sin\phi_1)$ and $(b_1, b_2) = (\frac{2}{\sqrt{13}}, -\frac{3}{\sqrt{13}})$. This closed path carries four singular points on which Chern numbers are not defined. The Chern numbers obtained so far are shown in Figure A.20, where the four

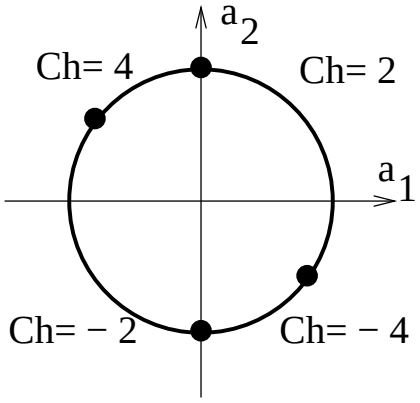

Figure A.20: Chern numbers along closed path **1** shown in figure 15.

dots on the circle denote the points in the parameter space corresponding to Hamiltonians with two eigenvalues possessing degeneracy points. Eigen-line bundles cannot be defined for Hamiltonian with these parameter values. The Chern number is constant in each arc between adjoining dots.

Acknowledgments: This work was started during the visit of B.Zh. to Kyoto in September - December 2010. The financial support of this visit by Kyoto University is greatly acknowledged.

References

[1] V.I. Arnold, Modes and quasimodes. Funkt. Anal. Appl. **6** (1972) 94-101.

[2] V.I. Arnold, Remarks on eigenvalues and eigenvectors of Hermitian matrices. Berry phase, adiabatic connections and quantum Hall effect. Selecta Mathematica **1**, 1-19 (1995).

[3] J.E. Avron, D. Osadchy, and R. Seiler, A topological look at the Hall effect. Physics Today, August 2003, 38-42.

[4] J.E. Avron, L. Sadun, J. Segert, and B. Simon, Chern numbers, quaternions, and Berry's phases in Fermi systems, Comm. Math. Phys. **124**, 595-627 (1989).

[5] S. Brodersen and B. I. Zhilinskii, The rotational structure of the vibrational states and substates of symmetry E in CF_4. J. Mol. Spectrosc. **172**, 303-318 (1995).

[6] W. Burnside. *Theory of groups of Finite Order.* Cambridge Univ. Press, N.Y. 1911.

[7] Y. Colin de Verdier, S. Vu Ngoc, Singular Bohr-Sommerfeld rules for 2D integrable systems. Ann. Ec. Norm. Sup. **36**, 1-55 (2003).

[8] R.H. Cushman, L.M. Bates, *Global aspects of classical integrable systems.* Birkhäuser. Basel, 1997.

[9] S. K. Donaldson and P.B. Kronheimer, *The Geometry of Four-Manifolds,* Oxford Mathematical Monographs, Oxford: Clarendon Press, 1997.

[10] H.H. Duistermaat, On global action angle coordinates, Commun. Pure Appl. Math. **33**, 687-706 (1980)

[11] K.E.Efstathiou, D. A. Sadovskii. Normalization and global analysis of perturbations of the hydrogen atom. Rev.Mod.Phys. **82**. 2099-20154 (2010).

[12] K. Efstathiou, D. A. Sadovskii, B. I. Zhilinskii, Analysis of rotation-vibration relative equilibria on example of a tetrahedral four atom molecule. SIAM Journal of Dynamical Systems, **3**, 261-351 (2004).

[13] F. Faure and B. I. Zhilinskii, Topological Chern indices in molecular spectra Phys. Rev. Lett., **85**, 960-963 (2000).

[14] F. Faure and B. I. Zhilinskii, Topological properties of the Born-Oppenheimer approximation and implications for the exact spectrum. Let. Math. Phys. **55**, 239-247 (2001).

[15] F. Faure and B. Zhilinskii, Qualitative features of intra-molecular dynamics. What can be learned from symmetry and topology. Acta Appl. Math. **70**, 265-282 (2002)

[16] F. Faure and B. I. Zhilinskii, Topologically coupled energy bands in molecules. Phys. Lett. A **302**, 242-252 (2002).

[17] *Geometric phase in physics,* Eds: F. Wilczek and A. Shapere, World Scientific, 1989.

[18] L. Grondin, D. Sadovskii and B. Zhilinskii, Monodromy in systems with coupled angular momenta and rearrangement of bands in quantum spectra. Phys. Rev. A., **65**, 012105 (2002).

[19] A. Guichardet, On rotation and vibration motion of molecules. Ann. Inst. Henri Poincarè. **40** 329-342 (1984)

[20] M.S. Hansen, F. Faure, and B. I. Zhilinskii, Fractional monodromy in systems with coupled angular momenta J.Phys. A: Math.Theor. **40**, 13075–13089 (2007)

[21] G. Herzberg, *Molecular spectra and molecular structure.* Vol. 2, Krieger, 1989.

[22] G. Herzberg and H.C. Longuet-Higgins, Intersection of potential energy surfaces in polyatomic molecules. Disc. Faraday Soc. 1963, **35**, 77-82.

[23] T. Iwai, A. Tachibana, The geometry and mechanics of multi-particle systems. Ann. Inst. Henri Poincarè, **70**. 525-559 (1999).

[24] T. Iwai and B. Zhilinskii, Rearrangement of energy bands: Chern numbers in the presence of symmetry. Acta Appl. Math, submitted (2011).

[25] C.L. Kane and E.J. Mele, Z_2 topological order and the quantum spin Hall effect. Phys.Rev. Lett. **95**, 146802 (2005).

[26] A. Kitaev, Periodic table for topological insulators and superconductors. arXiv:0901.2686v2 (2009).

[27] L.Michel and B. Zhilinskii. Symmetry, invariants topology. Basic tools. Phys. Rep. **341**, 11-84 (2001).

[28] T. Molien, Uber die Invarianten der linearen Substitutionsgruppen. Sitzungber. Konig. Preuss. Akad. Wiss. **52**, 1151-1156 (1897).

[29] J.E. Moore and L. Balents, Topological insulators of time-reversal-invariant band structures. Phys. Rev. B **75**,121306 (R) (2007).

[30] N.N. Nekhoroshev, Action-angle variables and their generalizations, Trans. Moscow Math. Soc. **26**, 1880-198 (1972).

[31] N. N. Nekhoroshev, D.A. Sadovskii B. I. Zhilinskii, Fractional Hamiltonian monodromy. Ann. Henri Poincare. **7**, 1099–1211 (2006).

[32] N. N. Nekhoroshev, D.A. Sadovskii B. I. Zhilinskii, Fractional monodromy of resonant classical and quantum oscillators. C.R. Acad. Sci. Paris I, **335**, 985-988 (2002).

[33] Y. A. Nisnevich, The structure of a class of finite ramified coverings and canonical forms of analytic matrix functions in a neighborhood of a ramified turning point. Proc. Natl Acad. Sci US, **99**, 7361-7366 (2002).

[34] J. Patera, R. Sharp, P. Winternitz. Polynomial irreducible tensors for point groups. J. Math. Phys. **19**, 2362-2376 (1978).

[35] V. B. Pavlov-Verevkin, D. A. Sadovskii and B. I. Zhilinskii On the dynamical meaning of diabolic points, Europhys. Lett. **6**, 573-78 (1988).

[36] J.M. Robbins, Topological phase effects. In: *Encyclopedia of Applied Physics*, Vol 21, 1997, Wiley-VCH.

[37] D. A. Sadovskii and B. I. Zhilinskii, Qualitative analysis of vibration-rotation Hamiltonians for spherical top molecules, Molec. Phys. **65** 109-28 (1988).

[38] D. A. Sadovskii and B. I. Zhilinskii Group theoretical and topological analysis of localized vibration-rotation states, Phys. Rev. A **47**, 2653-71 (1993).

[39] D. A. Sadovskii and B. I. Zhilinskii. Counting levels within vibrational polyads. Generating function approach, J. Chem. Phys. **103**, 10520-36 (1995).

[40] D. A. Sadovskii and B. I. Zhilinskii, Monodromy, diabolic points, and angular momentum coupling Phys. Lett. A **256**, 235-44 (1999).

[41] J. Schwinger. On angular momentum. In: *Quantum Theory of Angular Momentum.* N.Y.., 1965, p.229.

[42] R. Stanley, Invariants of finite groups and their application to combinatorics. Bull. Am. Math. Soc. **1**, 475-511 (1979).

[43] R. Stanley, *Enumerative combinatorics.* Vol. 1, Wadsworth Brooks, Montrey, CA (1986).

[44] R. Thom, *Structural stability and morphogenesis.* (Reading, MA: Addison-Wesley 1972).

[45] David J. Thouless, *Topological Quantum Numbers in Nonrelativistic Physics.* 1998 World Scientific, Singapore

[46] E. Wigner, *Group theory and its application to the quantum mechanics of atomic spectra.* Academic, N.Y. 1959.

[47] B. Zhilinskii, Symmetry, invariants and topology in molecular models. Phys. Rep. **341**. 85-172 (2001).

[48] B. I. Zhilinskii and S. Brodersen, The symmetry of the vibrational components in T_d molecules. J. Mol. Spectrosc. **163**, 326-338 (1994).